14th INTERNATIONAL SHIP AND
OFFSHORE STRUCTURES CONGRESS 2000
2-6 OCTOBER 2000
NAGASAKI, JAPAN

VOLUME 1

COMMITTEE VI.2

ULTIMATE HULL GIRDER STRENGTH

COMMITTEE MANDATE

Evaluate and develop procedures for estimating the ultimate strength of ship hull girders. Due consideration shall be given to relevant load combinations, including overall bending, torsion and shear as well as local pressure loads. The influence of fabrication imperfections, corrosion and in-service damage on the strength shall be discussed. The procedures shall be assessed by comparison with model tests and more refined calculation methods. Recommendations for ultimate strength assessment methods shall be given.

COMMITTEE MEMBERS

Chairman:	Prof.	T. Yao
	Dr.	O.C. Astrup
	Dr.	P. Caridis
	Dr.	Y.N. Chen
	Prof.	S.-R. Cho
	Dr.	R.S. Dow
	Dr.	O. Niho
	Dr.	P. Rigo

KEYWORDS

Ultimate Hull Girder Strength, Longitudinal Bending, Buckling/Plastic Collapse, Benchmark Calculations, Structural Design, Combined Loads, Initial Imperfection, Corrosion Damage, In-Service Damage, Average Stress-Average Strain Relationship

CONTENTS

1. INTRODUCTION

The most fundamental aspect of the strength of a ship is that of ***longitudinal strength***, that is, its ability to withstand longitudinal bending under operational and extreme loads without suffering failure. The assessment of the longitudinal strength involves the evaluation the capacity of the hull girder under longitudinal bending and also the estimation of the maximum bending moment which may act on it.

ThomasYoung, whose name is well known with *Young's modulus*, was the first to attempt to calculate the longitudinal bending moment of ships. He treated the hull girder as a beam that is subjected to distributed loads due to weight and buoyancy forces that correspond to assumed wave modes (Timoshenko 1953). On the other hand, it was Sir Isambard K. Brunel who was the first to assess hull girder strength under extreme load conditions (Rutherford and Caldwell 1990). When Sir Isambard designed the *Great Eastern*, a huge iron ship, he calculated bending stresses in the deck and bottom assuming a grounded condition, and determined the panel thickness so as to prevent breaking of the panel.

After Sir Isambard, John (1987) presented a fundamental idea to assess longitudinal strength of a ship's hull. He calculated the bending moment assuming the wave whose length is equal to the ship length. Based on the results of calculation, he proposed an approximate formula to evaluate the bending moment at a midship section. John calculated the maximum stress in the deck and compared it with the breaking strength of the material to determine the panel thickness.

The basic idea proposed by John to assess the longitudinal strength has remained in use until today. However, the methods of analysis that are used to calculate working stress and the wave loading have improved substantially. Furthermore, the criteria to determine the thickness has changed from breaking strength to yield strength and buckling strength. The most recent development is to also take into account the ultimate strength when calculating the hull girder strength.

In order to ensure critical and safe design of a ship's hull, it is necessary to accurately evaluate the capacity of the hull girder considering extreme loads. The need for this has urged the ISSC as a body to establish special task committees to deal with extreme loading and hull girder strength.

This report describes the results of works performed by members of the committee whose task has been to compare and critically evaluate existing procedures that are used to calculate the ultimate longitudinal strength of a ship hull girder.

Chapter 2 of the report reviews the existing methods for evaluation of ultimate hull girder strength of a ship subjected to longitudinal bending. The methods are categorised into two groups; direct calculation method and methods based on progressive collapse analysis.

Chapter 3 describes the results of benchmark calculations on ultimate compressive strength of stiffened plates composing the cross-section of a ship's hull girder. Ninety (90) stiffened plates are analysed applying twelve different methods.

Chapter 4 represents the results of benchmark calculations on ultimate longitudinal strength of four hull girders of existing ships and a 1/3-scale test model applying nine different methods. The influence of element characteristics on ultimate hull girder strength is discussed.

Chapter 5 describes the influences of load combined loading conditions on the ultimate strength of structural members and hull girders. The efffects of transverse thrust and lateral pressure on member strength are reviewed and discussed, and then those of shear forces and torsional moment as well as hirozontal bending on the ultimate hull girder strength. The influence of corrosion damage is also demonstratred.

Chapter 6 shows the sensitivities of the ultimate hull girder strength with respect to various design parameters such as the thickness of panels and stiffeners, the yield stress, the initial deflection and welding residual stress.

Chapter 7 describes some considerations on ultimate hull girder strength from the point of view of design. The relationship between the design load and the ultimate hull girder strength is discussed in relation to existing vessels, including those analysed in Chapter 4.

Chapter 8 includes a technical guide that can be used to select a suitable method to assess the ultimate longitudinal strength of a ship hull girder. Relevant features of existing methods are listed and used to enable a potential users to choose a method according to his requirements. Chapter 9 summarises concluding remarks.

2. EXISTING METHODS OF ANALYSES TO EVALUATE ULTIMATE HULL GIRDER STRENGTH

There exist two methods to evaluate the ultimate hull girder strength of a ship's hull under longitudinal bending. One is to calculate the ultimate hull girder strength directly, and the other is to perform progressive collapse analysis on a hull girder. In this chapter, existing methods are introduced with a brief historical review. More comprehensive reviews can be found in the papers by Rigo (1998) and Yao (1999).

2.1 Direct Method to Evaluate Ultimate Hull Girder Strength

2.1.1 Caldwell's Method

Caldwell (1965) was the first who tried to theoretically evaluate the ultimate hull girder strength of a ship subjected to longitudinal bending. He introduced a so-called *Plastic Design* considering the influence of buckling and yielding of structural members composing a ship's hull.

He idealised a stiffened cross-section of a ship's hull to an unstiffened cross-section with equivalent thickness. If buckling takes place at the compression side of bending, compressive stresses cannot reach the yield stress, and the fully plastic bending moment cannot be attained. Caldwell introduced a stress reduction factor at the compression side of bending, and the bending moment produced by the reduced stress was considered as the ultimate hull girder strength. He performed a series of calculations changing the reduction factors, and discussed the influence of buckling on the ultimate hull girder strength.

In Caldwell's method, reduction in the capacity of structural members beyond their ultimate strength was not taken into account. This causes an overestimation of the ultimate strength in general. In addition to this, in Caldwell's time, the exact values of reduction factors for structural members were not available, and the real ultimate strength itself could not be evaluated. However, Caldwell's original method seems to be rational, and has since been improved with respect to:

(1) the derivation of exact reduction factors due to buckling,

(2) the introduction of phase lag in collapse of individual structural members,

(3) the introduction of load-shedding effect of structural members beyond their ultimate strength.

2.1.2 Improved Methods

Twenty-four years later, Maestro and Marino (1989) extended the Caldwell's formulation to the case of bi-axial bending, and modified the method to estimate the influence of damage due to grounding and/or collision on the ultimate hull girder strength. Nishihara (1983) applied Caldwell's method to calculate the ultimate strength of a ship's hull improving the accuracy of the strength reduction factors. Many researchers proposed similar formulae. For examples, Endo *et al.*(1988) and Mansour *et al.*(1990) proposed simple calculation methods to evaluate the ultimate hull girder strength using their own formulae. Paik and Mansour (1995) also proposed a simple method to predict the ultimate hull girder strength. Applying this method, Paik *et al.*(1998) performed reliability analysis considering corrosion damage.

Although these methods described above do not explicitly take into account of strength

reduction in the members beyond their ultimate strength, the evaluated ultimate hull girder strength showed good correlation with the measured/calculated results in many cases. For instance, Paik and Mansour (1995) compared the predicted results with those by experiments and ISUM analysis, and the differences were reported to be between -1.9% and +9.1%.

2.1.3 Empirical Formulations and Interaction Formulations

An other class of methods, different from the rational Caldwell's method (and improved methods), are some empirical formulations usually assessed for a type of specific vessels (Viner 1986, Frieze *et al.* 1991).
In order to raise the problem of combined loads (vertical and horizontal bending moments and shear forces), several authors have proposed interaction equations to predict the ultimate strength associated with each load (supposed to act separately). These are discussed in more detail in Chapter 5.

2.2 Progressive Collapse Analysis

In Caldwell's method (and later improvements), the ultimate hull girder strength is calculated without considering the strength reduction in individual members after they have attained their ultimate strength locally. This does not represent the real collapse behaviour of the structural members. As shall be demonstrated later in Chapter 4, neglection of the reduction in capacity of individual members beyond their ultimate strength greatly affects the ultimate strength of the whole cross-section.
For this reason, it is very important to take into consideration the strength reduction (load shedding) of each structural member when the collapse behaviour of a ship's hull is simulated. This simulation method is called Progressive Collapse Analysis. In the following, major methods of progressive collapse analysis and some calculated results are discussed.

2.2.1 Simplified Method (Smith's method)

It is fundamentally possible to perform progressive collapse analysis applying the Finite Element Method (FEM) considering both material and geometrical nonlinearities. However, large computing resources are required as well as manpower to obtain reliable results. Because of this, some simplified methods have been developed and the most well known is the so-called Smith's method. The fundamental idea is to take into account of the strength reduction of structural members after their ultimate strength as well as the time lag in collapse of individual members. Smith (1977) was the first who demonstrated by analysis that the cross-section cannot sustain fully plastic bending moment. In the Smith's method, the cross-section is divided into small elements composed of a stiffener and attached plating, and the average stress-average strain relationships of individual elements are derived before performing a progressive collapse analysis.
According to Smith (1983), the progressive collapse behaviour of the cross-section subjected to combined vertical and horizontal bending is simulated as follows:

(1) Axial rigidities of individual elements are calculated using the average stress-average strain relationships.
(2) Flexural rigidity of the cross-section is evaluated using the axial rigidities of elements.
(3) Vertical and horizontal curvatures of the hull girder are applied incrementally with the assumption that the plane section remains plane and that the bending occurs about the instantaneous neutral axes of the cross-section.
(4) The corresponding incremental bending moments are evaluated and so the strain and stress increments of individual elements.
(5) Incremental curvatures and bending moments of the cross-section as well as incremental strains and stresses are summed up to provide their cumulative values.

The accuracy of the calculated results by the Smith's method depends largely on the accuracy

of the average stress-average strain relationships of the elements. Main difficulties concern the modelling of initial imperfections (deflection and welding residual stress) and the boundary conditions (multi-span model, interaction between adjacent elements, *etc.*). This is the reason why most of the recent works are focussing on the development of more reliable stress-strain curves (Gordo and Guedes Soares 1993, Paik 1999).

Smith himself performed a series of elastoplastic large deflection analysis by FEM to derive the average stress-average strain relationships of elements. On the other hand, some analytical methods have been proposed to get average stress-average strain relationships of stiffened plate elements. Ostapenko (1981) applied analytical solutions with some assumptions, and derived the average stress-average strain relationships of compression flange under combined inplane bending and shear as well as under combined thrust and hydraulic pressure. Rutherford and Caldwell (1990) proposed an analytical method combining the ultimate strength formulae and solution of the rigid-plastic mechanism analysis. In both methods, the strength reduction after the ultimate strength is considered.

To evaluate the ultimate hull girder strength by the Smith's method, Gordo and Guedes Soares (1993, 1996a) and Gordo *et al.*(1996b) applied a simplified approach to represent collapse behaviour of a beam-column subjected to axial compression. In addition, Bureau Veritas implemented in the MARS scantlings PC code a progressive collapse model (RESULT), based on the Smith's method and the Gordo-Soares average stress-average strain curves for plates and stiffeners (Beghin *et al.* 1995).

Yao (1993a) also proposed an analytical method to derive average stress-average strain relationship for the element composed of a stiffener and attached plating. In this method, the average stress-average strain relationship of the panel surrounded by stiffeners is first derived combining the elastic large deflection analysis and the rigid-plastic mechanism analysis in analytical forms (Yao and Nikolov 1991, 1992). Then, considering the equilibrium condition of forces and bending moments acting on the element, the average stress-average strain relationship of a stiffener element is derived. When the stiffener part is elastic, a sinusoidal deflection mode is assumed, but after the yielding has started, a plastic deflection component is introduced which gives constant curvature at the yielded mid-span region. This method is implemented in the computer code HULLST for progressive collapse analysis.

Rahman and Chowdhury (1996) combined the Smith's method with simplified average stress-average strain curves based on the calculation of the ultimate strength of a stiffened panel developed by Hughes (1988).

A few practical applications are mentioned: Smith (1983) discussed the advantage of the longitudinal stiffening systems from the viewpoint of ultimate longitudinal strength and he derived a strength interaction curve for combined vertical and horizontal bending moments; Dow *et al.*(1981, 1991) studied a British destroyer and a frigate model applying the Smith's method; Faulkner *et al.*(1984) carried out analysis by the same method on a British torpedo-boat-destroyer and Okamoto *et al.*(1985) performed a progressive collapse analysis to assess the strength of a new unidirectional-girder structural system.

To investigate the cause of the casualty of *Energy Concentration*, Rutherford and Caldwell (1990) and Viner (1986) performed a progressive collapse analysis. Similar calculations were performed on *Nakhodka* (JMT, 1997). Yao *et al.*(1993b, 1994) carried out progressive collapse analyses on existing ships, and discussed the influence of thickness reduction due to corrosion on the ultimate hull girder strength. Committee III.1 of ISSC'94 also performed a series of progressive collapse analyses on ten vessels (Jensen *et al.* 1994) and noticed that the initial yielding strength, cannot be a conservative measure of the ultimate hull girder strength especially when a cross-section is subjected to the sagging bending moment.

2.2.2 Finite Element Method (FEM)

Usually, simplified methods are applied for the progressive collapse analysis of a ship's hull under longitudinal bending, and the applications of ordinary FEM are very few. This is because the influences of both material and geometrical nonlinearities have to be considered

in the analysis applying an incremental procedure. A ship's hull girder may be too large for such kind of analysis to get rational results easily. Nevertheless, some results have been reported.

Chen *et al.*(1983) performed static and dynamic FEM analyses modelling a part of the ship hull with plate and beam-column elements. They also used orthotropic plate elements to represent stiffened plates. This reduced the numbers of nodal points and elements. The yielding condition was represented by sectional forces such as axial force, shear force and bending moment. This also reduced the computation time by avoiding numerical integration towards the thickness direction. The computer code, USAS was developed for this analysis. Kutt *et al.*(1985) performed the same analysis also using USAS on two general cargo vessels. They discussed the sensitivities of the ultimate hull girder strength with respect to yield stress, plate thickness and initial imperfection based on the calculated results. Valsgaard *et al.*(1991) applied a nonlinear code FENCOL to analyse the progressive collapse behaviour of the girder models tested by Mansour *et al.*(1990) and *Energy Concentration.*

The results of the FEM analysis to evaluate ultimate hull girder strength are not so many at the moment because the number of elements and nodal points become very huge if rational results are required. However, the Investigation Committee of the Cause of Casualty on *Nakhodka* performed elastoplastic large deflection analysis in an incremental manner with nearly 200,000 elements (JMT 1997) using the computer code LSDYNA-3D. Similar analysis was performed on exsisting handy size tanker, panamax size tanker and VLCC to investigate into the influence of corrosion damage on ultimate hull girder strength (JSRA 2000).

2.2.3 Idealized Structural Unit Method (ISUM)

The Idealized Structural Unit Method (ISUM) is another simple method besides the Smith's method. In this method, a larger structural unit is considered as one element, which reduces the computation time. The essential point of this method is to develop effective and simple element (dynamical model) considering the influences of both buckling and yielding.

Ueda *et al.*(1984) developed plate and stiffened plate elements that accurately simulate buckling/plastic collapse behaviour under combined bi-axial compression/tension and shear loads. In their method, a stiffened plate surrounded by longitudinal girders and transverse frames is considered as one unit (element), and the stiffness matrix in an incremental form is derived for this unit taking account of the influences of buckling and yielding. Paik improved this unit, and performed different progressive collapse analyses (Paik *et al.* 1990a, 1990b, 1992a, 1992b). Ueda and Rashed (1991) also performed a progressive collapse analysis on a double-hull tanker applying their newly improved units. Paik (1994b) tried to introduce the influence of tensile behaviour of elements in ISUM.

Bai *et al.*(1993) developed beam element, plate element and shear element based on the Plastic Node Method (Ueda and Yao 1982) and using these elements he achieved progressive collapse analysis.

In the Smith's method, characteristics of the element are represented by average stress-average strain relationship under uni-axial load. Therefore, accurate results are obtained if only the bending moment is acting. On the other hand, ISUM can be applicable for the case with any combination of compression/tension, bending, shear and torsion loadings. However, sophisticated elements are required to get accurate results. From this point of view, new ISUM elements are still under development.

For instance, Masaoka *et al.*(1998) have developed a new rectangular plate element including all stages of behaviours such as elasto-plastic, buckling and post-buckling, taking into account of initial deflection and residual stress. Fujikubo *et al.*(2000a) developed a new rectangular plate element including the influence of the localisation of plastic deformation in the post-ultimate strength range. It is expected that more accurate and rational progressive collapse analysis can be peformed on ship hull cross-section combining this kind of plate elements with stiffener elements.

3 BENCHMARK CALCULATIONS ON ELEMENT CHARACTERISTICS

3.1 Stiffened Plates for Benchmark Calculations

As shall be demonstrated later in Chapter 4, collapse behaviour of structural members composing a cross-section of a hull girder largely affects the collapse behaviour of the cross-section and its ultimate strength as a whole. From this viewpoint, it is very important to know how accurately the applied method simulates the collapse behaviour and predicts the ultimate strength of individual structural members as stiffened plates.
In this chapter, benchmark calculations are performed on ninety stiffened plates changing the combination of slenderness ratios of the panels and the stiffeners and also changing the type and the size of the stiffener. A continuous stiffened plate is considered with equally spaced stiffeners of the same size. The size of the local panel between stiffeners is taken as:

$$a \text{ x } b = 2{,}400 \text{ x } 800;\quad 4{,}000 \text{ x } 800 \square (\text{mm})$$

and the panel thickness as:

$$t_p = 10;\ 13;\ 15;\ 20;\ 25 \square (\text{mm})$$

Three types of stiffeners are considered, which are a flat-bar, an angle-bar and a tee-bar. For each type, three sizes are assumed as indicated in Table 3.1.

TABLE 3.1
DIMENSIONS OF STIFFENERS

type	size 1	size 2	size 3
at-bar $(h \times t_w)$	150×17	250×19	350×35
angle-bar $(h \times b_f \times t_w/t_f)$	$150 \times 90 \times 9/12$	$250 \times 90 \times 10/15$	$400 \times 100 \times 12/17$
tee-bar $(h \times t_w + b_0 \times t_f)$	$138 \times 9 + 90 \times 12$	$235 \times 10 + 90 \times 15$	$383 \times 12 + 100 \times 17$

(in mm)

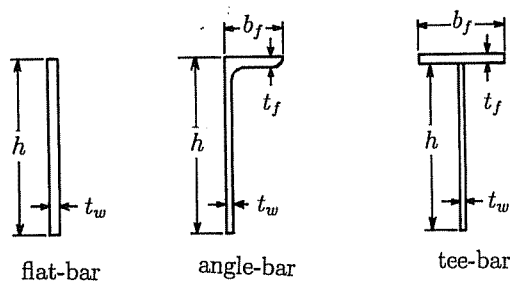

flat-bar angle-bar tee-bar

flat-bar h x t
angle-bar h x b x t_w/t_f
tee-bar: h x $t_w + b$ x t_f

In each case, initial deflection of the following mode is prescribed, see Figures 3.1 (a) and (b).

plate:

$$w_{0p} = A_0 \sin \frac{m\pi x}{a} \sin \frac{\pi y}{b} + B_0 \sin \frac{\pi x}{a} \tag{3.1}$$

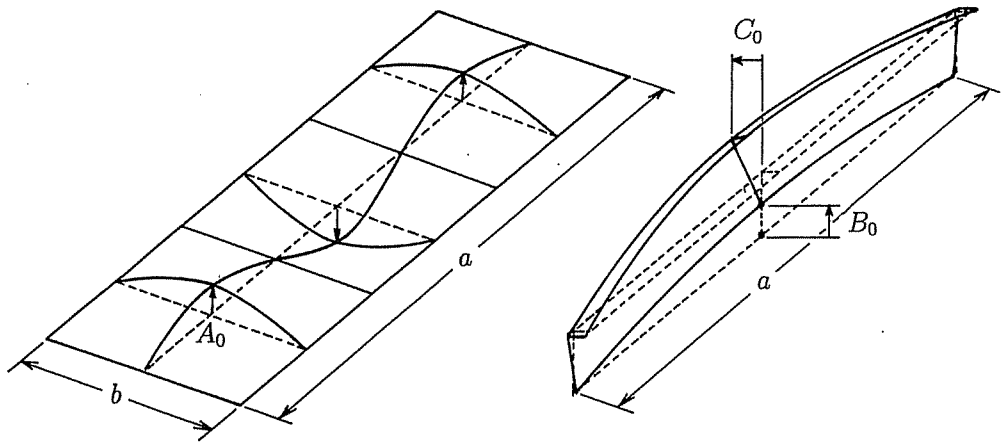

Figure 3.1: Assumed initial deflections in stiffened plates

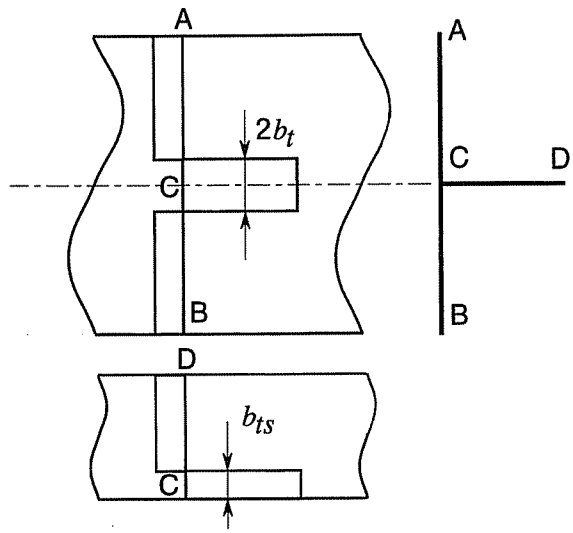

Figure 3.2: Assumed welding residual stresses

stiffener(span length = a):

$$w_{0s} = B_0 \sin\frac{\pi x}{a}, \qquad v_{0s} = C_0 \sin\frac{\pi x}{a} \tag{3.2}$$

where m is taken as 3 and 5 for the panels with a/b ratios of 3.0 and 5.0, respectively. The magnitudes of initial deflection are taken as:

$$A_0 = 0.01 \times t_p; \quad B_0 = 0.001 \times a; \quad C_0 = 0.001 \times a \tag{3.3}$$

Two cases are analysed, which are with and without welding residual stress of a rectangular distribution shown in Figure 3.2. The magnitude of compressive residual stress is evaluated as:

$$\sigma_{cp} = \frac{2b_t}{b-2b_t}\sigma_{Yp}, \qquad \sigma_{cs} = \frac{2b_s}{b-2b_s}\sigma_{Ys} \tag{3.4}$$

or

$$\sigma_{cp} = \sigma_{cs} = \frac{2b_t t_p \sigma_{Yp} + b_s t_w \sigma_{Ys}}{(b-2b_t)t_p + A_s - b_s t_w} \tag{3.5}$$

where

$$\left.\begin{array}{ll} b_t = t_w/2 + 0.26\Delta Q/(t_w + 2t_p) & (\text{mm}) \\ b_s = (t_w/t_p) \times (b_t - t_w/2) & (\text{mm}) \end{array}\right\} \tag{3.6}$$

$$\Delta Q = 78.8\ell^2 \tag{3.7}$$

$$\ell = \begin{cases} 0.7 \times t_w \ (\text{mm}) & (\text{when } 0.7 \times t_w < 7.0\text{mm}) \\ 7.0 \ (\text{mm}) & (\text{when } 0.7 \times t_w \geq 7.0\text{mm}) \end{cases} \tag{3.8}$$

σ_{Yp} and σ_{Ys} in Eqns. 3.4 and 3.5 are the yield stress of the plate and the stiffener, respectively, and are taken as 313.6 MPa. Eqn. 3.4 represents the case when self-equilibrium condition of welding residual stress is considered in the panel and the stiffener independently, whereas Eqn. 3.5 is the case when it is totally considered. Young's modulus of the material is taken as 205.8 GPa.

The stiffened plates are denoted as X *i j k l m* Y, indicating that:

X: = F: flat-bar;□ = A: angle-bar; □= T: tee-bar *i*: aspect ratio (*a/b*)

lm: = 15: size 1; = 25: size 2; = 35: size3 *jk*: plate thickness

Y: = n: no WRS(welding residual stress); = y: with WRS

For example, A51325y represents a stiffened plate of which aspect ratio and thickness of the local panel are 5 and 13 mm, respectively, the stiffener is an angle-bar of the size 2 and is accompanied by welding residual stress.

3.2 Applied Methods of Analyses

Benchmark calculations were performed applying twelve different methods. The methods are characterised by the following items:

(a) methods of analysis:
a1: analytical method;□a2: empirical formulae;□a3: FEM;□a4: ISUM

(b) modelling:
b1: beam-column (stiffener with attached plate);□b2: panel and stiffener, separately;
b3: stiffened plate

(c) number of spans for analysis:
c1: single span model;□c2: double span model;□c3: triple span model

(d) dynamical characteristics:
d1: average stress-average strain relationship;□
d2: nodal force-nodal displacement relationships;
d3: empirical formulae to evaluate ultimate strength;
d4: analytical buckling strength

(e) reduction in capacity after ultimate strength (load shedding effect):
e1: not considered;□e2: considered

(f) load combinations:
f1: not considered;□f2: lateral pressure;□f3: transverse thrust

(g) initial deflection in panels:
g1: not considered;□g2: buckling mode;□g3: any mode including hungry-horse mode

(h) initial deflection in stiffeners:
h1: not considered;□h2: flexural buckling mode;□h3: flexural-torsional buckling mode;
h4: any mode

(i) welding residual stresses:
i1: not considered;□i2: considered only in panel;
i3: considered both in panel and stiffener

(j) tripping of stiffeners:
j1: not able to deal with;□j2: able

(k) plate induced failure:
k1: not able to deal with; □k2: able
(l) stiffener induced failure:
l1: not able to deal with; □l2: able

The characteristics of individual methods for the above items are summarised in Table 3.2.

TABLE 3.2
CHARACTERISTICS OF APPLIED METHODS

methods	(a)	(b)	(c)	(d)	(e)	(f)	(g)	(h)	(i)	(j)	(k)	(ℓ)
Astrup(1)	a1	b3	c1	d4	e2	f3	g1	h2	i1	j2	k2	ℓ2
Astrup(2)	a3	b2	c2	d2	e1	f2/3	g3	h3	i2	j2	k2	ℓ2
Chen	a4	b3	c1	d2	e1	f3	g1	h1	i1	j1	k2	ℓ2
Cho	a2	b1	c1	d1/4	e1	f1	g1	h1	i1	j1	k1	ℓ1
Masaoka	a4	b2	c1	d2	e2	f3	g2	h1	i2	j1	k2	ℓ1
Rigo(1)	a1	b1	c1	d1/4	e2	f1	g1	h1	i1	j1	k2	ℓ2
Rigo(2)	a2	b1	c1	d3	e2	f1	g1	h1	i1	j1	k1	ℓ2
Soares	a1	b1	c1	d1	e2	f1	g2	h2	i2	j1	k2	ℓ2
Yao(1)	a1	b1	c2	d1	e2	f1	g2	h3	i2	j2	k2	ℓ2
Yao(2)	a1	b1	c2	d4	e1	f1	g2	h3	i2	j2	k2	ℓ2
Yao(3)	a3	b2	c2/3	d2	e2	f2/3	g3	h3	i2	j2	k2	ℓ2

Astrup(1) is based on a beam-column approach, and a Shanley's model is used (Steen 1999). Astrup (2) and Yao (3) are elastoplastic large deflection FEM analyses applying ABAQUS and ULSAS, respectively. Cho used NASTRAN for non-linear analysis on stiffened plates with small initial deflection and no welding residual stress, while used empirical formulae for stiffened plates with large initial deflection and welding residual stress (Cho *et al* .1998b). Masaoka used plate ISUM elements both for panels and stiffeners (Ueda and Masaoka 1993, 1995). Buckling collapse as a stiffened plate is not considered in his approach. Rigo (1) is based on Rahman-Hughes's model (Hughes 1988), and Perry-Robertson formula was applied. Rigo (2) is based on a model developed by Paik and Mansour (1995).
Soare's method is based on a beam-column approach considering the load-shedding according to the slenderness of the panel and the stiffener (Gordo and Guedes Soares 1993). Yao (1) is also based on a beam-column approach, and the average stress-average strain relationship is derived considering the influence of buckling and yielding of panels between stiffeners (Yao and Nikolov 1991, 1992). This method is explained in *2.2.1* in more detail. Yao (2) is a new simplified method (Fujikubo *et al.* 1999a, 1999b) improving the Carlsen's model (Carlsen 1980). In Yao's method, interaction between panel and stiffener web is considered when local buckling strength of a panel is evaluated (Fujikubo and Yao 2000b).

3.3 Calculated Results and Discussions

The results of benchmark calculations are summarised in Tables 3.3 through 3.8, where the ultimate strength made non-dimensional by the yield stress is indicated.
The parameters, β and λ, are the slenderness ratios of the panel and the stiffener with attached plating, respectively, and are given as:

$$\beta = b/t_p \cdot \sqrt{\sigma_{Yp}/E}, \quad \lambda = \sqrt{\sigma_{Ys}/\sigma_E} \tag{3.9}$$

where E and σ_E are Young's modulus and elastic buckling strength of the stiffener with attached plating.

TABLE 3.3
COMPRESSIVE ULTIMATE STRENGTH OF STIFFENED PLATES
(a/b = 3.0; WITH FLAT-BAR STIFFENERS)

No.	Astrup(1)	Astrup(2)	Cho	Masaoka	Rigo(1)	Rigo(2)	Soares	Yao(1)	Yao(2)	Yao(3)	β	λ
F31015n	0.562	0.649	0.687	0.739	0.613	-	0.472	0.679	0.643	0.670	3.123	0.738
F31315n	0.637	0.691	0.682	0.741	0.676	-	0.593	0.741	0.667	0.720	2.402	0.788
F31515n	0.700	0.656	696	0.885	0.723	-	0.651	0.808	0.678	0.702	2.082	0.818
F32015n	0.568	0.589	0.659	0.999	0.804	-	0.708	0.861	0.623	0.653	1.561	0.882
F32515n	0.502	0.537	0.600	0.999	0.804	-	0.730	0.805	0.582	0.613	1.249	0.931
F31025n	0.861	0.725	0.762	0.769	0.654	-	0.658	0.721	0.725	0.747	3.123	0.583
F31325n	0.846	0.844	0.781	0.821	0.719	-	0.698	0.804	0.783	0.830	2.402	0.462
F31525n	0.845	0.927	0.811	0.891	0.771	-	0.749	0.878	0.824	0.914	2.082	0.419
F32025n	0.834	0.937	0.930	0.999	0.882	-	0.839	0.954	0.869	0.944	1.561	0.448
F32525n	0.814	0.925	1.024	0.999	0.918	-	0.918	0.953	0.850	0.939	1.249	0.473
F31035n	0.888	0.828	0.893	0.810	0.701	-	0.424	0.830	0.841	0.847	3.123	0.586
F31335n	0.887	0.933	0.920	0.848	0.752	-	0.654	0.865	0.899	0.922	2.402	0.556
F31535n	0.864	0.975	0.946	0.905	0.797	-	0.746	0.906	0.926	0.964	2.082	0.530
F32035n	0.868	0.979	1.008	0.999	0.898	-	0.848	0.971	0.947	0.973	1.561	0.454
F32535n	0.869	0.979	1.060	0.999	0.932	-	0.928	0.970	0.942	0.973	1.249	0.380
F31015y	-	-	0.638	0.739	0.455	0.494	0.536	0.638	0.513	0.544	3.123	0.738
F31315y	-	-	0.663	0.770	0.570	0.561	0.615	0.666	0.585	0.636	2.402	0.788
F31515y	-	-	0.679	0.832	0.636	0.592	0.647	0.719	0.619	0.642	2.082	0.818
F32015y	-	-	0.721	0.993	0.746	0.641	0.702	0.832	0.583	0.612	1.561	0.882
F32515y	-	-	0.762	0.999	0.762	0.665	0.721	0.806	0.551	0.583	1.249	0.931
F31025y	-	-	0.740	0.769	0.502	0.573	0.644	0.728	0.590	0.621	3.123	0.583
F31325y	-	-	0.752	0.782	0.612	0.660	0.717	0.746	0.690	0.725	2.402	0.462
F31525y	-	-	0.761	0.833	0.682	0.703	0.768	0.790	0.750	0.819	2.082	0.419
F32025y	-	-	0.785	0.993	0.813	0.772	0.835	0.917	0.801	0.875	1.561	0.448
F32525y	-	-	0.807	0.999	0.859	0.810	0.893	0.920	0.792-	0.880	1.249	0.473
F31035y	-	-	0.802	0.809	0.511	0.597	0.475	0.803	0.677	0.777	3.123	0.586
F31335y	-	-	0.795	0.813	0.626	0.691	0.714	0.841	0.795	0.809	2.402	0.556
F31535y	-	-	0.792	0.855	0.693	0.738	0.768	0.858	0.844	0.860	2.082	0.530
F32035y	-	-	0.796	0.994	0.820	0.817	0.858	0.943	0.860	0.965	1.561	0.454
F32535y	-	-	0.806	0.999	0.865	0.862	0.909	0.961	0.865	0.966	1.249	0.380

TABLE 3.4
COMPRESSIVE ULTIMATE STRENGTH OF STIFFENED PLATES
(a/b = 5.0; WITH FLAT-BAR STIFFENERS)

No.	Astrup(1)	Cho	Masaoka	Rigo(1)	Rigo(2)	Soares	Yao(1)	Yao(2)	Yao(3)	β	λ
F51015n	0.431	0.513	0.739	0.493	-	0.424	0.502	0.453	0.465	3.123	1.230
F51315n	0.406	0.419	0.803	0.482	-	0.434	0.479	0.417	0.427	2.402	1.314
F51515n	0.371	0.425	0.855	0.469	-	0.430	0.444	0.390	0.404	2.082	1.364
F52015n	0.303	0.290	0.999	0.427	-	0.398	0.379	0.339	0.352	1.561	1.470
F52515n	0.264	0.284	0.999	0.388	-	0.360	0.337	0.306	0.318	1.249	1.552
F51025n	0.809	0.730	0.770	0.637	-	0.504	0.692	0.688	0.704	3.123	0.647
F51325n	0.807	0.769	0.820	0.699	-	0.647	0.776	0.728	0.803	2.402	0.678
F51525n	0.774	0.797	0.982	0.748	-	0.702	0.844	0.764	0.820	2.082	0.699
F52025n	0.736	0.837	0.999	0.847	-	0.797	0.900	0.740	0.781	1.561	0.746
F52525n	0.715	0.790	0.999	0.871	-	0.839	0.891	0.703	0.744	1.249	0.789
F51035n	0.847	0.888	0.811	0.690	-	0.517	0.809	0.814	0.822	3.123	0.548
F51335n	0.849	0.919	0.847	0.740	-	0.641	0.854	0.874	0.911	2.402	0.483
F51535n	0.852	0.959	0.905	0.785	-	0.702	0.892	0.901	0.945	2.082	0.437
F52035n	0.831	1.032	0.999	0.884	-	0.816	0.950	0.905	0.947	1.561	0.438
F52535n	0.821	1.051	0.999	0.918	-	0.902	0.950	0.895	0.944	1.249	0.450
F51015y	-	0.558	0.739	0.407	0.389	0.437	0.496	0.381	0.402	3.123	1.230
F51315y	-	0.629	0.770	0.452	0.438	0.453	0.478	0.393	0.402	2.402	1.314
F51515y	-	0.676	0.832	0.453	0.461	0.453	0.444	0.372	0.384	2.082	1.364

TABLE 3.4
COMPRESSIVE ULTIMATE STRENGTH OF STIFFENED PLATES
(a/b = 5.0; WITH FLAT-BAR STIFFENERS; continued)

No.	Astrup(1)	Cho	Masaoka	Rigo(1)	Rigo(2)	Soares	Yao(1)	Yao(2)	Yao(3)	β	λ
F52015y	-	0.777	0.993	0.422	0.496	0.421	0.379	0.328	0.340	1.561	1.470
F52515y	-	0.849	0.999	0.385	0.513	0.379	0.337	0.298	0.309	1.249	1.552
F51025y	-	0.684	0.770	0.491	0.515	0.568	0.648	0.564	0.578	3.123	0.647
F51325y	-	0.726	0.782	0.598	0.591	0.679	0.711	0.646	0.705	2.402	0.679
F51525y	-	0.752	0.833	0.663	0.626	0.721	0.757	0.700	0.748	2.082	0.639
F52025y	-	0.809	0.993	0.784	0.682	0.788	0.868	0.689	0.730	1.561	0.746
F52525y	-	0.855	0.999	0.819	0.710	0.820	0.864	0.662	0.704	1.249	0.789
F51035y	-	0.770	0.810	0.504	0.567	0.542	0.773	0.655	0.704	3.123	0.548
F51335y	-	0.790	0.813	0.617	0.656	0.692	0.824	0.773	0.791	2.402	0.483
F51535y	-	0.803	0.855	0.683	0.701	0.746	0.837	0.811	0.843	2.082	0.437
F52035y	-	0.832	0.994	0.808	0.775	0.832	0.922	0.823	0.867	1.561	0.438
F52535y	-	0.858	0.999	0.852	0.816	0.886	0.921	0.823	0.873	1.249	0.450

TABLE 3.5
COMPRESSIVE ULTIMATE STRENGTH OF STIFFENED PLATES
(a/b = 3.0; WITH ANGLE-BAR STIFFENERS)

No.	Astrup(1)	Cho	Rigo(1)	Rigo(2)	Soares	Yao(1)	Yao(2)	Yao(3)	β	λ
A31015n	0.734	0.730	0.618	-	0.558	0.645	0.651	0.668	3.123	0.569
A31315n	0.782	0.758	0.690	-	0.663	0.771	0.734	0.758	2.402	0.602
A31515n	0.746	0.766	0.744	-	0.714	0.851	0.763	0.779	2.082	0.626
A32015n	0.714	0.788	0.851	-	0.797	0.919	0.732	0.739	1.561	0.679
A32515n	0.661	0.747	0.875	-	0.848	0.912	0.691	0.701	1.249	0.724
A31025n	0.770	0.768	0.644	-	0.548	0.659	0.697	0.705	3.123	0.563
A31325n	0.858	0.807	0.715	-	0.682	0.789	0.800	0.808	2.402	0.460
A31525n	0.845	0.839	0.771	-	0.739	0.874	0.842	0.895	2.082	0.405
A32025n	0.835	0.938	0.887	-	0.864	0.961	0.894	0.947	1.561	0.382
A32525n	0.815	1.029	0.924	-	0.925	0.960	0.877	0.944	1.249	0.404
A31040n	0.838	0.788	0.672	-	0.395	0.683	0.694	0.723	3.123	0.652
A31340n	0.884	0.826	0.735	-	0.603	0.748	0.790	0.823	2.402	0.592
A31540n	0.875	0.856	0.787	-	0.717	0.885	0.860	0.899	2.082	0.548
A32040n	0.870	0.946	0.898	-	0.839	0.966	0.923	0.959	1.561	0.440
A32540n	0.871	1.043	0.936	-	0.937	0.970	0.935	0.964	1.249	0.351
A31015y	-	0.704	0.527	0.530	0.593	0.585	0.569	0.596	3.123	0.569
A31315y	-	0.719	0.620	0.604	0.666	0.695	0.676	0.693	2.402	0.602
A31515y	-	0.730	0.683	0.638	0.705	0.755	0.716	0.730	2.082	0.626
A32015y	-	0.758	0.804	0.692	0.784	0.883	0.695	0.704	1.561	0.679
A32515y	-	0.787	0.836	0.719	0.829	0.883	0.662	0.674	1.249	0.724
A31025y	-	0.777	0.538	0.584	0.622	0.604	0.603	0.620	3.123	0.563
A31325y	-	0.779	0.633	0.673	0.717	0.725	0.727	0.733	2.402	0.460
A31525y	-	0.784	0.698	0.716	0.756	0.790	0.781	0.822	2.082	0.405
A32025y	-	0.800	0.829	0.787	0.842	0.922	0.838	0.891	1.561	0.382
A32525y	-	0.817	0.874	0.826	0.902	0.934	0.828	0.896	1.249	0.404
A31040y	-	0.799	0.574	0.604	0.456	0.634	0.618	0.650	3.123	0.652
A31340y	-	0.789	0.660	0.699	0.682	0.671	0.728	0.753	2.402	0.592
A31540y	-	0.788	0.721	0.745	0.753	0.790	0.805	0.832	2.082	0.548
A32040y	-	0.796	0.845	0.824	0.855	0.928	0.876	0.906	1.561	0.440
A32540y	-	0.809	0.888	0.869	0.918	0.960	0.885	0.918	1.249	0.351

Representative results are plotted against the slenderness ratio of the local panel, β for each group of stiffener type and size in Figures 3.3 (a), (b) and (c).

For the case of stiffened plate with flat-bar stiffeners of which local panel is 2,400x800 mm, FEM analyses are performed using two codes, ULSAS and ABAQUS, and the evaluated ultimate strength is plotted in Figure 3.3 (a) by solid and broken lines. It is known that both results show good correlations, which indicates that the result of FEM analyses could be an appropriate measure of the ultimate strength. For some of these cases, the average stress-average strain relationships are compared in

TABLE 3.6
COMPRESSIVE ULTIMATE STRENGTH OF STIFFENED PLATES
(a/b = 5.0; WITH ANGLE-BAR STIFFENERS)

No.	Astrup(1)	Cho	Rigo(1)	Rigo(2)	Soares	Yao(1)	Yao(2)	Yao(3)	β	λ
A51015n	0.641	0.623	0.575	-	0.533	0.585	0.558	0.559	3.123	0.929
A51315n	0.588	0.616	0.617	-	0.577	0.641	0.568	0.570	2.402	0.997
A51515n	0.544	0.604	0.636	-	0.603	0.667	0.534	0.539	2.082	1/039
A52015n	0.476	0.527	0.618	-	0.635	0.576	0.469	0.475	1.561	1.130
A52515n	0.420	0.453	0.564	-	0.635	0.504	0.421	0.427	1.249	1.205
A51025n	0.758	0.749	0.633	-	0.587	0.693	0.699	0.685	3.123	0.543
A51325n	0.785	0.788	0.702	-	0.669	0.736	0.752	0.762	2.402	0.565
A51525n	0.777	0.823	0.756	-	0.708	0.843	0.792	0.845	2.082	0.584
A52025n	0.740	0.884	0.866	-	0.816	0.925	0.797	0.813	1.561	0.630
A52525n	0.718	0.854	0.897	-	0.864	0.920	0.762	0.778	1.249	0.671
A51035n	0.830	0.789	0.665	-	0.488	0.703	0.723	0.736	3.123	0.701
A51340n	0.865	0.836	0.728	-	0.660	0.762	0.802	0.796	2.402	0.542
A51540n	0.862	0.868	0.780	-	0.714	0.864	0.848	0.885	2.082	0.461
A52040n	0.857	0.967	0.890	-	0.823	0.955	0.914	0.948	1.561	0.368
A52540n	0.839	1.056	0.927	-	0.918	0.953	0.904	0.946	1.249	0.384
A51015y	-	0.612	0.499	0.439	0.536	0.547	0.500	0.496	3.123	0.929
A51315y	-	0.670	0.568	0.495	0.580	0.576	0.541	0.544	2.402	0.997
A51515y	-	0.708	0.601	0.520	0.606	0.625	0.513	0.518	2.082	1.039
A52015y	-	0.791	0.606	0.558	0.638	0.576	0.455	0.461	1.561	1.130
A52515y	-	0.851	0.558	0.574	0.638	0.504	0.411	0.417	1.249	1.205
A51025y	-	0.727	0.530	0.538	0.625	0.648	0.606	0.596	3.123	0.543
A51325y	-	0.760	0.623	0.617	0.686	0.679	0.684	0.705	2.402	0.565
A51525y	-	0.780	0.686	0.653	0.721	0.747	0.737	0.783	2.082	0.584
A52025y	-	0.826	0.810	0.711	0.800	0.890	0.749	0.768	1.561	0.630
A52525y	-	0.863	0.850	0.740	0.842	0.888	0.723	0.741	1.249	0.671
A51040y	-	0.785	0.568	0.584	0.520	0.662	0.647	0.673	3.123	0.701
A51340y	-	0.805	0.654	0.675	0.689	0.730	0.738	0.749	2.402	0.542
A51540y	-	0.818	0.714	0.719	0.743	0.794	0.794	0.835	2.082	0.461
A52040y	-	0.847	0.837	0.792	0.842	0.919	0.862	0.893	1.561	0.368
A52540y	-	0.870	0.880	0.833	0.902	0.919	0.856	0.898	1.249	0.384

TABLE 3.7
COMPRESSIVE ULTIMATE STRENGTH OF STIFFENED PLATES
(a/b = 3.0; WITH TEE-BAR STIFFENERS)

No.	Astrup(1)	Cho	Rigo(1)	Rigo(2)	Soares	Yao(1)	Yao(2)	Yao(3)	β	λ
T31015n	0.673	0.717	0.618	-	0.548	0.645	0.649	0.649	3.123	0.556
T31315n	0.748	0.740	0.690	-	0.660	0.760	0.735	0.762	2.402	0.598
T31515n	0.757	0.746	0.744	-	0.702	0.841	0.769	0.802	2.082	0.623
T32015n	0.705	0.754	0.851	-	0.781	0.919	0.754	0.761	1.561	0.678
T32515n	0.660	0.706	0.875	-	0.826	0.912	0.715	0.723	1.249	0.723
T31025n	0.765	0.755	0.644	-	0.558	0.688	0.676	0.703	3.123	0.628
T31325n	0.846	0.796	0.715	-	0.688	0.789	0.788	0.806	2.402	0.484
T31525n	0.842	0.829	0.771	-	0.737	0.869	0.833	0.895	2.082	0.410
T32025n	0.828	0.930	0.887	-	0.861	0.961	0.893	0.957	1.561	0.377
T32525n	0.814	1.032	0.924	-	0.922	0.960	0.881	0.955	1.249	0.403
T31040n	0.779	0.757	0.672	-	0.408	0.730	0.606	0.719	3.123	0.840
T31340n	0.880	0.808	0.735	-	0.635	0.760	0.746	0.813	2.402	0.723
T31540n	0.872	0.842	0.787	-	0.727	0.887	0.813	0.905	2.082	0.645
T32040n	0.886	0.923	0.898	-	0.848	0.971	0.908	0.965	1.561	0.483
T32540n	0.868	1.020	0.936	-	0.937	0.970	0.924	0.970	1.249	0.370
T31015y	-	0.675	0.527	0.530	0.590	0.584	0.567	0.603	3.123	0.556
T31315y	-	0.695	0.620	0.604	0.654	0.687	0.676	0.679	2.402	0.598
T31515y	-	0.709	0.683	0.638	0.695	0.744	0.721	0.753	2.082	0.623
T32015y	-	0.744	0.804	0.692	0.768	0.883	0.716	0.724	1.561	0.678
T32515y	-	0.777	0.836	0.719	0.810	0.883	0.685	0.694	1.249	0.723

TABLE 3.7
COMPRESSIVE ULTIMATE STRENGTH OF STIFFENED PLATES
(a/b = 3.0; WITH TEE-BAR STIFFENERS; continued)

No.	Astrup(1)	Cho	Rigo(1)	Rigo(2)	Soares	Yao(1)	Yao(2)	Yao(3)	β	λ
T31025y	-	0.745	0.538	0.584	0.622	0.638	0.585	0.642	3.123	0.628
T31325y	-	0.758	0.633	0.673	0.711	0.735	0.716	0.733	2.402	0.484
T31525y	-	0.768	0.698	0.716	0.753	0.788	0.773	0.822	2.082	0.410
T32025y	-	0.791	0.829	0.787	0.842	0.922	0.836	0.901	1.561	0.377
T32525y	-	0.812	0.874	0.826	0.896	0.935	0.832	0.905	1.249	0.403
T31040y	-	0.747	0.574	0.604	0.472	0.690	0.548	0.650	3.123	0.840
T31340y	-	0.754	0.660	0.699	0.692	0.729	0.692	0.742	2.402	0.723
T31540y	-	0.762	0.721	0.745	0.756	0.815	0.763	0.839	2.082	0.645
T32040y	-	0.784	0.845	0.824	0.855	0.935	0.855	0.910	1.561	0.483
T32540y	-	0.804	0.888	0.869	0.922	0.961	0.875	0.921	1.249	0.370

TABLE 3.8
COMPRESSIVE ULTIMATE STRENGTH OF STIFFENED PLATES
(a/b = 5.0; WITH TEE-BAR STIFFENERS)

No.	Astrup(1)	Cho	Rigo(1)	Rigo(2)	Masaoka	Yao(1)	Yao(2)	Yao(3)	β	λ
T51015n	0.599	0.580	0.575	-	0.510	0.592	0.570	0.572	3.123	0.927
T51315n	0.618	0.565	0.617	-	0.552	0.653	0.588	0.590	2.402	0.996
T51515n	0.566	0.549	0.636	-	0.571	0.673	0.554	0.558	2.082	1.038
T52015n	0.475	0.471	0.618	-	0.589	0.576	0.486	0.491	1.561	1.130
T52515n	0.421	0.328	0.564	-	0.574	0.504	0.436	0.442	1.249	1.205
T51025n	0.770	0.738	0.633	-	0.584	0.695	0.692	0.685	3.123	0.530
T51325n	0.787	0.774	0.702	-	0.660	0.734	0.752	0.764	2.402	0.561
T51525n	0.788	0.802	0.756	-	0.714	0.851	0.800	0.854	2.082	0.582
T52025n	0.748	0.862	0.866	-	0.804	0.926	0.806	0.825	1.561	0.629
T52525n	0.715	0.825	0.897	-	0.848	0.920	0.773	0.791	1.249	0.671
T51040n	0.772	0.787	0.665	-	0.517	0.735	0.688	0.743	3.123	0.761
T51340n	0.842	0.821	0.728	-	0.663	0.765	0.794	0.802	2.402	0.565
T51540n	0.853	0.843	0.780	-	0.714	0.861	0.843	0.887	2.082	0.472
T52040n	0.837	0.956	0.890	-	0.819	0.955	0.911	0.950	1.561	0.363
T52540n	0.832	1.046	0.927	-	0.915	0.953	0.904	0.949	1.249	0.383
T51015y	-	0.588	0.499	0.439	0.513	0.545	0.510	0.511	3.123	0.927
T51315y	-	0.652	0.568	0.495	0.555	0.603	0.554	0.560	2.402	0.996
T51515y	-	0.694	0.601	0.520	0.577	0.627	0.533	0.535	2.082	1.038
T52015y	-	0.785	0.606	0.558	0.599	0.576	0.472	0.476	1.561	1.130
T52515y	-	0.849	0.558	0.574	0.583	0.504	0.426	0.432	1.249	1.205
T51025y	-	0.712	0.530	0.538	0.615	0.647	0.600	0.597	3.123	0.530
T51325y	-	0.748	0.623	0.617	0.679	0.678	0.684	0.704	2.402	0.561
T51525y	-	0.771	0.686	0.653	0.714	0.762	0.743	0.790	2.082	0.582
T52025y	-	0.821	0.810	0.711	0.791	0.890	0.759	0.778	1.561	0.629
T52525y	-	0.861	0.850	0.740	0.832	0.888	0.734	0.753	1.249	0.671
T51040y	-	0.772	0.568	0.584	0.552	0.698	0.618	0.666	3.123	0.761
T51340y	-	0.798	0.654	0.675	0.702	0.729	0.730	0.753	2.402	0.565
T51540y	-	0.813	0.714	0.719	0.740	0.794	0.789	0.838	2.082	0.472
T52040y	-	0.844	0.837	0.792	0.839	0.919	0.857	0.894	1.561	0.363
T52540y	-	0.869	0.880	0.833	0.902	0.919	0.856	0.899	1.249	0.383

Figure 3.4 together with those by the simplified method (Yao(1)) used in HULLST for progressive collapse analysis of a hull girder. It can be seen that relatively good correlations exist in the calculated results by different methods.

In Figure 3.3, some scatters are seen in the ultimate strength calculated by simplified methods. The difference may be attributed to the difference between the collapse mode assumed in a simplified method and that simulated by the FEM. Two typical collapse modes by the FEM are shown in Figures 3.5 (a) and (b). In both cases, Euler buckling as a column takes place, and the yielded zone is concentrated at the mid-span part. However, in F31025n, Euler buckling is accompanied by tripping of

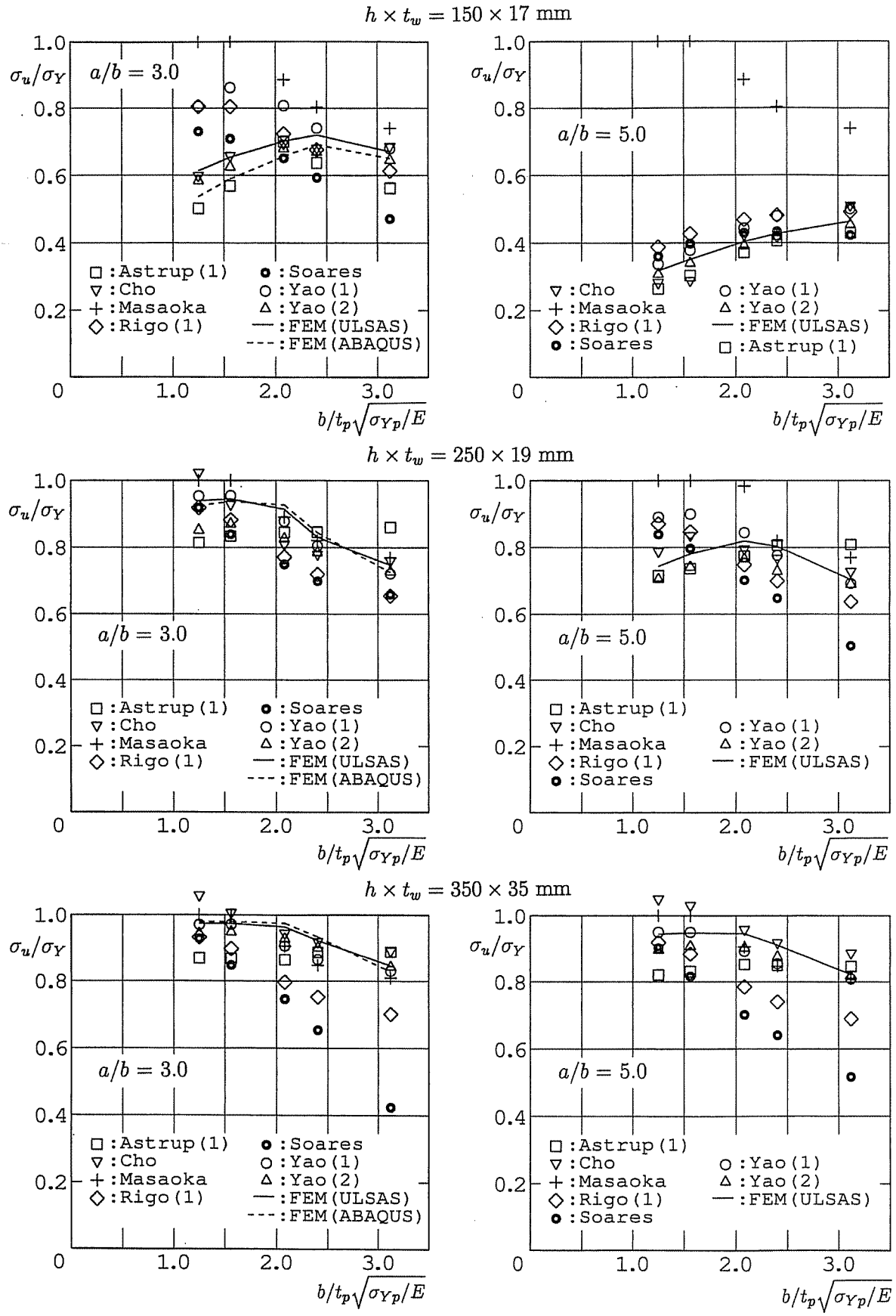

(a) Stiffened panel with flat-bar stiffener (no welding residual stress)

Figure 3.3: Compressive ultimate strength of stiffened plate plotted against slenderness ratio of panel

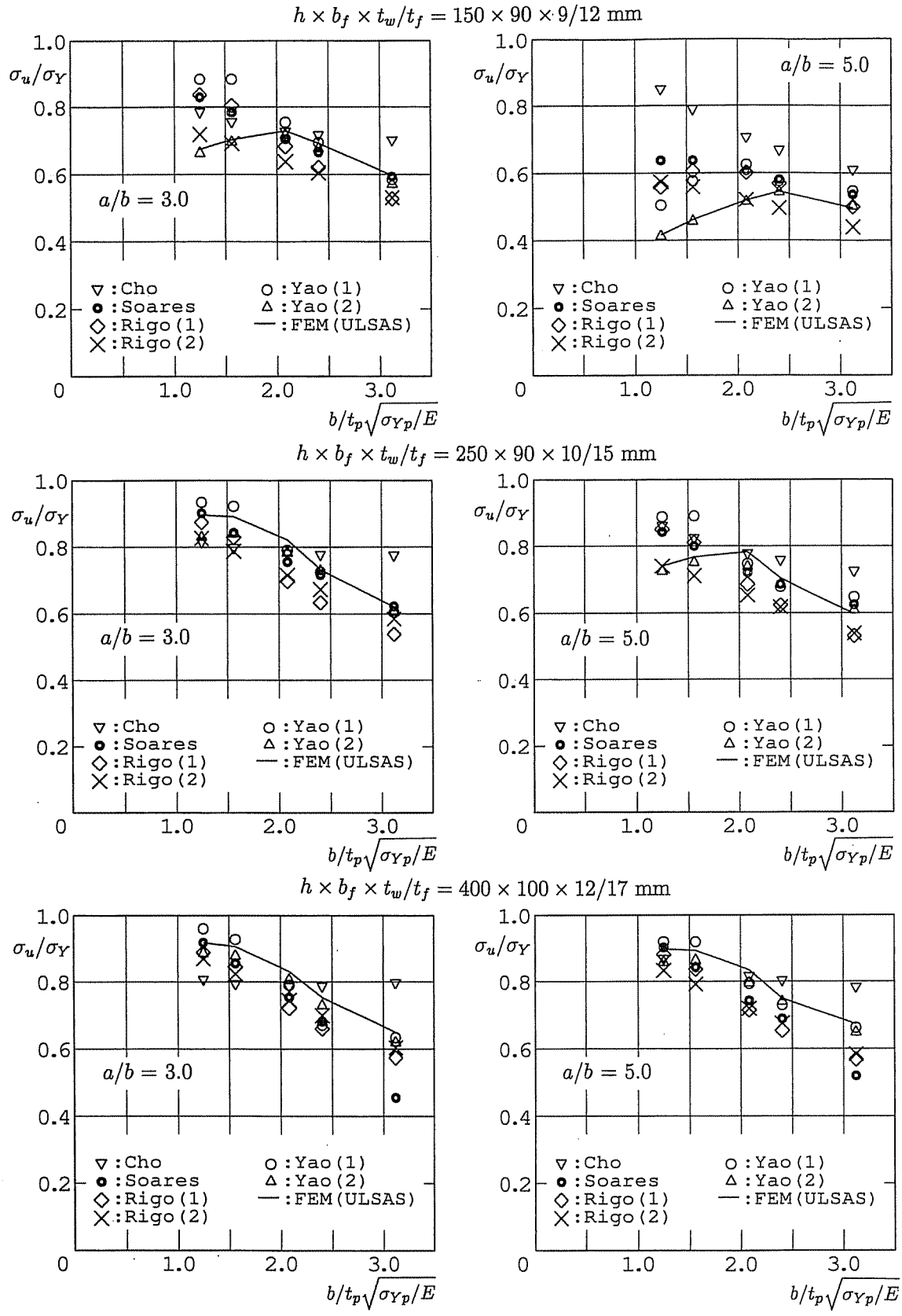

(b) Stiffened panel with angle-bar stiffener (with welding residual stress)

Figure 3.3:□Compressive ultimate strength of stiffened plate plotted against slenderness ratio of panel (continued)

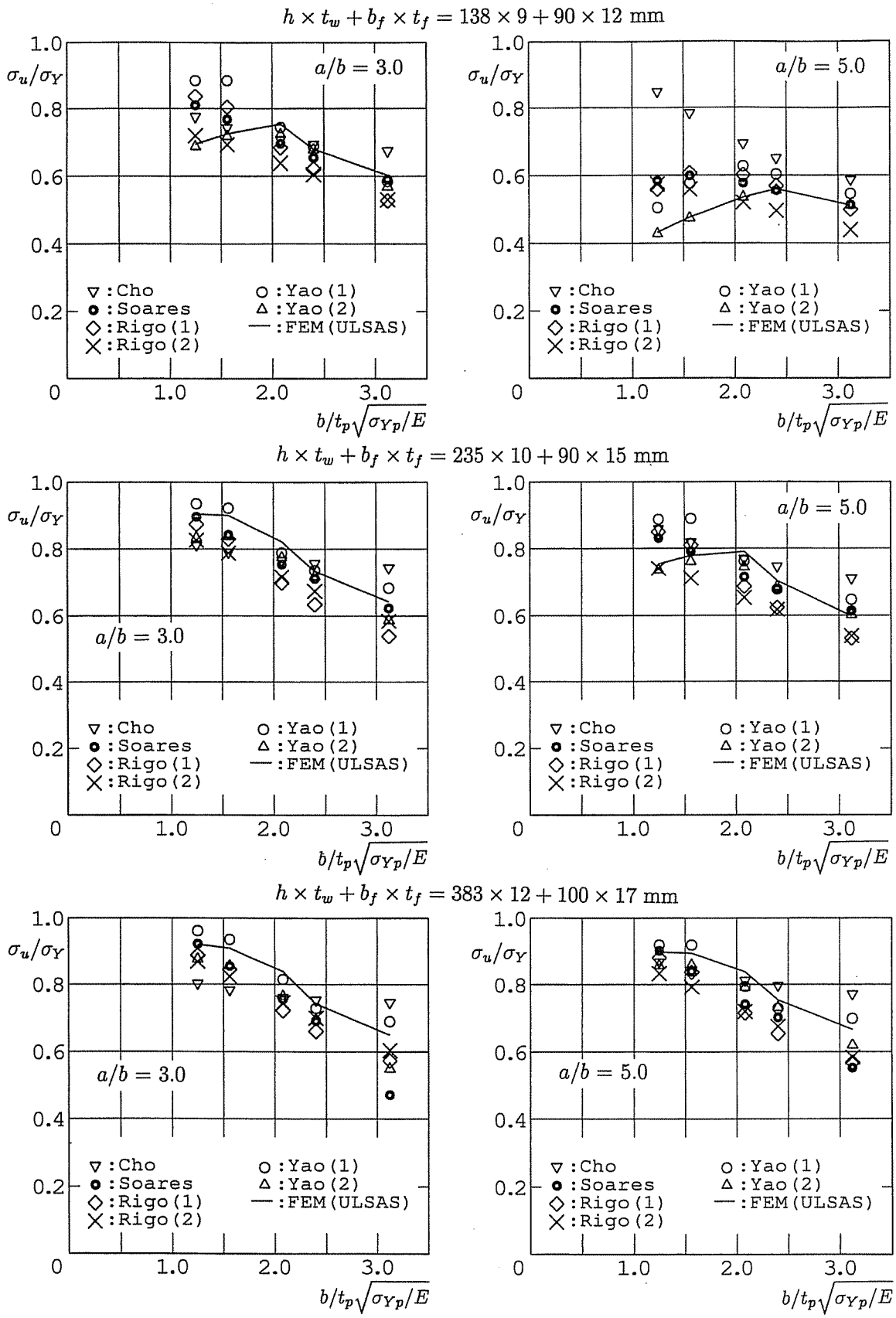

(c) Stiffened panel with tee-bar stiffener (with welding residual stress)

Figure 3.3: Compressive ultimate strength of stiffened plate plotted against slenderness ratio of panel (continued)

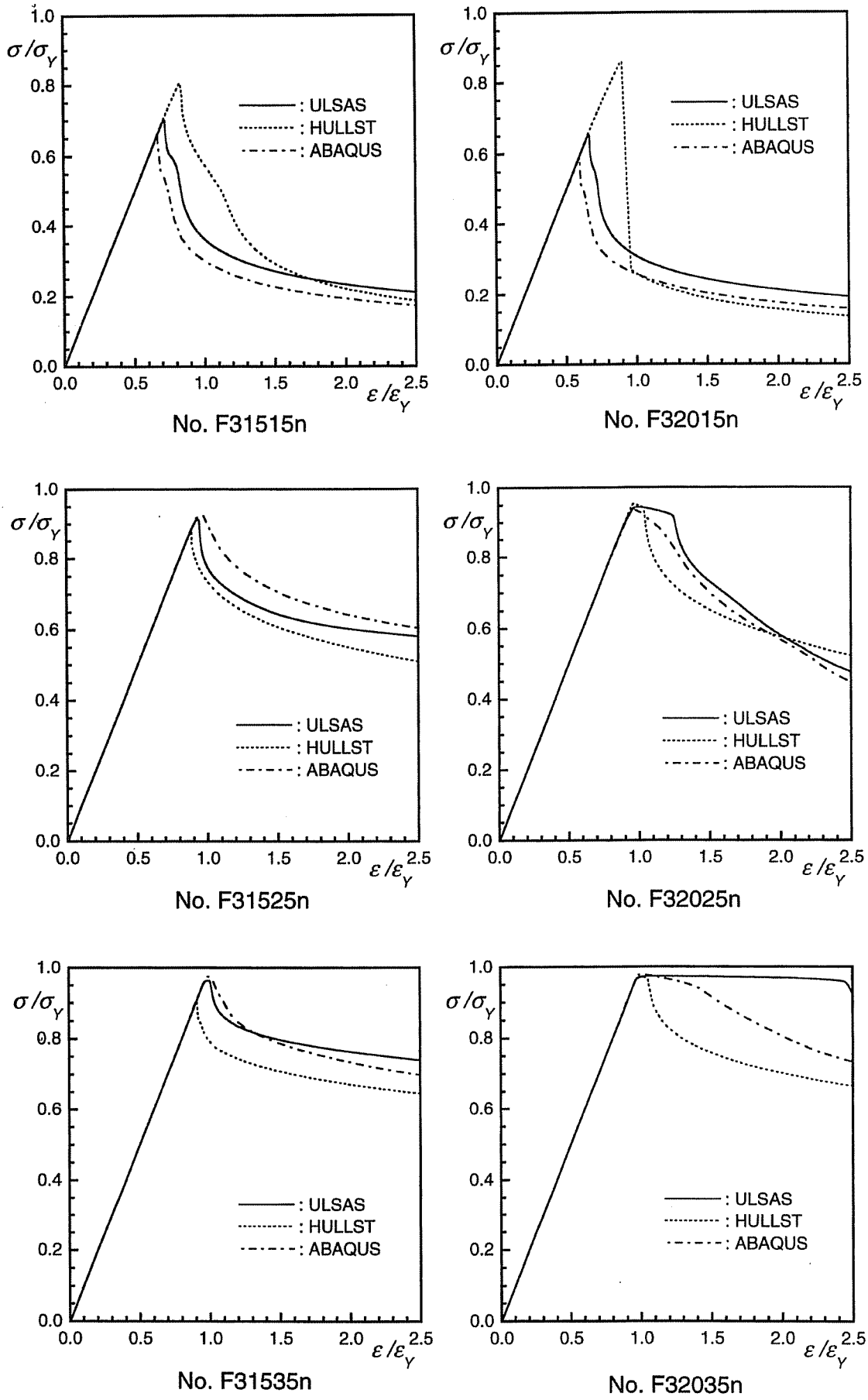

Figure 3.4: Comparison of average stress-average strain relationships

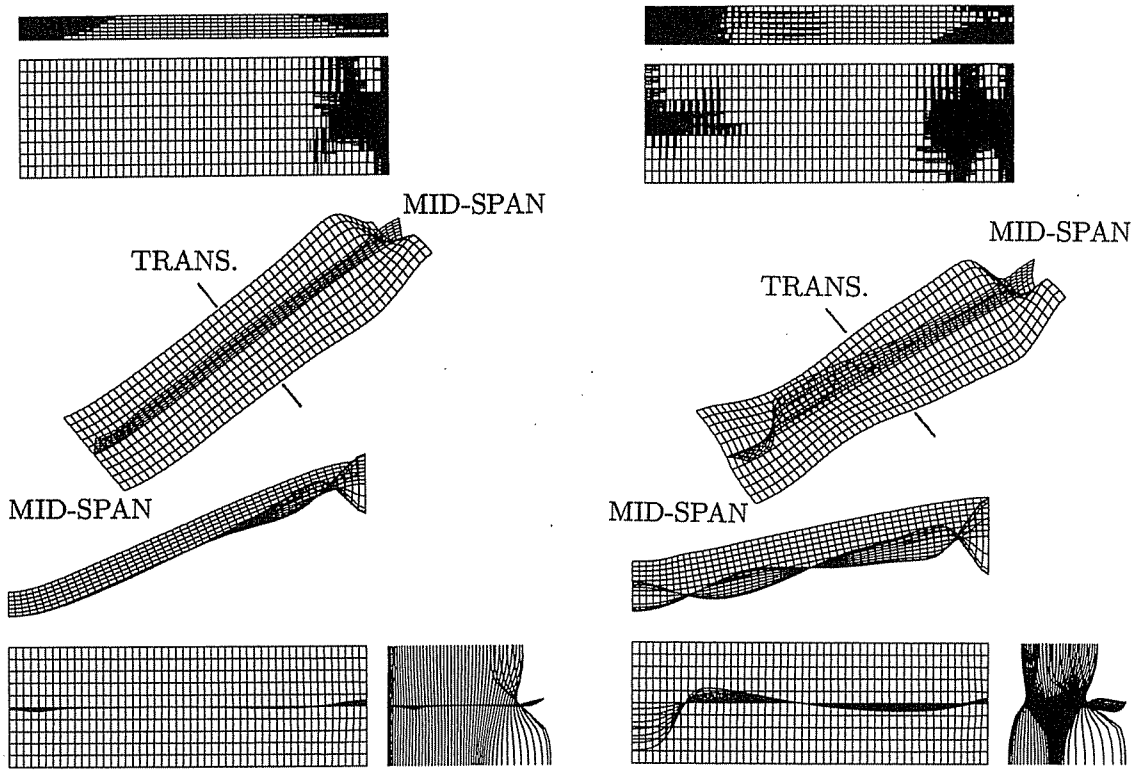

Figure 3.5:Typical collapse modes of stiffened plates under thrust
(FEM; Double-span model)

the stiffener which comes in the compression side of bending. The accuracy of the ultimate strength calculated by a simplified method depends how accurately the collapse mode can be simulated. For example, Masaoka's method yields a too high ultimate strength when the overall buckling as a stiffened plate dominates the collapse behaviour, since this failure mode cannot be simulated by his method.

From this viewpoint, it is essential to realise the potential collapse modes of the stiffened panel as well as to know the assumptions made in the calculation method to be applied.

It is seen from Figure 3.3 that the slenderness ratio of the local panel cannot be a unique parameter to represent the ultimate strength of the stiffened plate, and it should be used in combination with type and size of the stiffener and also with the aspect ratio of the local panel.

On the other hand, slenderness ratio of the stiffener with associated plating is sometimes used as an unique parameter to represent the ultimate strength of a stiffened plate. For this use, however, slenderness ratio of the stiffener should be used as a unique parameter regardless of the type and size of the stiffener as well as the slenderness ratio of the associated panel.

To examine this possibility, the ultimate strength by Yao(3) (results of FEM analyses) is plotted against the slenderness ratio of the stiffener in Figures 3.6 (a) and (b), where flexural buckling strength and flexural/torsional buckling strength (Yao and Nikolov 1992) are used as σ_E to calculate the slenderness ratio, $(\sigma_{Ys}/\sigma_E)^{1/2}$. It is seen that the ultimate strength shows different tendency depending on the size and type of the stiffener as well as on the aspect ratio and slenderness of the local panel. This implies that the slenderness ratio of a stiffener cannot be used as an unique parameter to represent the ultimate strength of a stiffened plate, and it should be used in combination with the slenderness as well as the aspect ratio of the local panel as was done in Figure 3.3.

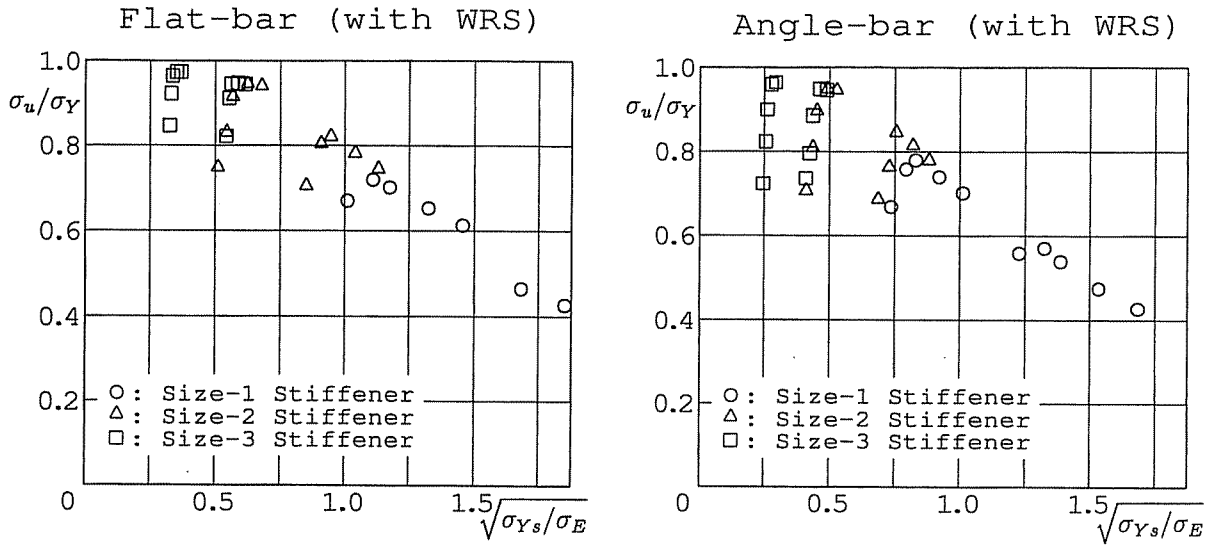

(a) Against slenderness ratio using flexural buckling strength

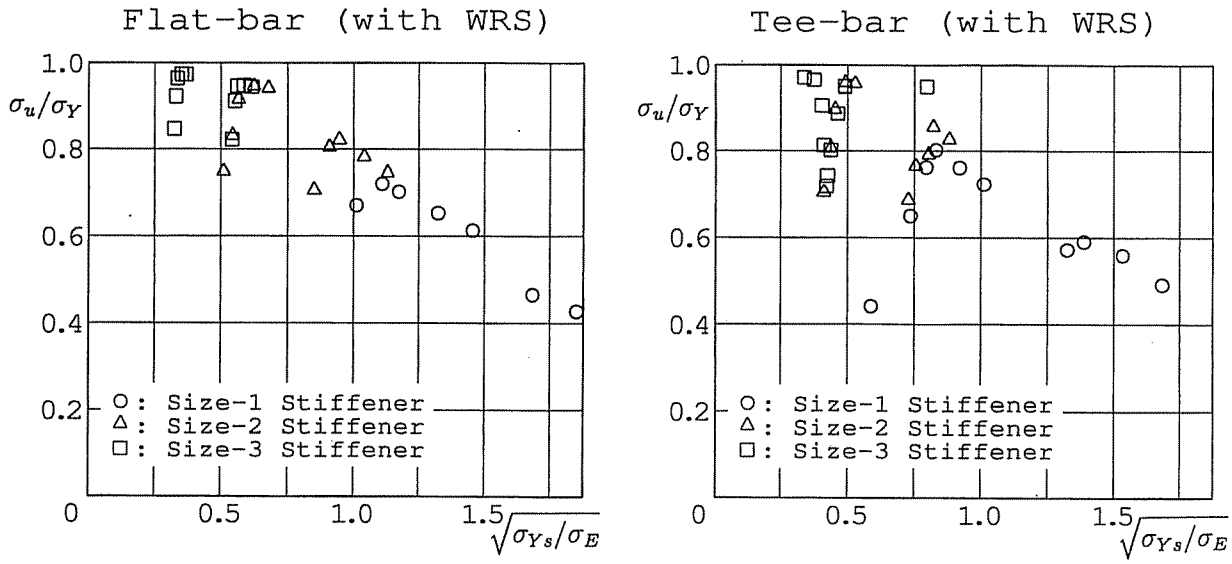

(b) Against slenderness ratio using flexural/torsional buckling strength

Figure 3.6: Ultimate strength plotted against slenderness ratio of stiffener

4 BENCHMARK CALCULATIONS ON ULTIMATE HULL GIRDER STRENGTH

4.1 Five Hull Girders for Benchmark Calculations

Hull girders of five vessels indicated in Table 4.1 are chosen for benchmark calculations to evaluate ultimate hull girder strength. The cross-sections of the five hull girders are shown in Figures 4.1 through 4.5 and the dimensions or locations of the longitudinal stiffeners in Tables 4.2 through 4.6. Dimensions of stiffeners in the tables are defined as indicated in Figure 4.6. Among five vessels, the ultimate hull girder strength of the Frigate Model under the sagging condition is measured by Dow (1991). The single Hull VLCC is *Energy*

Concentration who sank at Rotterdam harbour in 1980, and the working bending moment at collapse under the hogging condition was estimated by Rutherford and Caldwell (1990).
Two cases are analysed for five hull girders, which are:

Case (1): with small initial deflection and no welding residual stress.

Case (2): with actual initial deflection and welding residual stress

The assumed initial deflection in panels and stiffeners for Case (1) are the same as those shown in Figure 3.1, and are represented by Eqns. 3.1, 3.2 and 3.3. Their maximum magnitudes are assumed as $A_0/t_p = 0.01$ and $B_0/a = C_0/a = 0.001$.
For Case (2), the same initial deflection is assumed for stiffeners. For panels, the mode is the same with Case (1), but the magnitude is given as:

$$A_0 = \eta w_{0max} \tag{4.1}$$

where

$$w_{0max} = 0.1\, b/t_p \cdot \sqrt{\sigma_{Yp}/E} \times t_p \tag{4.2}$$

η is the coefficient of effective initial deflection (Ueda and Yao 1985), and is, for example, 0.3321 when the aspect ratio of the panel, *a/b* is 3.0. η decreases with the increase in an aspect ratio.
The assumed welding residual stress in Case (2) is represented by Eqns. 3.4 through 3.8.
In Case (2) of the Single Hull VLCC (*Energy Concentration*), thickness of the panel and the stiffener web is reduced by 1 mm and that of the stiffener flange by 2 mm according to the measured results (Rutherford and Caldwell 1990).

TABLE 4.1
PRINCIPAL DIMENSIONS OF FIVE VESSELS FOR BENCHMARK CALCULATIONS

TYPE	LENGTH	BREADTH	DEPTH
BULK CARRIER	285	50	26.7
CONTAINER SHIP	230	32.2	21.5
DOUBLE HULL VLCC	315	58	30.3
SINGLE HULL VLCC**	313	48.2	25.2
FRIGATE MODEL*	18	4.2	2.8

(in m)

*: 1/3 scale-model; Length is that of a test model.
**: *ENERGY CONCENTRATION*

4.2 Applied Methods of Analyses

Astrup:
A computer program NAUTICUS is used to evaluate the ultimate longitudinal strength of a hull girder. The program calculates the ultimate hull girder bending moment capacity based on DNV Rules for Ships Pt.3 Ch.1 Sec.16 D300.
A cross-section of the hull girder is divided into panels with stiffeners. It is assumed that the capacity of each panel in compression is equal to the critical buckling capacity calculated according to the DNV Class Note 30.1 (1995). On the other hand, that in tension is assumed to be the yield strength. Assuming that all the structural components in the cross-section are at their ultimate state either in compression or tension, the neutral axis for pure bending is calculated. The bending moment with respect to this neutral axis is considered as the ultimate hull girder strength.

TABLE 4.2
DIMENSIONS OF LONGITUDINALS OF BULK CARRIER

Stif. No.	dimensions	type	σ_Y (MPa)	Stif. No.	dimensions	type	σ_Y (MPa)
1	390 × 27	at-bar	392.0	8	283 × 9 + 100 × 17	tee-bar*	352.8
2	333 × 9 + 100 × 16	tee-bar*	352.8	9	333 × 9 + 100 × 18	tee-bar*	352.8
3	283 × 9 + 100 × 14	tee-bar*	352.8	10	333 × 9 + 100 × 19	tee-bar*	352.8
4	283 × 9 + 100 × 18	tee-bar*	352.8	11	383 × 9 + 100 × 17	tee-bar*	352.8
5	333 × 9 + 100 × 17	tee-bar*	352.8	12	383 × 10 + 100 × 18	tee-bar*	352.8
6	283 × 9 + 100 × 16	tee-bar*	352.8	13	383 × 10 + 100 × 21	tee-bar*	352.8
7	180 × 32.5 × 9.5	bulb-bar	235.2	14	300 × 27	at-bar	392.0

(dimensions in mm)

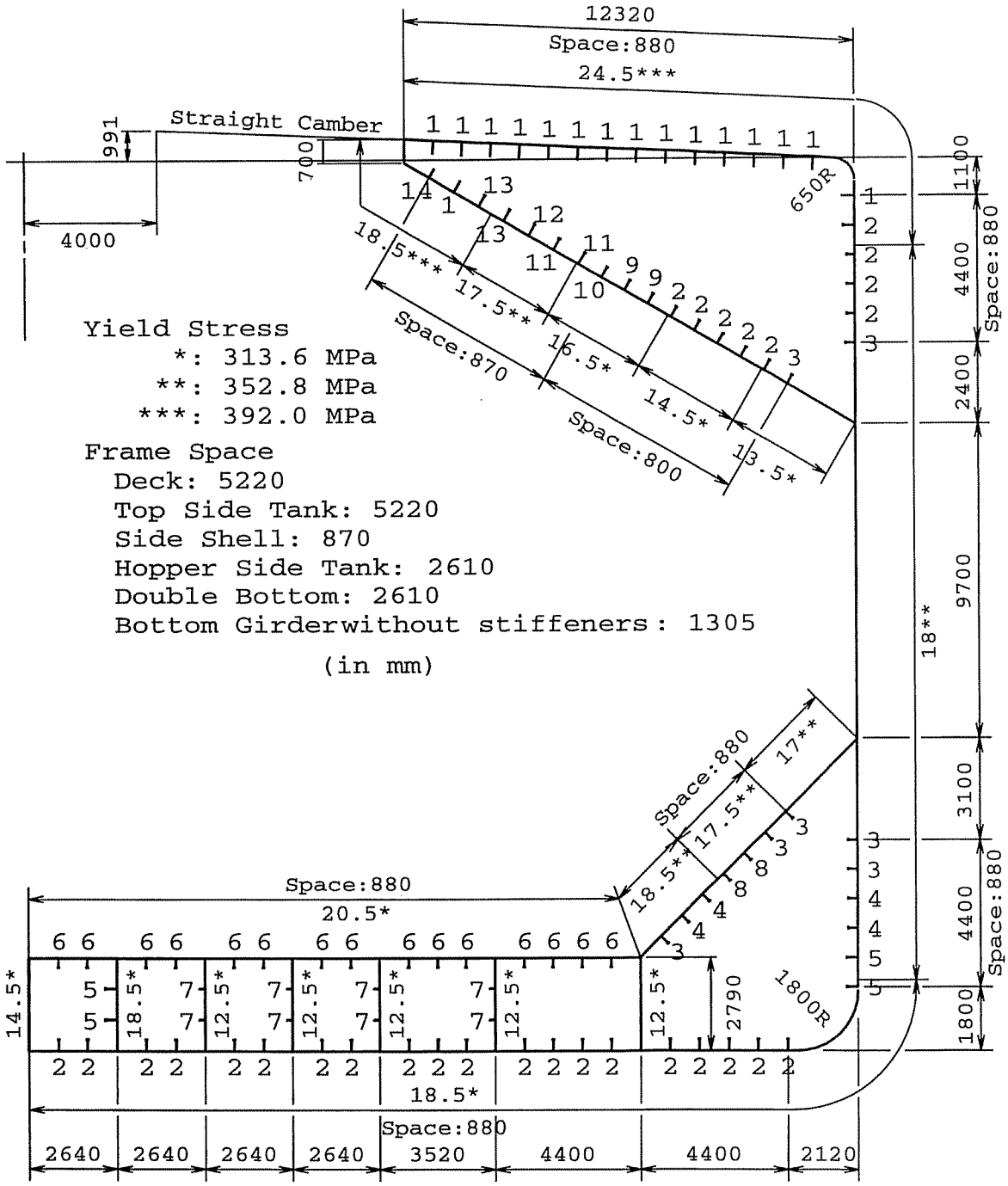

Figure 4.1: Cross-section of Bulk Carrier

TABLE 4.3
DIMENSIONS OF LONGITUDINALS OF CONTAINER SHIP

Stif. No.	dimensions	type	σ_Y (MPa)	Stif. No.	dimensions	type	σ_Y (MPa)
1	300 × 38	at-bar	352.8	9	230 × 10	at-bar	313.6
2	300 × 28	at-bar	313.6	10	300 × 90 × 13/17 IA	angle-bar	313.6
3	250 × 90 × 10/15 IA	angle-bar	313.6	11	150 × 90 × 12/12 IA	angle-bar	313.6
4	250 × 90 × 12/16 IA	angle-bar	313.6	12	250 × 90 × 12/15 IA	angle-bar	313.6
5	300 × 90 × 11/16 IA	angle-bar	313.6	13	150 × 12	at-bar	313.6
6	300 × 90 × 13/17 IA	angle-bar	313.6	14	150 × 90 × 9/9 IA	angle-bar	313.6
7	350 × 100 × 12/17 IA	angle-bar	313.6	15	150 × 10	at-bar	313.6
8	400 × 100 × 11.5/16 IA	angle-bar	313.6	16	300 × 90 × 11/16 IA	angle-bar	313.6

(dimensions in mm)

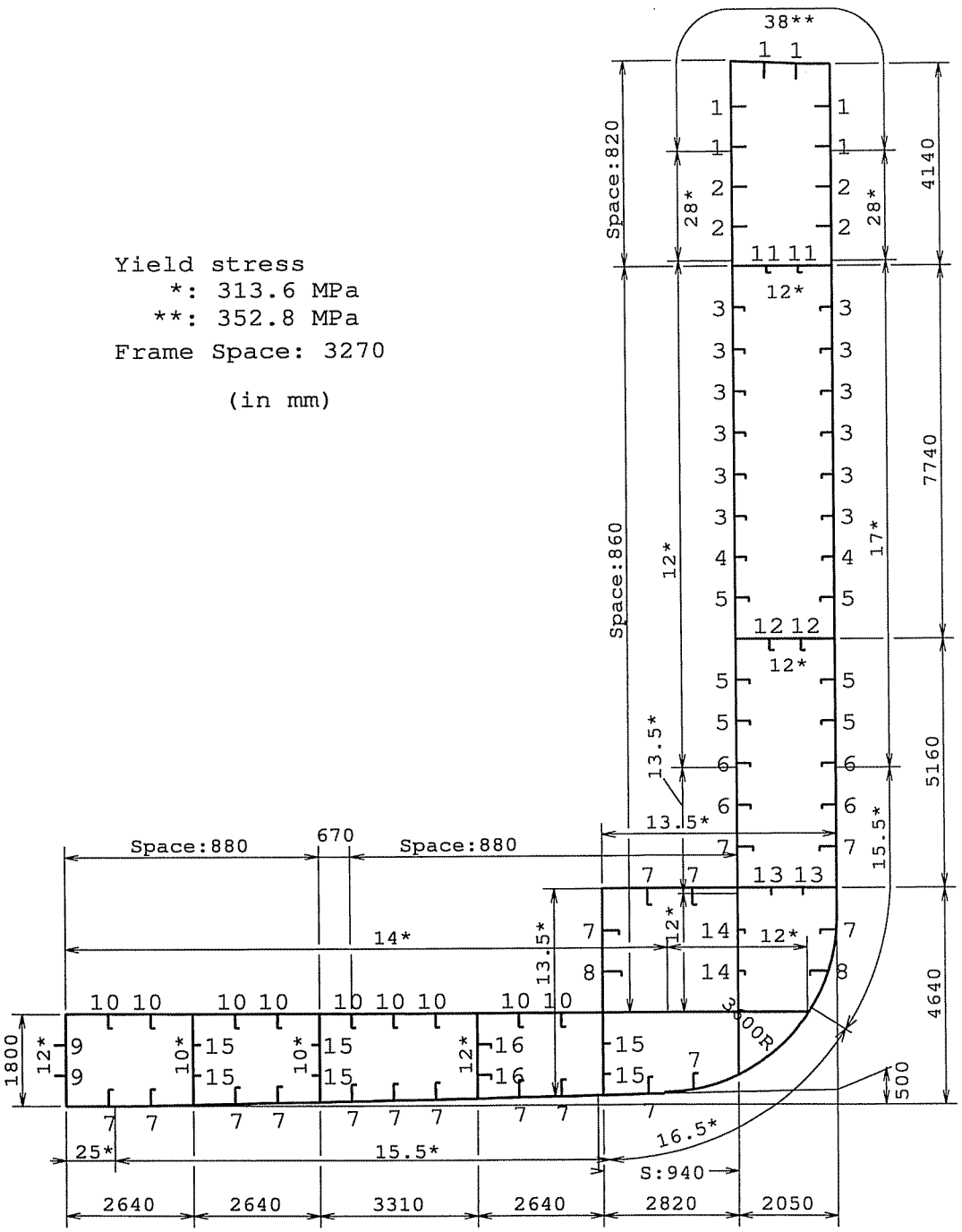

Figure 4.2: Cross-section of Container Ship

TABLE 4.4
DIMENSIONS OF LONGITUDINALS OF DOUBLE HULL VLCC

Stif. No.	dimensions	type	σ_Y (MPa)	Stif. No.	dimensions	type	σ_Y (MPa)
1	300 × 90 × 13/17 IA	angle-bar	313.6	25	250 × 90 × 12/16 IA	angle-bar	313.6
2	350 × 100 × 12/17 IA	angle-bar	313.6	26	450 × 11 + 150 × 22	tee-bar*	352.8
3	400 × 100 × 11.5/17 IA	angle-bar	313.6	27	450 × 11 + 150 × 19	tee-bar*	352.8
4	400 × 11 + 150 × 12	tee-bar*	313.6	28	450 × 11 + 150 × 16	tee-bar*	352.8
5	400 × 11 + 150 × 14	tee-bar*	313.6	29	450 × 11 + 150 × 14	tee-bar*	352.8
6	450 × 11 + 150 × 12	tee-bar*	313.6	30	450 × 11 + 150 × 12	tee-bar*	352.8
7	450 × 11 + 150 × 14	tee-bar*	313.6	31	450 × 11 + 150 × 14	tee-bar*	352.8
8	450 × 11 + 150 × 16	tee-bar*	313.6	32	400 × 100 × 11.5/16 IA	angle-bar	352.8
9	450 × 11 + 150 × 19	tee-bar*	313.6	33	350 × 100 × 12/17 IA	angle-bar	352.8
10	450 × 11 + 150 × 22	tee-bar*	313.6	34	300 × 90 × 13/17 IA	angle-bar	352.8
11	450 × 11 + 150 × 25	tee-bar*	313.6	35	850 × 17 + 150 × 19	L-bar*	352.8
12	500 × 11 + 150 × 28	tee-bar*	313.6	36	250 × 90 × 12/16 IA	angle-bar	352.8
13	500 × 11 + 150 × 30	tee-bar*	313.6	37	300 × 90 × 12/16 IA	angle-bar	352.8
14	500 × 11 150 × 32	tee-bar*	313.6	38	400 × 11 + 150 × 14	tee-bar*	352.8
15	500 × 11 150 × 34	tee-bar*	313.6	39	450m × 11 + 150 × 12	tee-bar*	352.8
16	550 × 12 150 × 30	tee-bar*	313.6	40	450 × 11 + 150 × 14	tee-bar*	352.8
17	550 × 12 150 × 25	tee-bar*	313.6	41	450 × 11 + 150 × 16	tee-bar*	352.8
18	350 × 100 × 12/17 IA	angle-bar*	313.6	42	450 × 11 + 150 × 19	tee-bar*	352.8
19	550 × 12.5 150 × 32	tee-bar*	352.8	43	450 × 11 + 150 × 22	tee-bar*	352.8
20	500 × 11.5 150 × 30	tee-bar*	352.8	44	450 × 11 + 150 × 25	tee-bar*	352.8
21	500 × 11.5 150 × 28	tee-bar*	352.8	45	450 × 11 + 150 × 28	tee-bar*	352.8
22	500 × 11 150 × 25	tee-bar*	352.8	46	500 × 11 + 150 × 25	tee-bar*	352.8
23	450 × 11 150 × 28	tee-bar*	352.8	47	500 × 11 + 150 × 28	tee-bar*	352.8
24	250 × 12.5	at-bar	313.6	48	230 × 12.5	at-bar	313.6

(*: fabricated by welding; dimensions in mm)

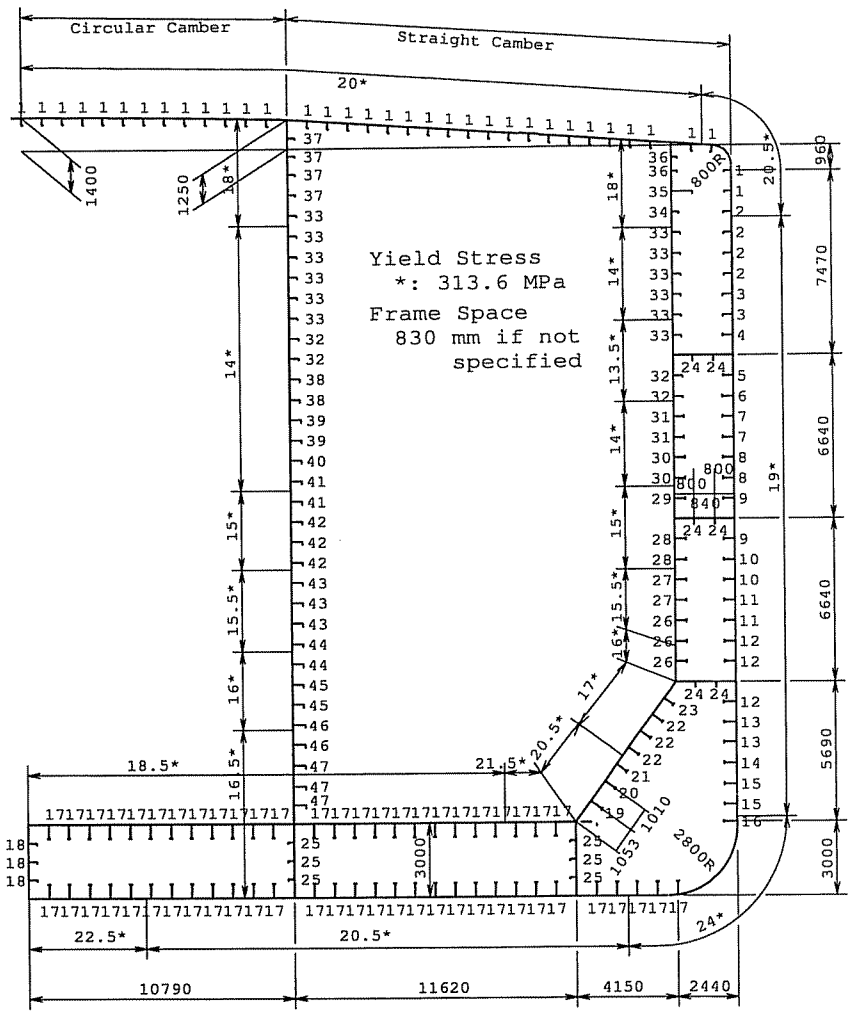

Figure 4.3: Cross-section of Double Hull VLCC

TABLE 4.5 : DIMENSIONS OF LONGITUDINALS OF SINGLE HULL VLCC, *Energy Concentration*

Stif. No.	dimensions	type	σ_Y (MPa)	Stif. No.	dimensions	type	σ_Y (MPa)
1	797 × 15 + 200 × 33	tee-bar*	313.6	17	747 × 12.7 + 180 × 25	angle-bar*	235.2
2	300 × 100 × 11.5/16	angle-bar	313.6	18	797 × 14 + 180 × 25	tee-bar*	235.2
3	370 × 16	at-bar	313.6	19	847 × 14 + 180 × 25	angle-bar*	313.6
4	425 × 25	at-bar	313.6	20	847 × 14 + 180 × 32	tee-bar*	235.2
5	480 × 32	at-bar	313.6	21	847 × 15 + 180 × 25	angle-bar*	313.6
6	300 × 100 × 11.5/16	angle-bar	313.6	22	847 × 15 + 180 × 32	angle-bar*	313.6
7	370 × 16	at-bar	313.6	23	897 × 15 + 200 × 25	angle-bar*	253.2
8	447 × 11.5 + 125 × 22	tee-bar*	313.6	24	945 × 16 + 200 × 25	angle-bar*	235.2
9	549 × 11.5 + 125 × 22	angle-bar*	235.2	25	897 × 15 + 200 × 25	angle-bar*	313.6
10	597 × 11.5 + 125 × 22	angle-bar*	235.2	26	797 × 15 + 180 × 25	angle-bar*	313.6
11	597 × 11.5 + 125 × 22	angle-bar*	235.2	27	347 × 11.5 + 125 × 22	angle-bar*	313.6
12	647 × 11.5 + 125 × 22	angle-bar*	235.2	28	397 × 25	at-bar	313.6
13	350 × 25.4	at-bar	235.2	29	300 × 25	at-bar	253.2
14	646 × 12.7 + 150 × 25	angle-bar*	235.2	30	230 × 12.7	at-bar	253.2
15	697 × 12.7 + 150 × 25	angle-bar*	235.2	31	230 × 12.7	at-bar	253.2
16	747 × 12.7 + 150 × 25	angle-bar*	313.6	32	397 × 11.5 + 100 × 25	tee-bar*	313.6

(*: fabricated by welding; dimensions in mm)

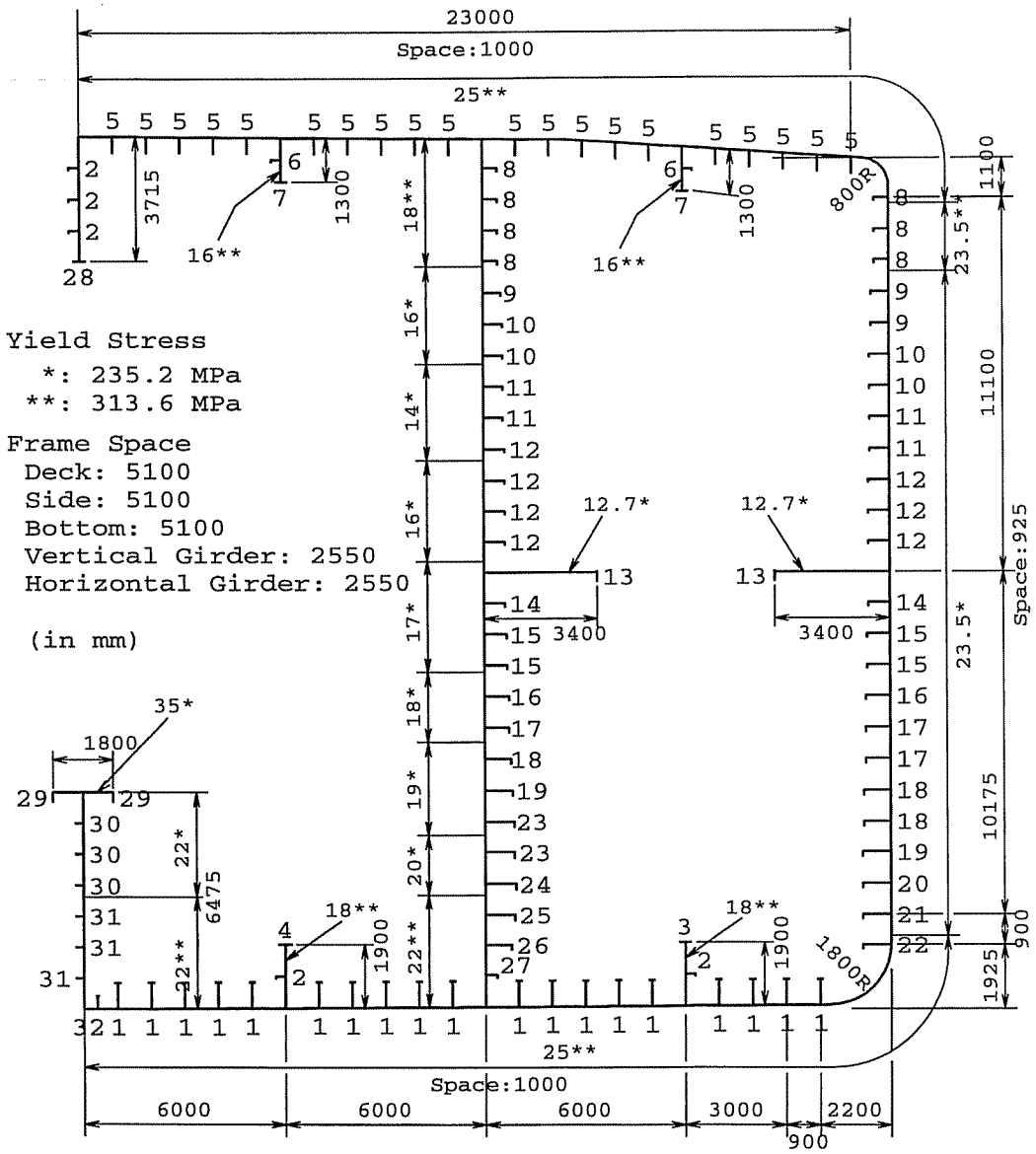

Figure 4.4: Cross-section of Single Hull VLCC; "*Energy Concentration* "

TABLE 4.6
LOCATION OF LONGITUDINALS OF 1/3-SCALE FRIGATE MODEL

Stif. ID	y(mm)	z(mm)	Sif. ID	y(mm)	z(mm)	Sif. ID	y(mm)	z(mm)
Keel	0.0	0.0	No.4 DK	1685.9	493.5	29L	2050.0	2264.5
1L	98.4	12.9	16L	1741.7	548.4	30L	2050.0	2464.5
2L	249.3	41.9	17L	1807.3	622.6	31L	2050.0	2658.1
3L	373.9	67.7	18L	1863.0	709.7	No.1 DK	2050.0	2800.0
4L	472.3	87.1	19L	1909.0	793.5	32L	1948.3	2800.0
5L	574.0	106.5	20L	1945.0	883.9	33L	1823.7	2800.0
6L	675.7	125.8	21L	1974.6	977.4	34L	1621.6	2800.0
7L	774.1	145.2	22L	1994.2	1077.4	35L	1418.3	2800.0
8L	882.3	167.7	23L	2010.6	1174.2	36L	1216.2	2800.0
9L	984.0	190.3	24L	2023.8	1274.2	37L	1012.9	2800.0
10L	1089.0	216.1	No.3 DK	2033.6	1367.7	38L	810.8	2800.0
11L	1197.2	241.9	26L	2040.2	1471.0	39L	607.5	2800.0
12L	1292.3	277.4	27L	2050.0	1671.0	40L	405.4	2800.0
13L	1394.0	316.1	28L	2050.0	1867.7	41L	202.0	2800.0
14L	1492.4	364.5	No. 2 DK	2050.0	2064.5	42L	0.0	2800.0
15L	1587.5	419.4						

(dimensions in mm)

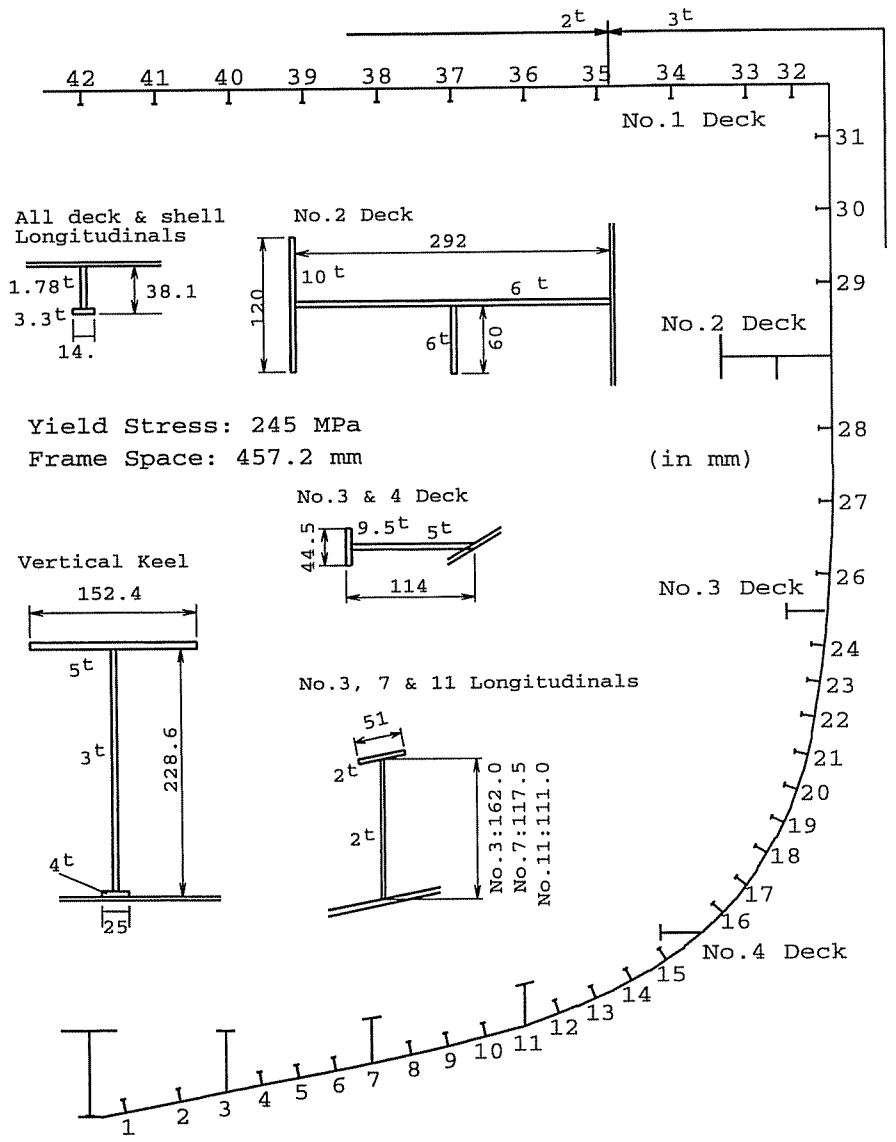

Figure 4.5: Cross-section of 1/3-scale Steel Welded Frigate Model

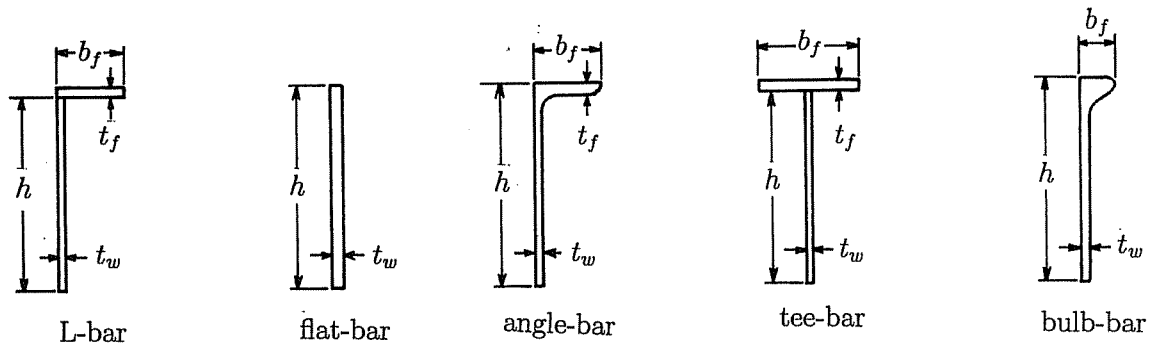

Figure 4.6: Dimensions of stiffeners

For the evaluation of the critical capacity of the members, influences of transverse thrust and lateral pressure are taken into account. For the evaluation of the yield strength, influence of other stress components is accounted.

Chen:
This method is a variation of the Idealized Structural Unit Method (ISUM) generally attributed to Ueda *et al.*(1984) and was further developed by Paik (1990b). The specific method employed here is a subset of Paik's work that is identified as Analysis of Large Plated Structures (ALPS; Paik 1992c).
In the present analysis, five types of ISUM elements are in use; namely, beam-column element, unstiffened plate element, stiffened plate element, hard element, and virtual element. The detail of these elements can be found in ALPS (Paik 1992).
Failure modes simulating instability and plasticity imbedded in the formulation include local buckling, panel buckling, overall buckling, yielding (including necking), ultimate tensile rupture, and ductile fracture. An element may fail in one of these modes initially and progress to another mode subsequently in the manifestation of the progressive collapse process

Cho:
The ordinary Smith's method is applied to simulate the progressive collapse behaviour of the hull girder cross-section using average stress-average strain relationships derived for stiffener elements with attached plating (Cho *et al.* 1998b).

Dow:
The method used to carry out the analysis is the Smith's method, which enables to calculate the progressive collapse behaviour of a ship hull girder subjected to combined vertical and horizontal bending incorporating the effects of shear and lateral loads (Dow, 1980). The fundamental procedure to apply this method is explained in *2.2.1.*

Masaoka:
The ISUM is applied for the analysis. The cross-section is divided into ISUM rectangular plate elements and elastoplastic beam elements. To derive the stiffness matrix of all the plate elements, edges of the plate are assumed to be simply supported. Stiffeners are also modelled by plate elements with a free edge and three simply supported edges.
Detail of the ISUM rectangular plate element used for the present analysis is described in the paper by Ueda and Masaoka (1995). In the analysis, a shift of the neutral axis during progressive collapse is considered, but overall buckling as a stiffened plate and tripping of stiffeners are not accounted. Geometrical nonlinearity is considered in ISUM element only locally by using eigen-function for deflection. Arc length method is applied for the nonlinear incremental calculation.

Rigo(1):
The ordinary Smith's method is applied with a simplified structural modelling proposed by Rahman and Chowdhury (1996), and a progressive collapse analysis is performed. The modelled structure is composed of only three components, which are the deck, the bottom and the side shell plating.
The average stress-average strain relationships are derived for these three elements (components) applying the Hughes' method (1988). Special approximation and simplification have to be performed when the analysed midship section is complex or composed of large curved part.

Rigo(2):
For each component composing a cross-section, the ultimate strength is estimated applying Paik's method (Paik and Thayamballi, 1997). Then, based on the credibly assumed stress distribution across the cross-section, the hogging and the sagging ultimate bending moments are directly calculated by a simple formulation (Paik and Mansour 1995). A progressive collapse analysis is not performed.
In this method, the stress-strain relationships are not defined, but the reduction in capacity beyond the ultimate strength in individual compressed components is implicitly and approximately accounted for by introducing an "assumed stress distribution" which may represent the real situation of the structural failure at the ultimate limit state. If the reduction of capacity is not considered, the assumed stress distribution could not be obtained.

Yao:
The ordinary Smith's method is applied using a computer code HULLST with the average stress-average strain relationships of elements composed of a stiffener and attached plating, which are derived analytically (Yao and Nikolov 1991; 1992). The bi-axial bending can be applied, and the influence of shear force can be accounted when it is necessary.

4.3 Calculated Results and Discussions

The calculated results of ultimate hull girder strength are summarised in Tables 4.7 through 4.11. The items in the tables are as follows:

I_y: moment of inertia with respect to horizontal neutral axis
z_G: location of neutral axis above keel under vertical bending
M_P: fully plastic bending moment of cross-section
M_{YS}: initial yielding strength of deck plating
M_{YH}: initial yielding strength of bottom plating
M_{BS}: buckling strength of deck plating
M_{BH}: buckling strength of bottom plating
M_{US}: ultimate bending moment of cross-section under sagging
M_{UH}: ultimate bending moment of cross-section under hogging
$|_{(1)}$: with small initial deflection and free from welding residual stress; Case (1)
$|_{(2)}$: with specified initial deflection and welding residual stress; Case (2)

The moment-curvature relationships obtained by different methods for Case (2) are plotted in Figure 4.7 (a) through (e).
It is seen that the scatter in the ultimate hull girder strength is not so large especially when the hull is subjected to hogging bending moment. This may be partly because the bottom plate is relatively thick, and the local buckling strength of a panel is nearly equal to the yield strength. On the other hand, the scatter of the ultimate hull girder strength in sagging is relatively large. This may be because different methods give somwhat different buckling strength of the deck which has in general lighter scantling and more sensitive to buckling than the bottom.

TABLE 4.7
ULTIMATE HULL GIRDER STRENGTH OF BULK CARRIER

Items	Chen	Cho	Masaoka	Rigo(1)	Rigo(2)	Soares	Yao
I_y (m^4)	694.87	693.44	689.8	-	702.48	679.31	682.50
z_G (m)	11.20	11.06	11.03	10.94	10.66	11.15	10.87
M_P ($\times 10^3$MN·m)	20.87	19.90	19.86	20.26	20.03	19.64	20.12
M_{YS} ($\times 10^3$MN·m)	15.82	15.64	15.53	-	15.45	15.41	15.21
M_{YH} ($\times 10^3$MN·m)	21.58	21.83	21.79	-	23.04	21.20	21.91
M_{BS} ($\times 10^3$MN·m)	13.19	13.05	12.95	-	12.89	12.85	12.79
M_{BH} ($\times 10^3$MN·m)	16.43	16.63	16.59	-	17.55	16.14	16.68
$M_{US}\|_{(1)}$ ($\times 10^3$MN·m)	15.35	14.40	16.82	15.03	-	13.72	15.67
$M_{UH}\|_{(1)}$ ($\times 10^3$MN·m)	18.71	19.55	18.90	19.13	-	17.43	17.78
$M_{US}\|_{(2)}$ ($\times 10^3$MN·m)	15.20	13.69	16.02	14.34	14.84	-	14.45
$M_{UH}\|_{(2)}$ ($\times 10^3$MN·m)	19.06	18.99	18.56	18.71	17.08	-	17.36

TABLE 4.8
ULTIMATE HULL GIRDER STRENGTH OF CONTAINER SHIP

Items	Chen	Cho	Masaoka	Rigo(1)	Rigo(2)	Soares	Yao
I_y (m^4)	250.94	226.7	235.6	-	254.3	238.73	238.21
z_G (m)	8.86	8.84	8.54	8.13	8.10	8.51	8.63
M_P ($\times 10^3$MN·m)	9.36	8.39	8.64	9.06	9.01	8.76	8.95
M_{YS} ($\times 10^3$MN·m)	7.00	6.32	6.41	-	6.70	6.48	6.53
M_{YH} ($\times 10^3$MN·m)	8.88	8.04	8.65	-	9.85	8.80	8.66
M_{BS} ($\times 10^3$MN·m)	6.72	6.06	6.16	-	6.43	6.22	6.28
M_{BH} ($\times 10^3$MN·m)	6.54	5.92	6.37	-	7.25	6.48	6.37
$M_{US}\|_{(1)}$ ($\times 10^3$MN·m)	5.54	5.29	7.79	6.93	-	6.68	6.84
$M_{UH}\|_{(1)}$ ($\times 10^3$MN·m)	6.82	7.05	8.06	8.00	-	7.75	6.90
$M_{US}\|_{(2)}$ ($\times 10^3$MN·m)	5.47	5.13	7.75	6.51	6.91	-	6.72
$M_{UH}\|_{(2)}$ ($\times 10^3$MN·m)	6.56	6.69	8.07	7.60	7.20	-	6.72

TABLE 4.9
ULTIMATE HULL GIRDER STRENGTH OF DOUBLE HULL VLCC

Items	Chen	Cho	Masaoka	Rigo(1)	Rigo(2)	Soares	Yao
I_y (m^4)	1347.3	1340.1	1360.0	-	1382.3	1355.8	1344.7
z_G (m)	12.88	12.92	12.79	12.83	13.18	13.03	12.84
M_P (MN·m)	32.40	31.74	32.07	30.99	32.86	31.77	32.96
M_{YS} ($\times 10^3$MN·m)	24.12	24.04	24.22	-	25.17	24.48	24.02
M_{YH} ($\times 10^3$MN·m)	32.80	32.53	33.35	-	32.89	32.63	32.84
M_{BS} ($\times 10^3$MN·m)	19.74	19.68	19.82	-	20.61	20.24	19.66
M_{BH} ($\times 10^3$MN·m)	27.14	26.91	27.59	-	27.21	26.99	27.17
$M_{US}\|_{(1)}$ ($\times 10^3$ MN·m)	23.83	22.11	26.82	20.62	-	19.85	21.23
$M_{UH}\|_{(1)}$ ($\times 10^3$ MN·m)	28.28	29.59	30.88	28.90	-	27.61	29.22
$M_{US}\|_{(2)}$ ($\times 10^3$ MN·m)	24.33	20.80	26.59	19.57	24.07	-	20.42
$M_{UH}\|_{(2)}$ ($\times 10^3$ MN·m)	27.40	28.66	30.59	28.32	25.61	-	28.88

TABLE 4.10
ULTIMATE LONGITUDINAL STRENGTH OF SINGLE HULL VLCC,
ENERGY CONCENTRATION

Items	Astrup	Chen	Cho	Dow	Masaoka	Rigo(1)	Rigo(2)	Soares	Yao
$I_y\|_{(1)}$ (m^4)	-	851.5	860.0		869.8	-	857.76	848.71	840.28
$z_G\|_{(1)}$ (m)	-	12.06	12.12	-	11.99	12.81	12.75	12.17	12.24
$M_P\|_{(1)}$ ($\times 10^3$MN·m)	-	22.63	22.85	21.03	23.08	21.29	21.53	22.62	22.73
$M_{YS}\|_{(1)}$ ($\times 10^3$MN·m)	-	20.32	20.62	-	20.65	-	21.61	20.43	20.33
$M_{YH}\|_{(1)}$ ($\times 10^3$MN·m)	-	22.14	22.25	-	22.75	-	21.10	21.87	21.53
$M_{BS}\|_{(1)}$ ($\times 10^3$MN·m)	-	16.90	17.14	-	17.17	-	17.96	16.98	16.90
$M_{BH}\|_{(1)}$ ($\times 10^3$MN·m)	-	18.41	18.50	-	18.91	-	17.54	18.18	17.90
$M_{US}\|_{(1)}$ ($\times 10^3$MN·m)	-	20.49	17.98	-	18.02	19.52	18.15	15.83	18.98
$M_{UH}\|_{(1)}$ ($\times 10^3$MN·m)	-	20.67	20.53	-	20.44	20.02	18.58	18.79	20.82
$I_y\|_{(2)}$ (m^4)	-	-	819.70	743.8	828.3	-	812.86	-	800.89
$z_G\|_{(2)}$ (m)	-	-	12.15	11.85	12.01	12.31	12.81	-	12.27
$M_P\|_{(2)}$ ($\times 10^3$MN·m)	-	-	21.76	19.85	21.96	20.35	20.39	-	21.75
$M_{YS}\|_{(2)}$ ($\times 10^3$MN·m)	-	-	19.70	17.47	19.69	-	20.57	-	19.43
$M_{YH}\|_{(2)}$ ($\times 10^3$MN·m)	-	-	21.16	19.68	21.63	-	19.90	-	20.47
$M_{BS}\|_{(2)}$ ($\times 10^3$MN·m)	-	-	16.09	14.28	16.09	-	16.81	-	15.87
$M_{BH}\|_{(2)}$ ($\times 10^3$MN·m)	-	-	17.29	16.08	17.67	-	16.26	-	16.73
$M_{US}\|_{(2)}$ ($\times 10^3$MN·m)	17.15	18.54	16.75	16.32	19.00	17.90	17.10	-	16.84
$M_{UH}\|_{(2)}$ ($\times 10^3$MN·m)	18.84	20.23	20.09	18.80	20.01	18.46	17.54	-	19.03

(estimated applied load at collapse in hogging: 17.94×10^3 MN·m (Rutherford and Caldwell 1990))

TABLE 4.11
ULTIMATE LONGITUDINAL STRENGTH OF 1/3-SCALE WELDED STEEL FRIGATE MODEL

Items	Chen	Cho	Dow	Masaoka	Rigo(1)	Rigo(2)	Yao
I_y (m^4)	0.0649	0.0595	0.0627	0.0638	-	0.0676	0.0608
z_G (m)	1.376	1.44	1.407	1.398	1.433	1.42	1.424
M_P (MN·m)	13.77	12.81	17.01	13.72	14.32	14.39	13.24
M_{YS} ($\times 10^3$MN·m)	11.17	10.72	11.03	11.08	-	12.00	10.83
M_{YH} ($\times 10^3$MN·m)	11.55	10.12	10.92	11.25	-	11.66	10.46
M_{BS} ($\times 10^3$MN·m)	3.32	3.19	3.28	3.30	-	3.57	3.22
M_{BH} ($\times 10^3$MN·m)	10.48	9.18	9.90	10.20	-	10.58	9.48
$M_{u,sag}\|_{(1)}$ (MN·m)	-	10.10	-	11.72	9.84	-	9.88
$M_{u,hog}\|_{(1)}$ (MN·m)	-	11.61	-	13.21	13.45	-	11.24
$M_{u,sag}\|_{(2)}$ (MN·m)	9.54	9.48	9.67	11.50	9.47	9.88	8.58
$M_{u,hog}\|_{(2)}$ (MN·m)	12.49	11.32	11.39	12.49	13.26	12.12	10.90

(measued collapse moment in sagging: 9.64 MN·m (Dow 1991))

The capacity beyond the ultimate strength is somewhat scattering compared to the ultimate hull girder strength. Significant reduction in the capacity is not observed in the two ISUM results, while it is seen when the Smith's method using average stress-average strain relationships based on a beam-column approach is applied. These behaviour strongly depends on the element characteristics, that is, whether the load shedding in the elements beyond their ultimate strength is correctly accounted or not. In this sense, the present ISUM elements seem to have been failed to simulate load shedding behaviour of the element. To simulate the capacity reduction beyond the ultimate hull girder strength, it is necessary to account the influences of the localisation of yielding and deformation after the ultimate strength has been attained. Figure 4.8 shows an example of such localisation of the deformation beyond the ultimate hull girder strength in case of a Suez-max size tanker (FEM analysis, JSRA 2000). Sensitivity of the ultimate hull girder strength to element characteristics shall be discussed in the following two sections.

The calculated ultimate strength, M_u, of the four existing vessels is compared in Figures 4.9 (a) through (d) together with two simple measures, the initial yielding strength, M_{ys} and M_{yh}, and the initial buckling strength, M_{bs} and M_{bh}, of the deck and the bottom plate, respectively. Here,

$$M_{ys} = \sigma_{Ypd} Z_d; \qquad M_{bs} = \sigma_{crd} Z_d \tag{4.3}$$

$$M_{yh} = \sigma_{Ypb} Z_b; \qquad M_{bh} = \sigma_{chb} Z_b \tag{4.4}$$

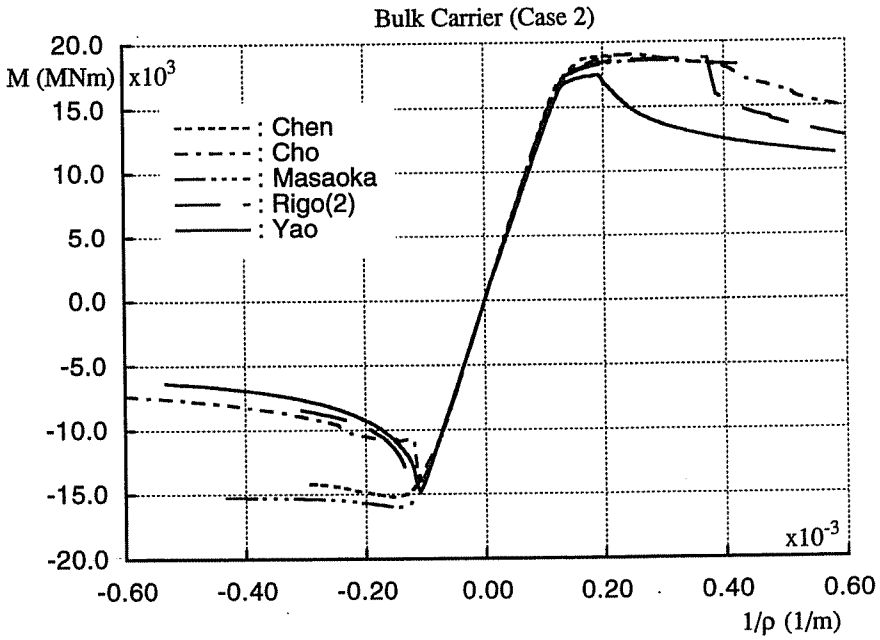

(a) Bulk Carrier (Cape size)

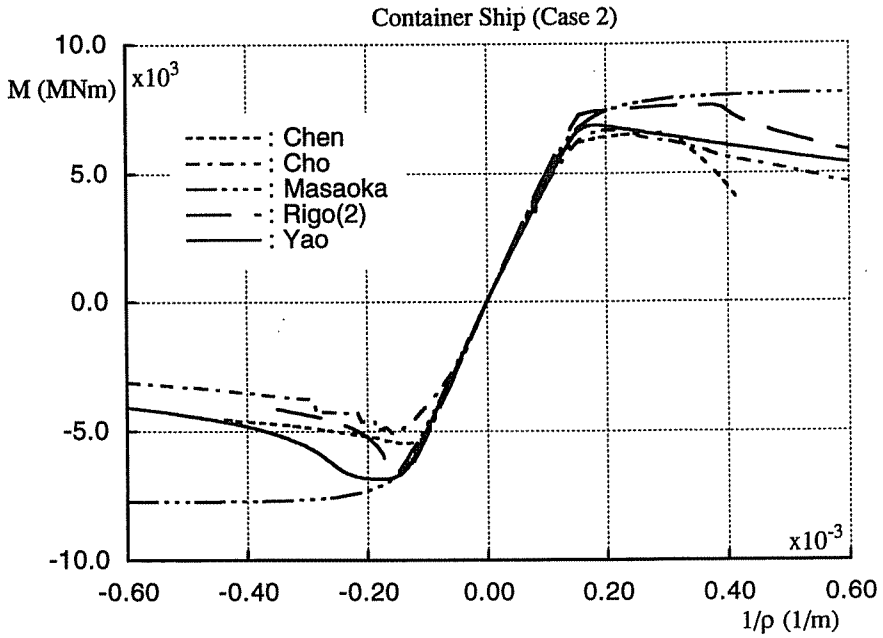

(b) Container Ship

Figure 4.7: Moment-curvature relationships

where Z_d and Z_b are elastic section modulus for the deck and the bottom, respectively, calculated by I_y and z_G in Tables 4.7 through 4.11. σ_{crd} and σ_{crb} are local buckling stress of the deck and the bottom panel assuming simply supported condition, and the plasticity correction given by Eqn. 7.5 is performed. σ_{Ypd} and σ_{Ypb} are the yield stress of the material of the deck and the bottom plating, respectively.

In Figure 4.9, all the moments are made non-dimensional by the corresponding fully plastic bending moment, M_P, indicated in Tables 4.7 through 4.11.

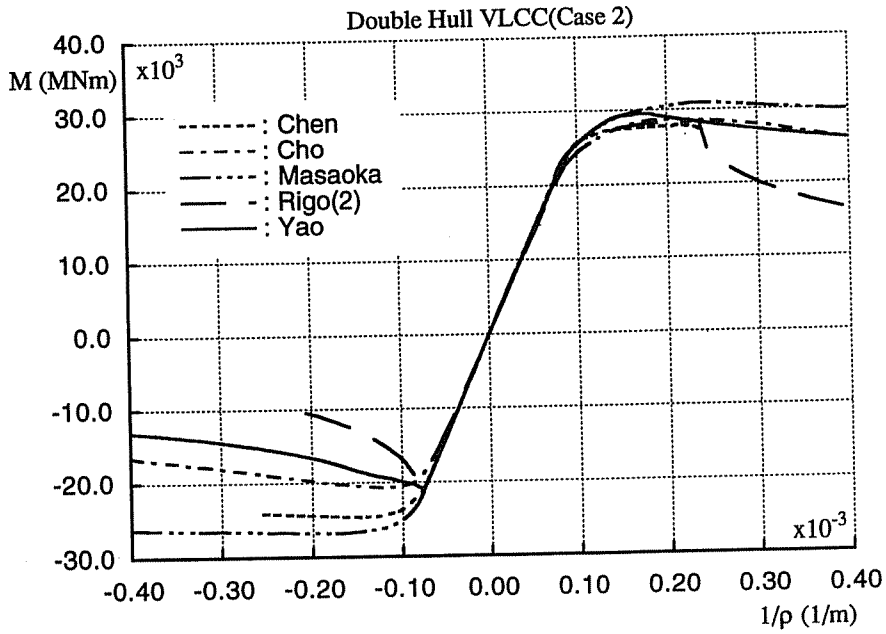

(c) Double Hull VLCC

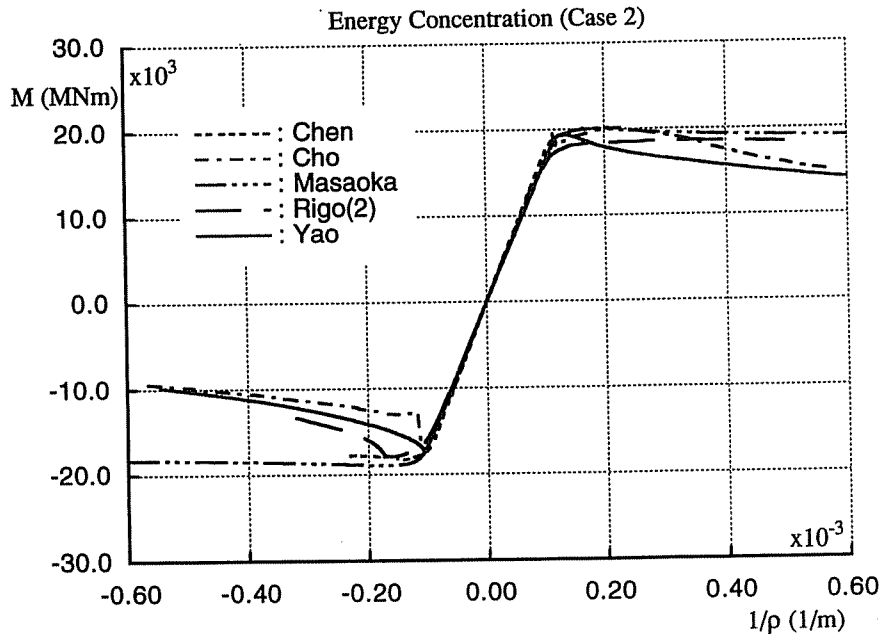

(d) Single Hull VLCC; *Energy Concentration*

Figure 4.7: Moment-curvature relationships (continued)

It is seen that initial yielding strength and initial buckling strength by different methods are almost the same although few exceptions exist. This implies that the modelling applying different methods are fundamentally correct.

The next point which should be noticed is the relationships between these simple measures and the evaluated ultimate hull girder strength. Although there are some exceptional cases, it can be said that, under the sagging condition, the initial yielding strength shows relatively good correlations with the ultimate hull girder strength but in general gives a little lower estimation.

On the other hand, under the hogging condition, the initial yielding strength, M_{yh}, is sometimes higher than the fully plastic bending moment, M_P. This is the case when neutral axis of the cross-section is located at lower part of the cross-section and the stress (based on the elastic moment of

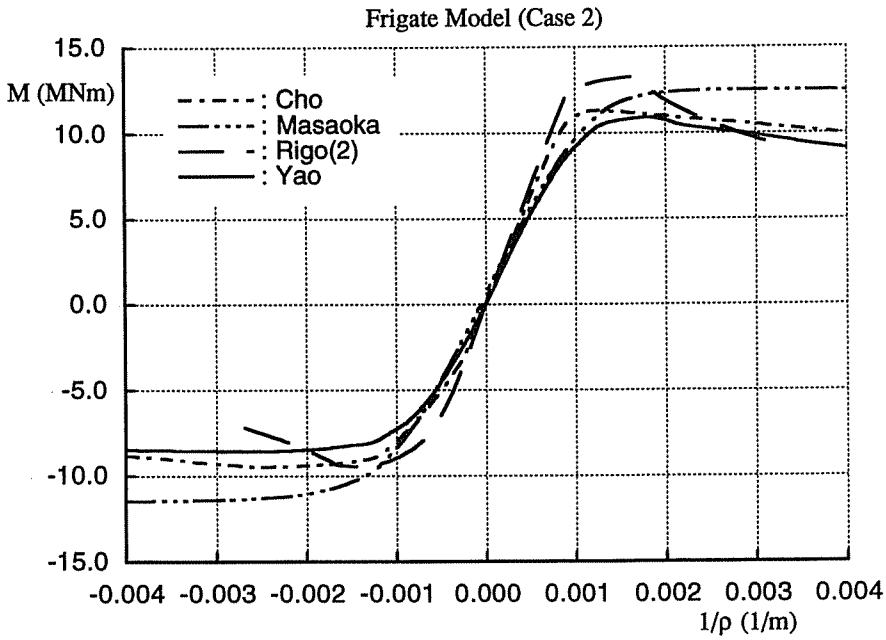

(e) 1/3-Scale Frigate Model

Figure 4.7: Moment-curvature relationships (continued)

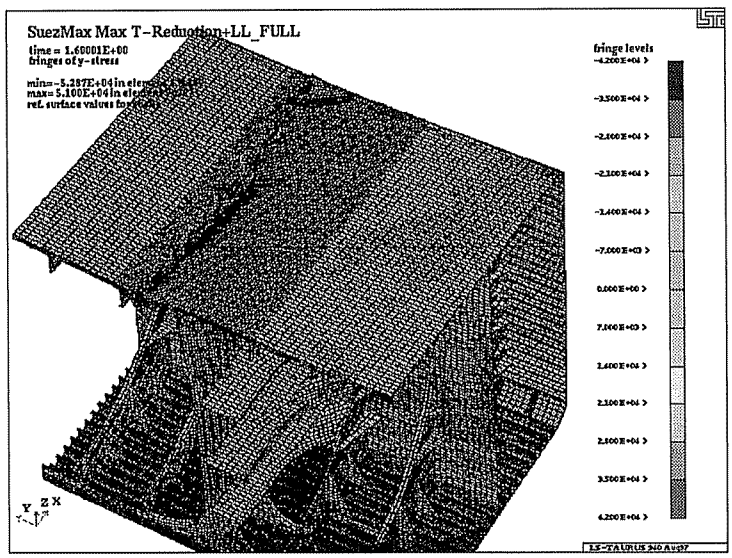

Figure 4.8: Collapse mode of handy-sized tanker in sagging (FEM analysis; JSRA 2000)

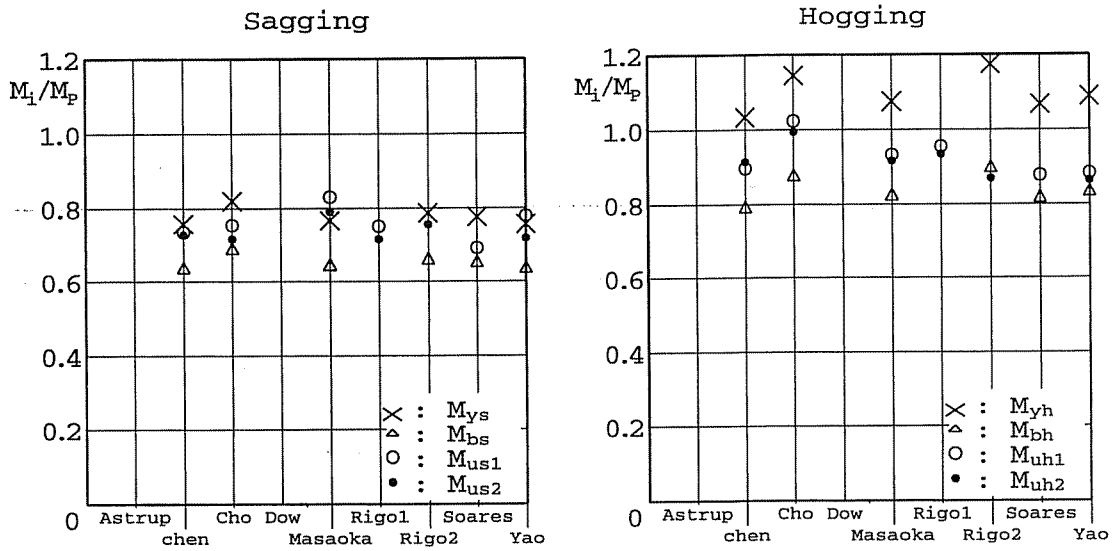

(a) Bulk Carrier

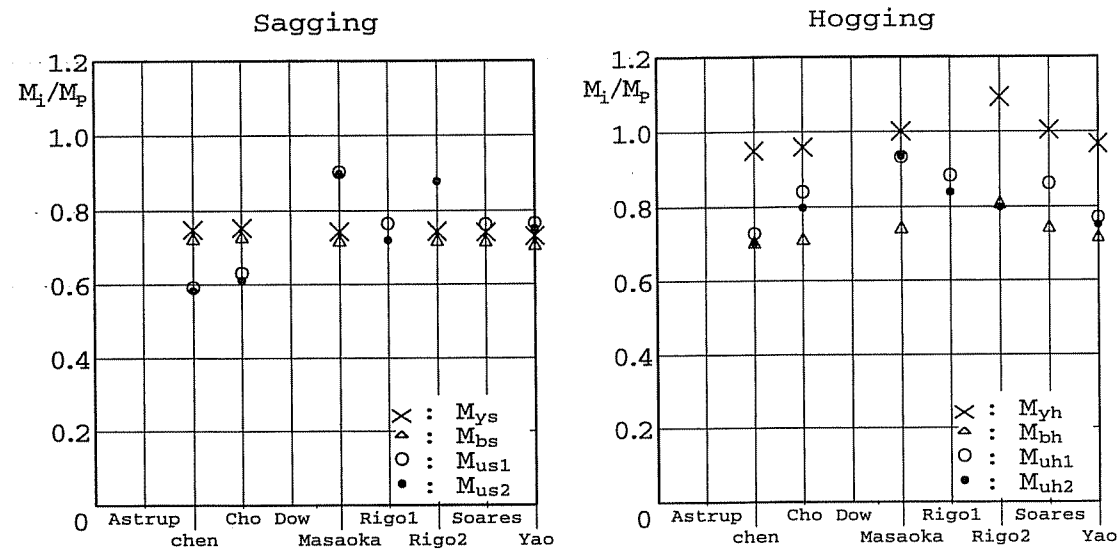

(b) Container Ship

Figure 4.9: Comparison of ultimate strength with simple measures

inertia) near the deck is higher than the yield stress. For this fictitious stress distribution, M_{yh} is higher than M_P. In this case, the initial buckling strength, $M_{bh} = \sigma_{crb} Z_b$ gives a better estimate of the ultimate hull girder strength than M_{yh} in general on the conservative side.

4.4 Influence of Element Characteristics on Progressive Collapse Behaviour

Buckling and yielding of structural members affect the overall collapse behaviour of a ship hull cross-section under longitudinal bending. Figure 4.10 (a) schematically illustrates an average stress-average strain relationship of a stiffened plate member composed of a stiffener and attached plating under axial

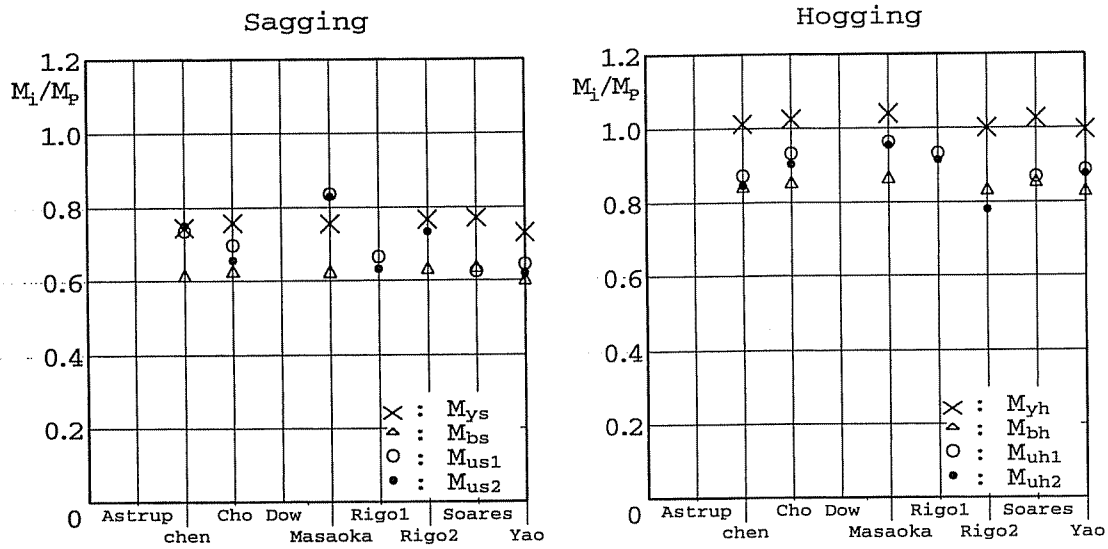

(c) Double Hull VLCC

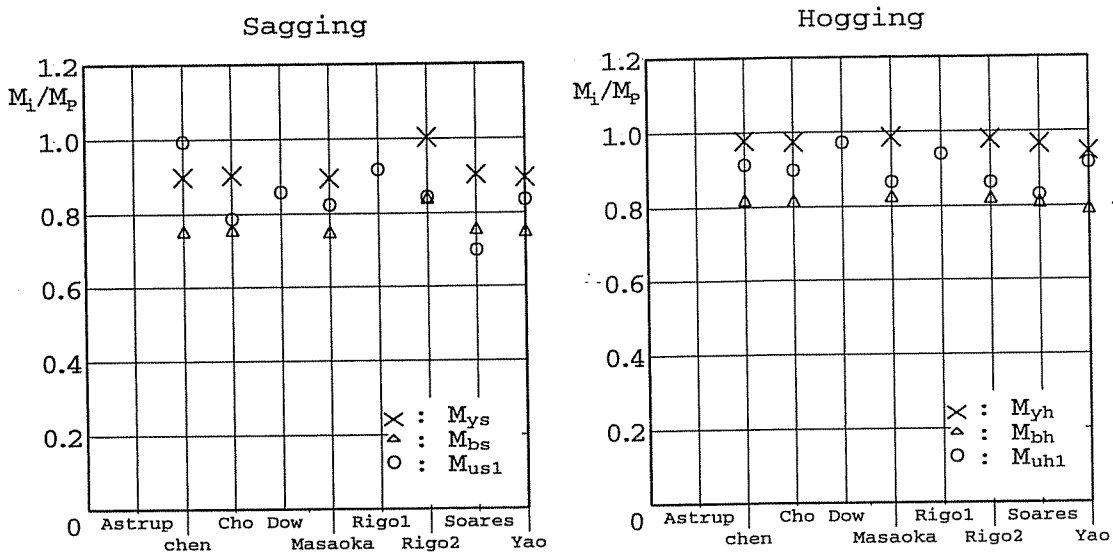

(d) Single Hull VLCC; *Energy Concentration*

Figure 4.9: Comparison of ultimate strength with simple measures (continued)

compression.

Four typical cases are considered, which are:

(1) Case A: linear relationship,

(2) Case B: bi-linear relationship assuming elastic-perfectly plastic material,

(3) Case C: relationship considering bucking but not the strength reduction beyond ultimatestrength,

(4) Case D: relationship considering buckling and the strength reduction beyond ultimate strength.

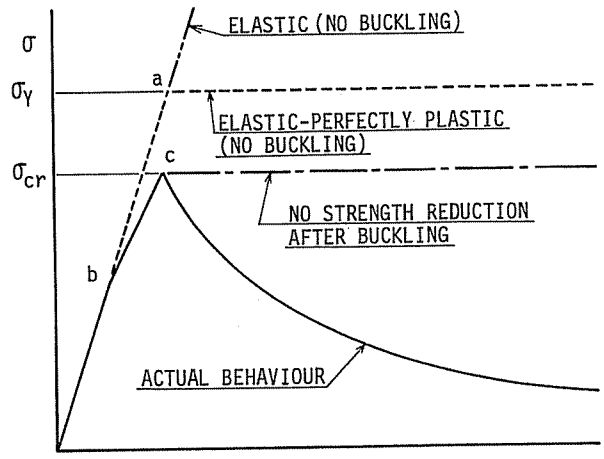

(a) Assumed average stress-average strain relationship of elements

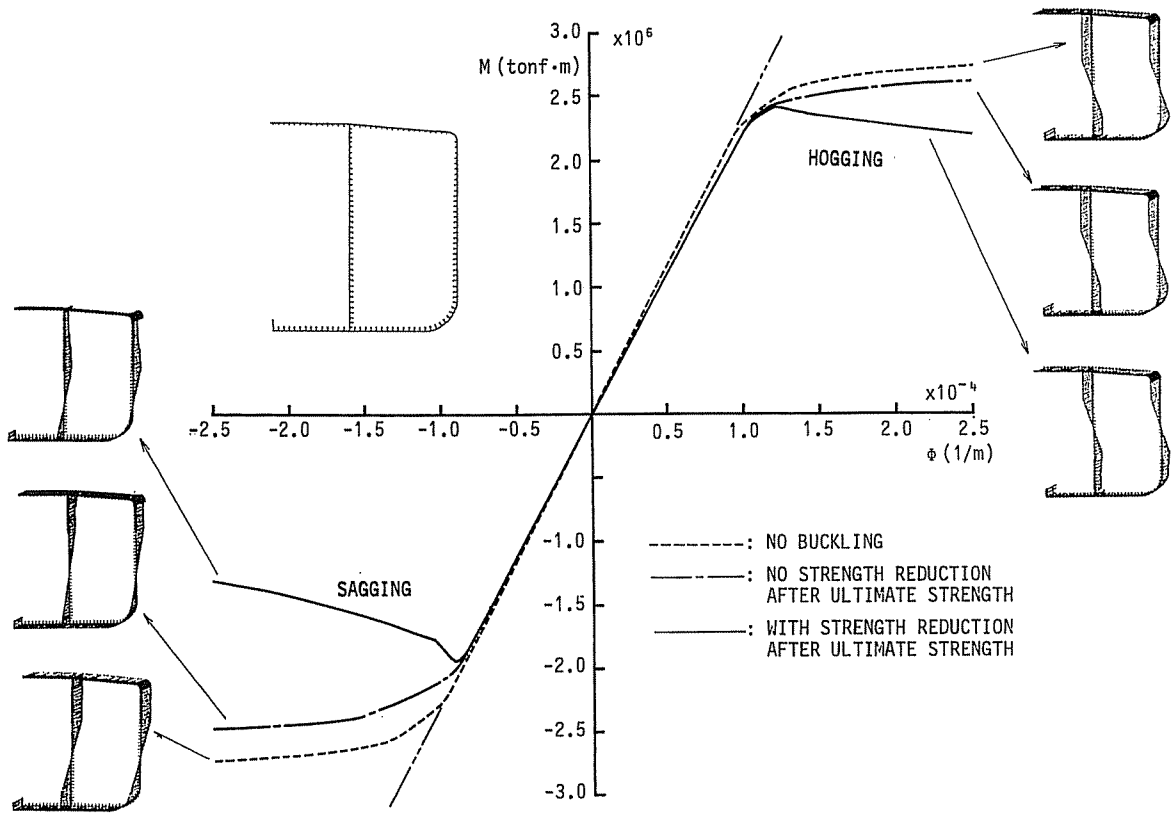

(b) Moment-curvature relationships of cross-section

Figure 4.10: Progressive collapse behaviour of cross-section of ship-hull girder subjected to longitudinal bending

When evaluating the ultimate longitudinal strength of a cross-section, it is often assumed that the structural members of which ultimate strength has been attained cannot carry additional load.

This implies that the capacity after the ultimate strength is constant. This behaviour corresponds to Case C, and is indicated by the chain line with one dot in Figure 4.10 (a). However, the capacity of structural members in a real structure decreases beyond the ultimate strength as indicated by the solid line in Figure 4.10 (a). This is Case D.

The progressive collapse analysis with these four classifications of average stress-average strain relationships shows the influence of buckling and yielding on the collapse behaviour. Figure 4.10 (b) shows the moment-curvature relationships corresponding to these four stress-strain relationships.
When both buckling and yielding do not occur, the moment-curvature relationship is linear as indicated by the chain line with two dots in Figure 4.10 (b). When the yielding of the material is introduced, the deck initially undergoes yielding, and then the bottom. With the increase in the curvature, yielded regions spread in the side shell and the longitudinal bulkhead towards the plastic neutral axis of the cross-section. In this case, the stresses in the yielded parts are kept constant, and a fully yielded condition is attained at the final stage. The maximum bending moment that the cross-section can carry is equal to the fully plastic bending moment.
In the above two cases where the buckling is excluded, the moment-curvature relationship under the sagging condition is equal with that under the hogging condition when the yield stress of the material in compression and tension are the same. On the other hand, the moment-curvature relationship and the maximum bending moment are different under the sagging and the hogging conditions when buckling takes place, since the buckling strength of the deck differs from that of the bottom. The chain line with one dot in Figure 4.10 (b) represents the moment-curvature relationship when strength reduction of the members beyond their ultimate strength is not considered. For the actual case where the capacity of individual members in compression decreases beyond their ultimate strength, the solid line in Figure 4.10 (b) represents the moment-curvature relationship. In this case, the bending moment shows a peak value at a certain value of the curvature, which is defined as the ultimate hull girder strength, and then decreases with the increase of curvature according to the reduction in capacity of individual members.
Such influences of element characteristics shall be discussed more systematically in the next section.

4.5 Assessment of the sensitivity of ultimate hull girder strength with respect to average stress-average strain relationships

Usually progressive collapse analysis to evaluate the ultimate bending moment of hull girder is achieved in three steps. Each step is characterised by a numerical model associated applying specific theoretical assumptions. For each available model, it is necessary to specify their assumptions and to assess their influence (sensitivity) on the result (ultimate bending moment of hull girder).
At the beginning of a "Progressive Collapse Analysis" (called PCA), there are the "raw data" that are the same for each model/user. These data concern:
- the scantling (plates, stiffeners, ..) of the midship section and the frame spacing,
- the initial imperfections (plate deflection, stiffener deflection and residual stress).

The three main steps of a complete "Progressive Collapse Analysis" (PCA) are the followings:
STEP 1: Modelling (the discretisation of the structure into elements, to establish the mesh),
STEP 2: Evaluate the average stress-average strain curve of each element. This requires a stress-strain model called "STR" model.
- STEP 2.1: To calculate the compressive ultimate strength of each element (defined as σ_u). This requires the modelling of the initial imperfections and boundary conditions.
- STEP 2.2: To fix the "shape" of the average stress-average strain curves

NB: Steps 2.1 and 2.2 can be performed together in the same routine (HULLST, Yao §*4.2*) or separately (Rahman and Chowdhury 1996).

STEP 3: Perform the progressive collapse analysis (using a "PCA" model including an incremental procedure)

In order to choose a method to evaluate the ultimate strength of a hull girder, the user has to select two models, one for STEP 2 (the "STR" model) and one for STEP 3 (the "PCA"

model).
Most of the PCA models are based on the Smith's model. This means that the fundamentals of the PCA models are the same. Only the quality of the numerical procedure can generate some differences between the different PCA models. Their quality is also strongly influenced by the discretisation (STEP 1). In fact, the mesh model of the considered structure (STEP 1) depends on the considered PCA model and the available elements: plates, stiffeners, stiffened plates, stiffened panels, curved elements, hard corners, *etc.*
In short, it can be said that a PCA model is "better" than others finer the discretisation is. For instance, the simplified Rahman progressive collapse model (Rahman and Chowdhury1996) uses the same fundamentals as the more sophisticated HULLST model (Yao, *4.2*) but is less accurate as it requires a simplified discretisation.
To provide reliable information to select a relevant "STR" model (Step 2), it is necessary to assess separately the sensitivity of STEP 2 on the ultimate bending moment. The next comparison is a quantification of this sensitivity.
Ultimate bending moment (M_u) of three ships (Double Hull VLCC, *Energy Concentration* and Container Ship) used in the previous benchmark calculation are evaluated with different STR models (Step 2) but with the same PCA model (Step 1 and Step 3). The PCA model is the one included in the HULLST software (Yao *4.2*). Rigo (1998) performed a link between this PCA model and four STR models developed by different authors (Paik *et al.* 1997; Hugues 1988; Rahman and Chowdhury 1996; Dowling *et al.* 1991; Yao and Nikolov 1992).
For each ship an identical mesh model is used, including hundred and five (105) elements for the VLCC, ninety (90) elements for Energy Concentration and ninety-nine (99) elements for the Container Ship. *Only the stress-strain curves differ.*
In addition to the HULLST stress-strain curve [*defined as the reference analysis*] that provides a fully computed average stress-average strain curves, simplified stress-strain curves are considered. They are composed of a perfect elastic deflection, a plastic deflection and a linear post-collapse deflection (Shape 1 to Shape 5 in Figure 4.11).
In order to compare different stress-strain curves of the same element, it is proposed to classify the curves on their main characteristics:
- the element ultimate compressive stress and strain which are denoted as "σ_u" and "ε_u",
- the "shape" of the stress-strain curves.

Based on the calculation of the ultimate strength of each element (σ_u) with the four different models, four average stress-average strain curves are obtained for each element with the same shape (same plastic and post-collapse deflection, shape 3). They only differ by the level of "σ_u".
These four sets of curves were used to compute the ultimate bending moment (M_u) using the same

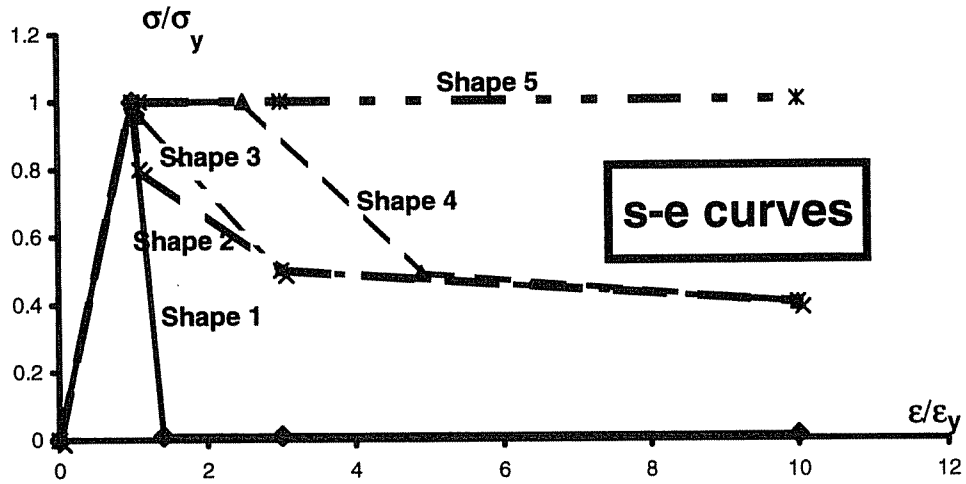

Figure 4.11: Assumed stress-strain relationships for sensitivity analysis

TABLE 4.12

SENSITIVITY OF THE ULTIMATE STRENGTH OF ELEMENTS ON ULTIMATE HULL GIRDER STRENGTH (SAME MESH (STEP 1); SAME $\sigma-\varepsilon$ CURVES (STEP 2.2); SAME PCA (STEP 3))

SAGGING	VLCC (105 elements)				ENERGY CONCENTRATION (90 elements)				CONTAINER SHIP (99 elements)			
	S(ult) of elements		Ult. Bending Moment		S(ult) of elements		Ult. Bending Moment		S(ult) of elements		Ult. Bending Moment	
sig-eps models (STR) (same shape)	Sm = Su(av)/Sy	Sm/Sm(av)	Mu 1000 MN.m	Mu/M(av)	Sm = Su(av)/Sy	Sm/Sm(av)	Mu 1000 MN.m	Mu/M(av)	Sm = Su(av)/Sy	Sm/Sm(av)	Mu 1000 MN.m	Mu/M(av)
model 1	0.823	1.035	21.02	1.069	0.874	1.022	16.32	1.043	0.756	1.000	6.01	1.025
model 2	0.820	1.031	20.94	1.065	0.871	1.019	16.43	1.050	0.776	1.026	6.08	1.036
model 3	0.757	0.952	18.01	0.916	0.837	0.979	14.73	0.941	0.753	0.996	5.63	0.960
model 4	0.782	0.983	18.71	0.951	0.838	0.980	15.11	0.966	0.740	0.979	5.74	0.979
	0.7955 = Sm(av)	**3.27%** Mean Variation	19.67 = M(av)	**6.66%** Mean Variation	0.855 = Sm(av)	**2.05%** Mean Variation	15.6475 = M(av)	**4.65%** Mean Variation	0.75625 = Sm(av)	**1.31%** Mean Variation	5.866 = M(av)	**3.09%** Mean Variation

Su = compressive ultimate strength of one element Sy = yield stress Mu = Ultimate bending moment

Su(av)= Su average value of all the elements of the ship (for instance :105 for the VLCC)

HOGGING	VLCC (105 elements)				ENERGY CONCENTRATION (90 elements)				CONTAINER SHIP (99 elements)			
	S(ult) of elements		Ult. Bending Moment		S(ult) of elements		Ult. Bending Moment		S(ult) of elements		Ult. Bending Moment	
sig-eps models (STR) (same shape)	Sm = Su(av)/Sy	Sm/Sm(av)	Mu 1000 MN.m	Mu/M(av)	Sm = Su(av)/Sy	Sm/Sm(av)	Mu 1000 MN.m	Mu/M(av)	Sm = Su(av)/Sy	Sm/Sm(av)	Mu 1000 MN.m	Mu/M(av)
model 1	0.823	1.035	28.60	1.013	0.874	1.022	18.71	1.023	0.756	1.000	6.472	1.016
model 2	0.820	1.031	29.29	1.037	0.871	1.019	18.64	1.019	0.776	1.026	6.5	1.020
model 3	0.757	0.952	27.26	0.965	0.837	0.979	17.76	0.971	0.753	0.996	6.26	0.982
model 4	0.782	0.983	27.82	0.985	0.838	0.980	18.05	0.987	0.740	0.979	6.26	0.982
	0.7955 = Sm(av)	**3.27%** Mean Variation	28.2425 = M(av)	**2.49%** Mean Variation	0.855 = Sm(av)	**2.05%** Mean Variation	18.29 = M(av)	**2.10%** Mean Variation	0.75625 = Sm(av)	**1.31%** Mean Variation	6.373 = M(av)	**1.77%** Mean Variation

TABLE 4.13
SENSITIVITY OF THE SHAPE OF STRESS-STRAIN RELATIONSHIP
ON ULTIMATE HULL GIRDER STRENGTH
(SAME MESH (STEP 1); SAME ELEMENT σ_u (STEP 2.1); SAME PCA (STEP 3))

SAGGING	VLCC 105 elements		ENERGY CONCENTRATION 90 elements		CONTAINER 99 elements	
Type of s-e shape (same S(ult), Eps(Ult))	Mu 1000 MN.m	Mu/M(ref)	Mu 1000 MN.m	Mu/M(ref)	Mu 1000 MN.m	Mu/M(ref)
M(ref) (Yao 1999)	20.42		16.84	1.000	6.72	
Shape 1	19.64	0.962	16.27	0.966	5.77	0.859
Shape 2	20.38	0.998	16.28	0.967	5.89	0.876
Shape 3	20.94	1.025	16.43	0.976	6.08	0.905
Shape 4	25.65	1.256	18.91	1.123	7.15	1.064
Shape 5	27.91	1.367	19.39	1.151	7.35	1.094
Mean Variation		13.77%		7.32%		10.35%

M(ref) = Ultimate bending moment obtained with the HULLST software

HOGGING	VLCC 105 elements		ENERGY CONCENTRATION 90 elements		CONTAINER 99 elements	
Type of s-e shape (same S(ult), Eps(Ult))	Mu 1000 MN.m	Mu/M(ref)	Mu 1000 MN.m	Mu/M(av)	Mu 1000 MN.m	Mu/M(av)
M(ref) (Yao 1999)	28.88		19.03	1.000	6.72	
Shape 1	28.89	1.000	18.49	0.972	5.95	0.885
Shape 2	28.89	1.000	18.49	0.972	6.27	0.932
Shape 3	29.29	1.014	18.69	0.982	6.50	0.967
Shape 4	31.03	1.074	19.87	1.044	7.06	1.050
Shape 5	31.26	1.082	20.41	1.072	7.11	1.058
Mean Variation		3.43%		3.82%		6.46%

PCA model. Table 4.12 gives the influence of the element ultimate strength (σ_u) on the ultimate bending moment (M_u). It is observed that a variation of 1% in the ultimate strength of the elements induces a variation of the ultimate bending moment of 1% and 2% for sagging and hogging, respectively. **This means that an uncertainty of 10% on σ_u induces an uncertainty of roughly 20% on the sagging ultimate bending moment.**

On the other hand, to assess the impact of the "shape" of the stress-strain curves on the ultimate bending moment (M_u), a second group of average stress-average strain curves is defined. They are characterised by the same element ultimate strength (σ_u) but different shapes. As five different standard shapes are considered, shown in Figure 4.11, five sets of σ-ε curves are defined. Using these new sets of curves to evaluate the ultimate bending moment (M_u), the sensitivity of the "shape" on the ultimate bending moment can be quantified (see Table 4.13).

Shape 1 has not post collapse strength. Shape 5 is the perfect elastoplastic curves. Shapes 2, 3 and 4 are between shapes 1 and 5. Shape 3 corresponds to the stress-strain curve proposed by Hughes (1988). Shape 4 is similar to shape 3 with an extended plastic plateau. These five standard shapes in Figure 4.11 are compared to a reference shape defined by HULLST (Yao in *4.2*).

Table 4.13 shows that the shape sensitivity on M_u is higher for sagging than hogging. Between shape 1 (no post collapse strength) and shape 5 (perfect elastoplastic strength) the variation is about 25% in sagging and 12% in hogging.

Comparison between shape 3 and shape 4 shows that the length of the plastic plateau is the more sensitive parameter. An overestimation of the plastic plateau (shape 4) increases the ultimate bending moment by 10 to 20%. On the other hand, shape 2, which has no plastic plateau, provides also acceptable results (M_u is accurate for the VLCC; M_u is underestimated by 3% for *Energy Concentration* and about 7% for Container Ship).
The above results demonstrate that the main significant factor in the complete procedure to evaluate the ultimate bending moment is the STEP 2.1: Evaluation of the ultimate compressive strength of the elements/components (σ_u). Moreover, results show that the "shape" (Step 2.2) is not negligible and particularly the length of the plastic plateau.
This conclusion is not surprising as the main uncertainties and numerical assumptions are linked with STEP 2.1 (for instance: modelling of the initial imperfections and the boundary conditions, considering local buckling like tripping, bi-axial compression, lateral loading, and so on).

5 EFFECTS OF LOAD COMBINATIONS AND IN-SERVICE DAMAGE ON ULTIMATE STRENGTH

5.1 Combined Load Effects on Element Characteristics

The stress picture in real ship structures tends to become very complicated. The load bearing capacity of the stiffened panel depends on the actual stress distribution, and may be the result of several load actions. Local panel stiffness variations and constraints add to the complexity. The task of determining the detailed stress distribution in a part of the ship structure, will in reality involve large scale numerical analysis using the Finite Element method. For some structures, it may even be necessary to perform fully non-linear FE analyses to determine the actual stress distribution due to the local non-linear response rising from initial deformations, residual stresses and fabrication tolerances. This picture becomes even more complicated when the goal is to assess the ultimate load carrying capacity of the structure.
It is therefore important that the simplified capacity models discussed in the previous chapter includes the most important effects on the ultimate load bearing capacity from combined load actions. The different loads are treated separately in order to assess the effect on the ultimate stiffened panel capacity.
The ultimate load of stiffened panels under combined loads can be obtained by using various combinations of load control, e.g. by displacement-displacement control, load-displacement control or load-load control. Fujikubo *et al.*(1997) and Yao *et al.*(1997b) has shown that the influence of loading method on the ultimate collapse load is negligible. This is also reflected by the majority of the studies on combined load effects reported in the literature.

5.1.1 Effect of Lateral Pressure

A lateral pressure will in general tend to reduce the elasto-plastic collapse load of the stiffened panel. The degree of reduction depends on which side the pressure is acting (plate or stiffener side) due to the anti-symmetric nature of the panel. However, for very slender stiffeners it can be observed that for lateral pressure ($p > 0$) acting on the plate side, may give rise to a higher collapse load than no lateral pressure. This phenomenon is particularly observed for strongly asymmetric panels. The reason for this behaviour is that the lateral pressure gives tension bending stresses in the stiffener flange which delays the onset of compressive yielding under axial loading (stiffener induced failure). On the other hand, bending stresses become larger as the water head increases. Because of this, yielding will take place earlier which results in reduced ultimate strength. Owing to these two opposing effects, the buckling/plastic collapse of a stiffened plate has its maximum value at a certain magnitude of lateral pressure.

The in-plane stiffness of the panel is an important characteristic which will influence the level of

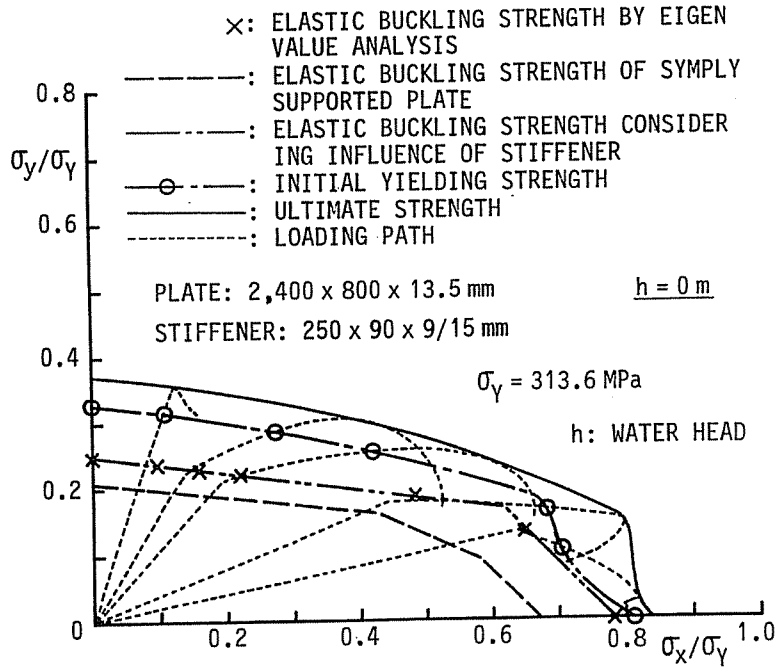

Figure 5.1: Loading path and ultimate strength interaction relationship for a stiffened panel under bi-axial thrust

redistribution of loads in large plated structures. Steen (1995) documented that the initial stiffness under the action of transverse loads are reduced by the order of 40% with the presence of initial imperfections consistent with normal shipbuilding standards. Steen (1995) also documented that the transverse buckling capacity is less sensitive to lateral pressures than the longitudinal buckling capacity.
Yao *et al.*(1997b) also proposed an empirical formula to calculate the buckling strength of a continuous stiffened plate field including the effect of lateral pressure which shows good correlation with numerical FEM analyses.

5.1.2 Effect of Transverse Thrust

Figure 5.1 shows a typical relationship between average stresses in the longitudinal and transverse direction for a stiffened plate field. The curves are obtained by elasto-plastic large deflection FEM analyses of a stiffened plate subjected to bi-axial thrust (Yao *et al.* 1997a). The dotted lines show the loading path, and the open circles represent the onset of yielding. The solid line obtained as the envelope of the dotted lines represents the ultimate strength interaction relationship.

5.1.3 Effect of Shear Loads

Available results on the effect of shear loads on the ultimate capacity of stiffened panels are scarce. Some results are reported by Steen and Balling Engelsen (1997) for un-stiffened plates using the non-linear Finite Element Method . Plates with aspect ratio 3 and 5 and slenderness ratio varying from 0.2 to 2.0 have been studied. The general observation made in Steen's paper is that the ultimate shear strength is close to the shear yield strength for all the plates. The slenderness dependencies for ultimate capacity are weak and the ideal elastic buckling level is far below the ultimate strength for the more slender plates. The reason for this significant strength reserve beyond the elastic buckling is due to the tension field developing along the diagonal in the plate. In order for the tension field to develop, the

tension forces must be transmitted to neighbouring plate fields in a real structure. This is a realistic assumption for large plate fields, but not for webs in girders.

5.2 *Combined Load Effects on Ultimate Hull Girder Strength*

5.2.1 *Effect of Horizontal Bending*

A ship is in general subjected to both horizontal and vertical bending moments, especially in a rough sea with significant roll motions.
Figure 5.2 shows the interaction between vertical and horizontal bending on the hull girder strength for double hull tanker (Yao *et al.* 1994). The dashed lines represents the horizontal/vertical moment paths for different curvature ratios. The enclosing envelope (solid line) represents ultimate strength interaction relationship. The broken line represents the interaction relationship of the initial yielding strength calculated using elastic section modulus. The reserve above initial yielding up to ultimate

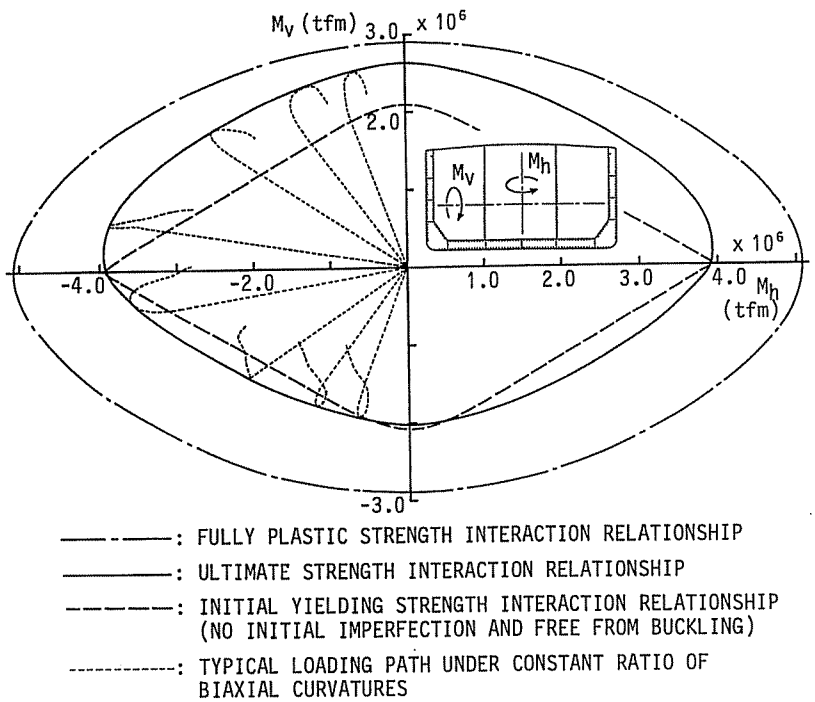

Figure 5-2: Ultimate hull girder strength interaction relationship under combined vertical and horizontal bending.

strength is small under pure vertical bending, and is even negative in sagging. This is because the buckling collapse of the deck part takes place below the linearly calculated initial yielding strength. In this case, buckling collapse directly results in overall collapse of the section with no possibilities for stress redistribution. The ultimate hull girder strength under horizontal bending is in general higher than that under vertical bending. This is because the ship's breadth is usually larger than its depth.
Ultimate hull girder strenth under combined vertical/horizontal bending is discussed also by Mansour *et al.*(1995) and Paik *et al.*(1996). Gordo and Guedes Soares (1997) proposed a simple formulation for tankers and container ships under combined bending. Rizzuto (1997) also discussed on this subject.

5.2.2 *Effect of Vertical Shear Force*

The vertical shear force in a ship hull is sustained by the side shell plating and additional longitudinal bulkheads. The effect of the vertical shear force can be accounted for in a simplified manner through the following steps (JMT 1997):

- The sharing ratio between side shell and additional bulkheads must be determined, either by a simplified method or by a shear flow calculation.
- Calculate the working shear stress in the cross-section;
- Reduce the yield stress at each element according to $\sigma_{Ys} = (\sigma_Y^2 - 3\ \tau^2)^{1/2}$ where τ is the shear stress corresponding to the vertical shear force in the ship hull cross-section;
- Reduce the compressive buckling strength according to the interaction relationship:

$$\left(\frac{\sigma_{cr}}{\sigma_{cr0}}\right)^2 + \left(\frac{\tau}{\tau_{cr0}}\right)^2 = 1$$

σ_{cr0} and τ_{cr0} are the buckling strength when pure compression and pure shear load are applied, respectively.

For merchant ships with a closed cross-section (i.e. tankers), the influence of the shear force is negligible for normal operational loads. For other ship types, (i.e. bulk carriers, ro-ro and container ships), data are not so enough to draw any firm conclusions on the effect of shear force on the ultimate hull girder strength, although some results are reported (Paik 1994a; Paik *et al.* 1996).

5.3 *Effects of In-Service Damage on Ultimate Hull Girder Strength*

5.3.1 *Effect of Corrosion Damage*

The effect of corrosion damage can be assessed indirectly by a sensitivity study on the influence of plate and stiffener thickness on ultimate hull girder capacity. Jensen *et al.*(1994) has carried out a sensitivity study on the ultimate hull girder capacity of four typical merchant ships (two VLCCs and two Bulk Carriers). The study clearly shows that a thickness reduction in the bottom plating largely

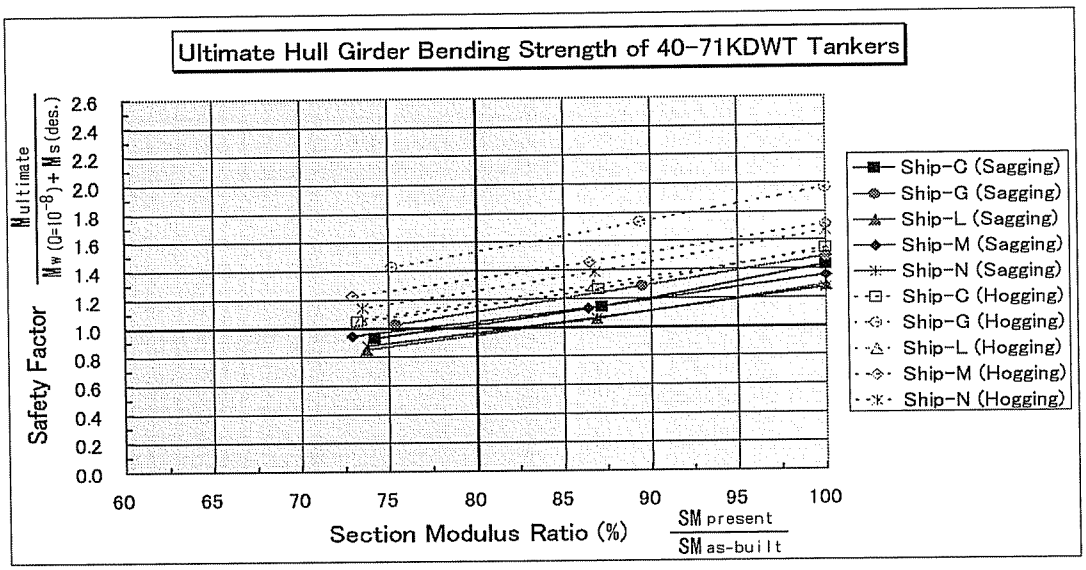

(a) Handy size tankers

Figure 5.3: Relationships between reductions of section modulus and ultimate hull girder strength

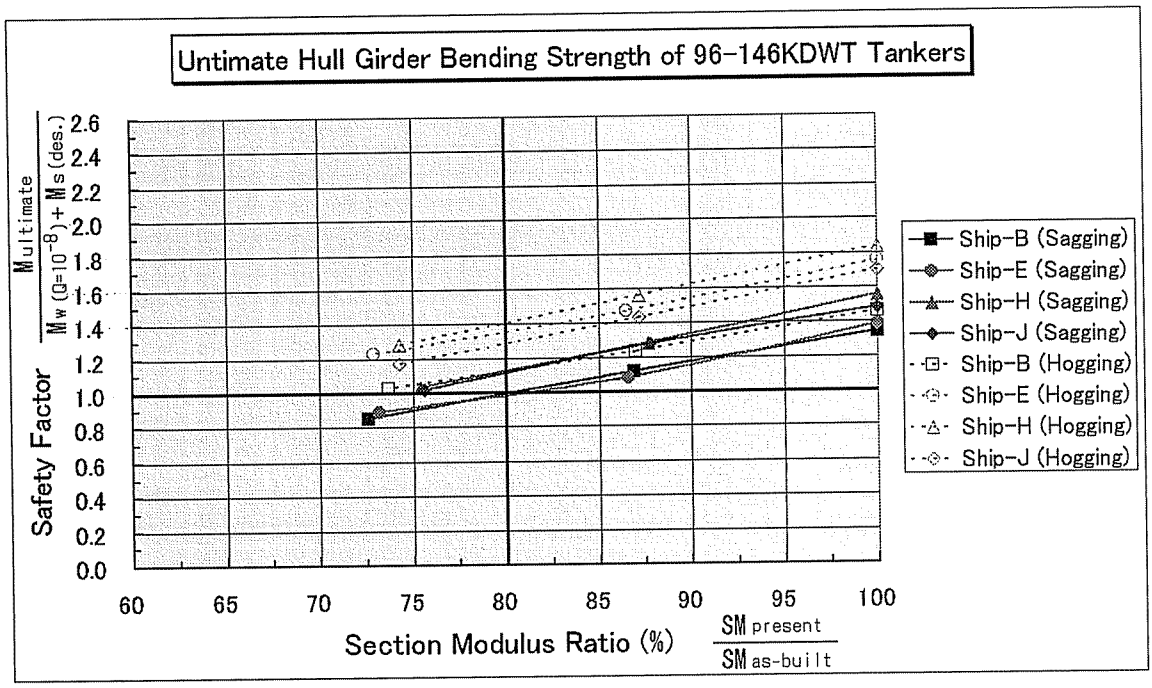

(b) Suez-max zise tankers

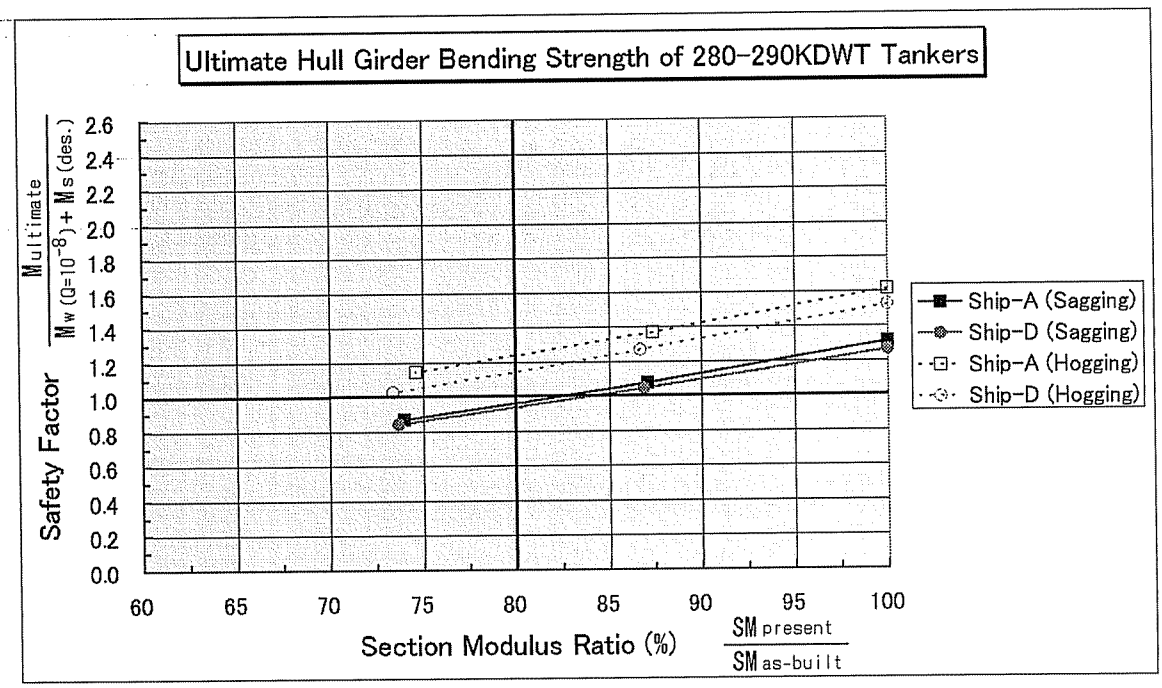

(c) VLCCs

Figure 5.3: Relationships between reductions of section modulus and ultimate hull girder strength (continued)

affects the hogging strength, while a thickness reduction in the deck plating largely reduces the sagging strength. This is a general observation for all four ships.

Yao *et al.*(1994) reported on a case study of a double hull tanker where the effect of corrosion damage on the hull girder capacity has been assessed. Yao calculated that a 30% overall reduction in the plate thickness leads to a strength reduction of 34% and 38% in the sagging and the hogging condition, respectively. Another studies also report on strength reduction of similar magnitudes for a bulk carrier (Yao *et al.* 1993b) and eleven single hull tankers

(JSRA 2000). The results for eleven single hull tankers are summarised in Figure 5.3. The ultimate hull girder strength divided by the design bending moment is plotted against the reduced elastic section modulus. It is known that the ultimate hull girder strength is almost linearly decreases with the reduction of the section modulus, and the reduction of 15% of the section modulus is allowable from the viewpoint of the safety for longitudinal strength.

5.3.2 Effect of Collision and Grounding

The ultimate hull girder strength of the collided or grounded hull girder can roughly be evaluated removing the fractured part of the cross-section due to collision or grounding. Such analysis can be easily performed applying simplified method such as the Smith's method.

6 SENSITIVITY OF ULTIMATE HULL GIRDER STRENGTH WITH RESPECT TO VARIOUS FACTORS

6.1 Method of Sensitivity Analysis

The sensitivity of the ultimate longitudinal strength, M_u, with respect to the i-*th* design variable, x_i, can be defined as:

$$S_i = \frac{\partial M_u}{\partial x_i} \tag{6.1}$$

This can be normalised by multiplying μ_{xi}/μ_{Mu} on S_i as:

$$\overline{S}_i = \frac{\mu_{x_i}}{\mu_{M_u}} \cdot S_i = \frac{\partial (M_u/\mu_{M_u})}{\partial (x_i/\mu_{x_i})} \tag{6.2}$$

where μ_{xi} and μ_{Mu} are the mean values of the i-*th* design variable and the ultimate hull girder strength, respectively.
For the sensitivity analysis, design variables shown in Table 6.1 are considered. In Table 6.1, the assumed mean values and their coefficients of variations are indicated, which are used later when the coefficient of variations of the ultimate hull girder strength is estimated.
The mean values of the ultimate hull girder strength is evaluated using the mean values of the design variables in Table 6.1 as:

$$\mu_{M_u} = M_u(\mu_{t_p},\ \mu_{t_s},\ \mu_{\sigma_{MS}},\ \mu_{\sigma_{HT32}},\ \mu_{\sigma_{HT36}},\ \mu_{\sigma_{HT40}},\ \mu_{\sigma_{rc}},\ \mu_{w_{p0}},\ \mu_{w_{s0}},\ \mu_{v_{s0}}) \tag{6.3}$$

The normalised sensitivity represnted by Eqn. 6.2 is evaluated numerically as follows:

$$\begin{aligned} \overline{S}_i = \frac{\partial M_u/\mu_{M_u}}{\partial x_i/\mu_{x_i}} &= \frac{(M_u^{+5\%} - M_u^{-5\%})/\mu_{M_u}}{(1.05\mu_{x_i} - 0.95\mu_{x_i})/\mu_{x_i}} \\ &= \frac{(M_u^{+5\%} - M_u^{-5\%})}{0.1\mu_{M_u}} \end{aligned} \tag{6.4}$$

where $M_u^{+5\%}$ and $M_u^{-5\%}$ are the ultimate hull girder strength by changing the design variable, x_i, by + 5 % and - 5 %, respectively.

TABLE 6.1
MEAN VALUES AND ASSUMED COEFFICIENT OF VARIATION OF DESIGN VARIABLES

Variables	Mean	COV(%)
t_p	Nominal values	0.6
t_s	Nominal values	0.6
σ_{MS}	29 kgf/mm^2	9.0
σ_{HT32}	37 kgf/mm^2	7.0
σ_{HT36}	41 kgf/mm^2	4.3
σ_{HT40}	45 kgf/mm^2	3.0
σ_{rc}	calculated value	30.0
w_{p0}	calculated value	50.0
w_{s0}	0.0005 L	20.0
v_{s0}	0.0005 L	20.0

t_p: thickness of plates
t_s: thickness of stiffeners
σ_{MS}: yielding stress of Mild Steel
σ_{HT32}: yielding stress of HT32
σ_{HT36}: yielding stress of HT36
σ_{HT40}: yielding stress of HT40
σ_{rc}: compressive residual stress in panel)
w_{p0}: initial deection in panels
w_{s0}: initial deection in stiffeners (e xural buckling mode)
v_{s0}: initial deection in stiffeners (tripping mode)
L: space between tranverse frames

Here, a first order approximation gives a standard deviation of the ultimate hull girder strength as:

$$\sigma_{M_u}^2 = \sum \left(\frac{\partial M_u}{\partial x_i}\sigma_{x_i}\right)^2 = \left(\frac{\partial M_u}{\partial t_p}\sigma_{t_p}\right)^2 + \left(\frac{\partial M_u}{\partial t_s}\sigma_{t_s}\right)^2 + \left(\frac{\partial M_u}{\partial \sigma_{MS}}\sigma_{\sigma_{MS}}\right)^2 + \left(\frac{\partial M_u}{\partial \sigma_{HT32}}\sigma_{\sigma_{HT32}}\right)^2 + \left(\frac{\partial M_u}{\partial \sigma_{HT36}}\sigma_{\sigma_{HT36}}\right)^2 + \left(\frac{\partial M_u}{\partial \sigma_{HT40}}\sigma_{\sigma_{HT40}}\right)^2 + \left(\frac{\partial M_u}{\partial \sigma_{rc}}\sigma_{\sigma_{rv}}\right)^2 + \left(\frac{\partial M_u}{\partial w_{0p}}\sigma_{w_{0p}}\right)^2 + \left(\frac{\partial M_u}{\partial w_{0s}}\sigma_{w_{0s}}\right)^2 + \left(\frac{\partial M_u}{\partial v_{0s}}\sigma_{v_{0s}}\right)^2 \tag{6.5}$$

Each term in the right-hand-side of Eqn. 6.5 can be calculated as follows.

$$\frac{\partial M_u}{\partial x_i}\sigma_{x_i} = \frac{\partial M_u/\mu_{M_u}}{\partial x_i/\mu_{x_i}} \cdot \frac{\mu_{M_u}}{\mu_{x_i}} \cdot \sigma_{x_i} = \frac{\partial M_u/\mu_{M_u}}{\partial x_i/\mu_{x_i}} \cdot \frac{\mu_{M_u}}{\mu_{x_i}} \cdot \mu_{x_i}\mathrm{COV}_{x_i}$$
$$= \frac{\partial M_u/\mu_{M_u}}{\partial x_i/\mu_{x_i}} \cdot \mu_{M_u}\mathrm{COV}_{x_i} \tag{6.6}$$

6.2 Results of Sensitivity Analysis

Calculation is carried out on the Double Hull VLCC, Container Ship, Bulk Carrier and *Energy Concentration* used for benchmark calculations in Chapter 4. The evaluated sensitivities are summarised in Table 6.2 for both sagging and hogging conditions.

TABLE 6.2
NORMALISED SENSITIVITYES OF ULTIMATE HULL GIRDER STRENGTH

variable	Double Hull VLCC		Container Ship		Bulk Carrier		*Energy Concen.*	
	Sagging	Hogging	Sagging	Hogging	Sagging	Hogging	Sagging	Hogging
t_p	0.06640	0.04157	0.8972	1.1366	1.1297	1.0096	1.0880	0.7943
t_s	0.2638	0.3438	0.2387	0.1847	0.3159	0.2486	0.3678	0.3615
σ_{MS}	-	-	-	-	-	-	0.00646	0.01545
σ_{HT32}	0.7836	0.8450	0.3038	0.6036	0.01578	0.3300	0.7248	0.9134
σ_{HT36}	0.01687	0.03834	0.4296	0.2412	0.1023	0.2205	-	-
σ_{HT40}	-	-	-	-	0.5848	0.2784	-	-
σ_{rc}	-0.04922	-0.04738	-0.02149	0.003143	-0.03705	-0.02123	-0.03157	-0.01097
w_{p0}	-0.01272	-0.01548	0.01882	-0.02356	-0.01440	-0.00798	-0.02816	-0.000751
w_{s0}	-0.02125	-0.01604	-0.02209	-0.00666	-0.06975	-0.02156	-0.00980	-0.00283
v_{s0}	0.000259	0.00141	0.000085	-0.0000024	0.000162	-0.001440	0.000079	-0.00237

t_p: thickness of plates
t_s: thickness of stiffeners
σ_{MS}: yielding stress of Mild Steel
σ_{HT32}: yielding stress of HT32
σ_{HT36}: yielding stress of HT36
σ_{HT40}: yielding stress of HT40
σ_{rc}: compressive residual stress in panel)
w_{p0}: initial deection in panels
w_{s0}: initial deection in stiffeners (e xural buckling mode)
v_{s0}: initial deection in stiffeners (tripping mode)

The sensitivities in Table 6.2 are the normalised values, and it is seen from this table which variable is more influencial by comparing the absolute values. According to the calculated results, the most influential parameter is the yielding stress of the material which is widely used in the structure in case of Double Hull VLCC. For other types of ships, thicknesses of the panel and the stiffener are more influencial to the ultimate hull girder strength. It is known that the sensitivity of the ultimate hull girder strength with respect to initial imperfections due to welding is in general small. The sensitivity under the sagging and the hogging condition is different.

6.3 Standard Deviation of Ultimate Hull Girder Strength

Using the evaluated sensitivities together with the coefficients of variations of design variables assumed in Table 6.1, the standard deviation and the coefficient of variation of the ultimate hull girder strength are evaluated by Eqn. 6.5. The calculated results are summarised in Table 6.3. It is known that the COV for a single hull tanker is the largest and that for Bulk Carrier the smallest.

TABLE 6.3
STANDARD DEVIATION AND COEFFICIENT OF VARIATION
OF ULTIMATE HULL GIRDER STRENGTH

	Double Hull VLCC		Container Ship		Bulk Carrier		*Energy Concen.*	
	Sagging	Hogging	Sagging	Hogging	Sagging	Hogging	Sagging	Hogging
σ_{M_u}(MN·m)	903.90	1220.14	241.15	362.22	418.56	548.51	1100.35	1477.99
COV (%)	4.434	5.305	3.121	4.563	2.735	2.841	5.398	6.426

σ_{M_u}: standard deviation of ultimate longitudinal strength
COV: coefcient of variation of ultimate longitudinal strength

7 CONSIDERATION ON ULTIMATE HULL GIRDER STRENGTH FROM DESIGN ASPECT

7.1 Present Design Method for Longitudinal Strength

7.1.1 Conventional Ships

Longitudinal strength of conventional commercial ships such as tankers, bulk carriers *etc.* is discussed from the viewpoint of structural design.
This section refers to the unified IACS (=International Association of Classification Societies) requirements for longitudinal strength including buckling strength formula for conventional commercial ships.
The strengths are conveniently divided into three categories: longitudinal strength, transverse strength and local strength. Longitudinal strength of the hull girder and local strength of the plate panel and the stiffeners are examined by conventional rule formulae. This examination is performed in an iterative way, because the surplus of longitudinal strength affects local strength requirements. On the other hand, transverse strength for larger ships is usually examined by direct calculations such as the FEM analysis (3-dimensional elastic analysis using shell and beam elements).
Assessment is generally based on safety factors. The criteria on the longitudinal strength are allowable stress (section modulus requirement) and deflection (moment of inertia requirement).

(1) IACS requirements

It is needless to say that longitudinal strength is one of the most essential strengths, since the loss of longitudinal strength leads to fatal damages - jackknifing -. The longitudinal strength requirements differed from classification society to classification society before 1991, but in 1991 the requirements were unified by IACS and new requirements were introduced in the rule of each classification society as "Longitudinal Strength Standard" - IACS Requirement S11 (Nitta *et al.* 1992). Followings are the unified requirements for bending strength of a hull girder in way of 0.4 L midship.

//SECTION MODULUS REQUIREMENT//

$$Z = \mathrm{Max}(Z_{min}, Z_{req}) \quad (\mathrm{m}^3) \tag{7.1}$$

- Minimun Section Modulus:

$$Z_{min} = CL^2B(C_b + 0.7)K \quad (\mathrm{m}^3) \tag{7.2}$$

where

$$\begin{aligned} C &= 10.75 - \left(\frac{300 - L}{100}\right)^{1.5} \quad for \quad 90 \leq L \leq 300 \\ &= 10.75 \quad for \quad 300 < L < 350 \\ &= 10.75 - \left(\frac{L - 350}{150}\right)^{1.5} \quad for \quad 350 \leq L \end{aligned}$$

and

L: length of vessel (m)
B: breadth of vessel (m)
C_b: block coefficient (greater than or equal to 0.6)
K: higher tensile strength steel factor (1.0/0.78/0.72 for MS/HT32/HT36)

- Required Section Modulus:

$$Z_{req} = \frac{M_s + M_w}{\sigma} \times 10^3 \quad (\mathrm{cm}^3) \tag{7.3}$$

where

M_s: design stillwater bending moment (kNm)
M_w: rule wave bending moment (kNm)
= 0.19 CL^2BC_b (hogging moment)
= 0.11 $CL^2 B$ (C_b + 0.7) (sagging moment)
σ: allowable stress
= 175/K

The relationship between Z_{min} and Z_{req} is illustrated in Figure 7.1.
The probability level of exceedance of M_w is assumed to be in the order of 10^{-8} (Nitta *et al.* 1992). Allowable stress of 175 (N/mm^2) corresponds to the safety factor of 1.4 (=245/175) against yielding.
Designers usually try to arrange tanks and holds in an appropriate position and plan loading pattern within the stillwater bending moment corresponding to Z_{min} (M_s*), if possible.
It has been a long practice to check the longitudinal strength under intact condition, but recently it has become required for bulk carriers to examine longitudinal strength under one hold flooded condition.

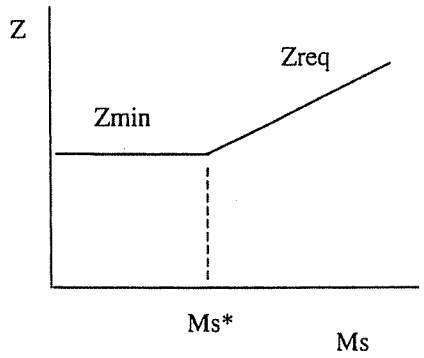

Figure 7.1: Relationship between section modulus and stillwater bending moment

//MOMENT OF INERTIA REQUIREMENT//

$$I_{min} = \frac{3Z_{min}L}{K} \tag{7.4}$$

Minimum moment of inertia is required in order to reduce excessive deformation, but in the ordinal ship design, this requirement does not become critical. It should be noted that no reduction by higher tensile strength steel is allowed.

//BUCKLING STRENGTH FORMULAE FOR LONGITUDINAL STRENGTH//

Buckling strength of longitudinal members is checked locally one by one applying the unified formulae.

PLATE

Euler buckling strength with elastoplastic correction:

$$\sigma_c = \sigma_T \left(1 - \frac{\sigma_Y}{4\sigma_{el}}\right) \tag{7.5}$$

where

$$\sigma_{el} = 0.9kE\left(\frac{t - t_k}{1000s}\right)^2 \qquad (\mathrm{N/mm^2})$$

and

σ_c: critical buckling stress □ σ_Y: yield stress
σ_{el}: elastic buckling stress □ □k: buckling coefficient
E: modulus of elasticity □ □ t: plate thickness (in mm)
t_k: corrosion addition □ s: space between longitudinals (in m)

STIFFENER

$$\sigma_{el} = 0.001E\frac{I_A}{Al^2} \qquad (\mathrm{N/mm^2}) \tag{7.6}$$

where

I_A: moment of inertia; A: sectional area; l: span of stiffener

Flexural-torsional buckling strength with elastoplastic correction:

$$\sigma_{el} = \frac{\pi^2 E I_w}{10^4 I_p l^2}\left(m^2 + \frac{K}{m^2}\right) + 0.385E\frac{I_T}{I_p} \qquad (\mathrm{N/mm^2}) \tag{7.7}$$

where

I_w: sectional moment of inertia with respect to connection line of stiffener to plate
I_p: polar moment of inertia with respect to connection line of stiffener to plate
m: number of half waves depending on coefficient K
I_T: St. Venant's moment of inertia

(2) Design characteristics dependent on ship kind

In order to investigate design characteristics of longitudinal strength dependent on ship kinds, section modulus calculation and loading manual are reviewed for typical commercial ships such as tankers (single hull, double hull), bulk carriers, container ships and pure car carriers. In addition to the above, four ships (DH VLCC, SH VLCC, Bulk Carrier, Container Ship) used for benchmark calculations of ultimate hull girder strength in Chapter 4 are investigated. In Table 7.1, these four ships can be distinguished with asterisk mark in the column of 'SHIP KIND'.

TABLE 7.1

DESIGN OF LONGITUDINAL STRENGTH (IACS BASE)

NO	SHIP KIND	YEAR OF DESIGN	CLASS	Lpp (m)	MS.design (HOG) x10^3(kN-m)	(SAG)	MW (HOG) x10^3(kN-m)	(SAG)	MS* (HOG) x10^3(kN-m)	(SAG)	MS,allow (HOG) x10^3(kN-m)	(SAG)	MS,act (HOG) x10^3(kN-m)	(SAG)	MATERIAL FACTOR (DK)	(BTM)	SURPLUS (DK) (%)	(BTM) (%)	REMARKS
1	DH TANKER	1995	NK	318	7,014	-4,709	9,884	-10,628	7,024	6,280	7,013	-6,273	6,958	4,554	0.72	0.78	1.23	20.72	Ballast tank inside
2	DH TANKER	1994	ABS	258	3,924	-3,532	5,011	-5,297	3,417	3,130	4,140	-3,853	3,903	3,462	0.78	0.78	2.26	35.17	Suez Max
3	DH TANKER	1990	DNV	258	4,120	0	5,077	-5,336	3,412	3,153	4,120	-3,467	4,002	3,260	0.72	0.78	0.52	13.36	Suez Max
4	DH TANKER	1992	DNV	210	2,551	0	2,458	-2,664	1,780	1,574	2,551	-1,574	2,441	1,095	0.78	0.78	2.26	25.11	Shuttle Tanker
5	DH TANKER	1991	DNV	233	3,139	0	3,585	-3,813	2,480	2,253	3,139	-2,253	3,052	1,979	0.78	0.78	0.48	15.09	Afra Max
6	DH TANKER*	1993	LR	315	5,720	-5,837	9,602	-10,214	6,647	6,035	6,650	-5,992	5,695	5,952	0.78	0.78	1.71	37.51	VLCC(Bench Mark)
7	SH TANKER	1989	NK	315	6,657	-5,845	9,231	-10,079	6,804	5,956	6,788	-5,941	6,657	5,845	0.72	0.78	0.88	6.20	VLCC
8	SH TANKER	1985	NK	305	5,144	-5,494	8,345	-8,993	5,962	5,314	5,431	-5,731	5,064	5,346	0.72	0.78	4.16	9.72	VLCC
9	SH TANKER	1987	LR	232	2,521	-2,521	3,611	-3,819	2,465	2,257	2,521	-2,521	2,481	2,032	0.78	0.78	2.01	10.21	Afra Max
10	SH TANKER	1981	ABS	175	863	-863	1,307	-1,398	917	826	1,072	-1,072	696	697	1	1	4.28	37.50	Double Bottom
11	SH TANKER	1981	LR	210	1,638	-1,638	2,190	-2,317	1,496	1,369	1,638	-1,638	1,528	1,006	0.78	0.78	7.53	12.62	Pana Max
12	SH TANKER*	1967	DNV	313	5,482	-4,964	7,960	-8,445	5,476	4,990	5,733	-5,628	4,910	4,800	0.78	0.78	6.93	13.33	ENERGY COCENTRATION
13	BULK	1996	NK	218	1,659	-1,692	2,761	-2,898	1,849	1,712	1,838	-1,701	1,610	1,643	0.72	0.78	0.36	19.50	Coal Carrier
14	BULK	1993	NK	181	982	-829	1,461	-1,566	1,030	925	1,029	-917	989	867	0.72	0.78	2.18	53.85	Handy Max
15	BULK	1993	NK	278	0	0	6,018	-6,311	4,021	3,729	4,011	-3,719	3,269	2,758	0.72	0.78	0.08	6.13	Cape Size
16	BULK	1986	NK	276	2,796	-2,836	5,739	-6,054	3,893	3,577	3,230	-3,469	2,796	3,292	0.68	0.78	-0.22	17.02	Cape Size
17	BULK	1984	NK	213	1,309	-1,055	2,314	-2,439	1,566	1,441	1,409	-1,309	1,309	1,278	0.78	0.78	3.07	28.76	Pana Max
18	BULK	1984	DNV	286	3,183	-3,936	6,586	-6,942	4,459	4,102	4,513	-4,905	3,188	3,938	0.72	0.78	-0.51	20.98	190BC
19	BULK	1983	NK	160	579	-498	907	-982	655	580	579	-579	564	497	0.78	0.78	4.49	50.06	26BC
20	BULK*	1985	NK	285	3,293	-3,733	6,744	-7,155	4,639	4,228	3,950	-4,200	3,293	3,733	0.68	0.78	-0.52	26.14	(Bench Mark)
21	CONTAINER	1996	NK	287	4,218	0	4,388	-5,144	3,797	3,040	4,218	0	4,218	0	0.72	0.78	13.62	19.13	6200TEU
22	CONTAINER	1993	LR	260	2,580	0	2,772	-3,363	2,578	1,987	2,580	-2,580	2,508	21	0.72	0.78	0.94	13.27	3800TEU
23	CONTAINER	1993	NK	283	4,591	0	3,712	-4,561	3,544	2,695	4,828	-4,047	4,275	598	0.68	0.72	2.68	6.94	4700TEU
24	CONTAINER	1989	LR	280	3,434	0	3,279	-3,924	2,965	2,319	3,434	0	3,362	0	0.72	0.78	1.46	13.08	3700TEU
25	CONTAINER	1986	NK	189	1,226	1,059	1,366	-1,632	1,231	965	1,253	0	1,213	0	0.72	1	10.62	46.78	2000TEU
26	CONTAINER	1985	NK	230	1,913	0	2,063	-2,509	1,928	1,482	1,955	0	1,893	0	0.72	1	12.09	14.43	2600TEU
27	CONTAINER*	1985	NK	230	2,011	2,011	1,991	-2,461	1,925	1,454	2,011	-1,795	1,936	0	0.72	0.78	14.60	46.74	(Bench Mark)
28	PCC	1987	NK	190	1,615	0	1,106	-1,465	1,224	866	1,600	0	1,572	0	1	1	32.65	125.03	5500CARS
29	PCC	1986	ABS	170	1,275	0	766	-1,040	888	614	1,275	0	1,220	0	1	1	37.18	107.65	4000CARS
30	PCC	1985	LR	150	834	0	585	-719	558	425	834	0	818	0	1	1	54.71	127.45	2500CARS
31	PCC	1982	DNV	180	1,844	910	1,100	-1,390	1,112	822	1,840	0	1,738	0	1	1	53.19	87.09	5600CARS

*: Ships for Bench Mark analysis

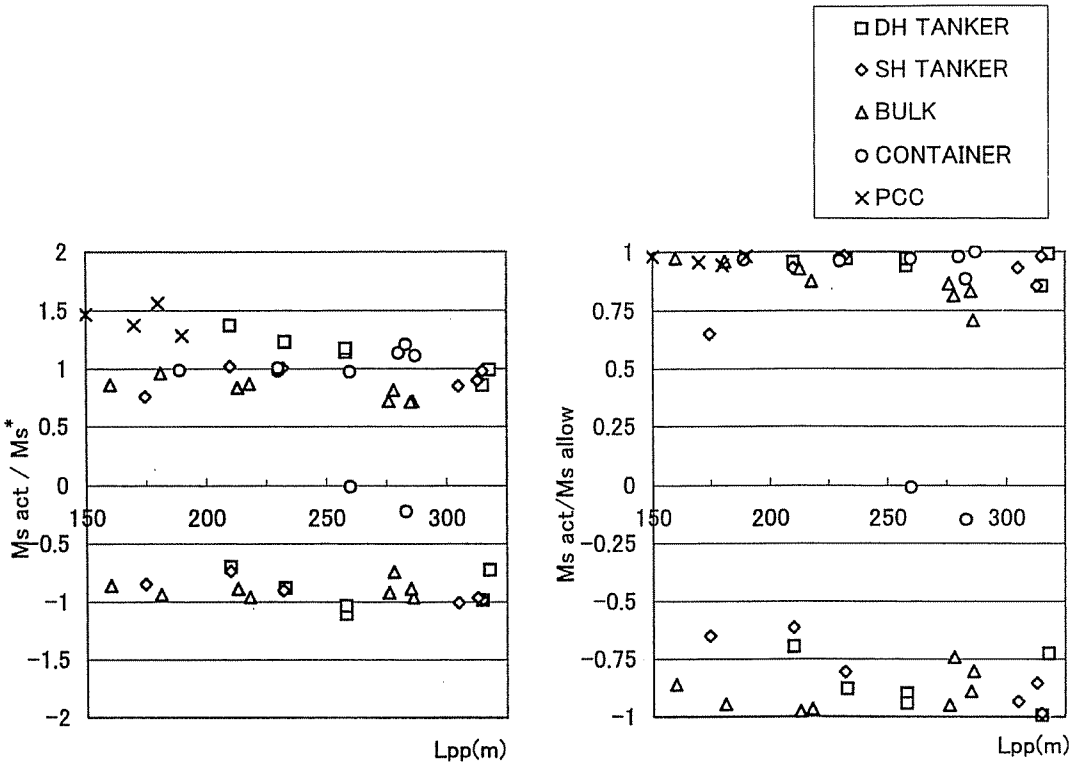

(a) $M_{s\,act} / M_s$*□□□□□□□□□□□□(b) $M_{s\,act} / M_{s\,allow}$

Figure 7.2: Comparison of stillwater bending moment

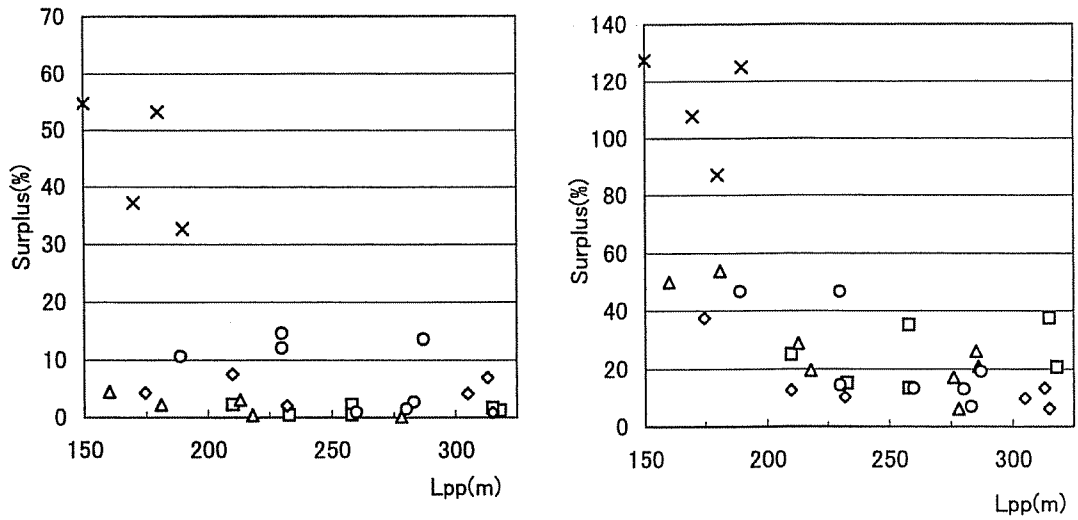

(a) Deck□□□□□□□□□□□□□□(b) Bottom

Figure 7.3: Surplus of section modulus ((Z_{act}/Z - 1)x100%)

Wave-induced bending moment can be obtained by rule formulae mentioned above, but stillwater bending moment is calculated considering cargo weight, lightweight and buoyancy distribution. When the cargo is light, no severe sagging moment will occur. Characteristics of stillwater bending moments relevant to kinds of vessels are also to be taken into consideration.

Required Section Modulus

Four to eight ships per each ship kind are selected for investigation as shown in Table 7.1, where the year of design ranges from 1981 to 1995 except No.12 SH TANKER (*Energy Concentration*, 1967).
Section modulus requirements for these ships at design stage are not consistent, because each classification society had its own formula before IACS's unification in 1991. Therefore, in this investigation, IACS's unified formula described in *(1)* is applied for consistency.
In case of container ships, there are special requirements in NK and LR Classes considering small block coefficient and torsional strength. These requirements are, however, neglected in this investigation.

Results of Investigation

1) $M_{s\,act}$ / M_s*

M_s* (stillwater bending moment corresponding to Z_{min}) is one of a target design bending moment for designers. So, in Figure 7.2 (a), $M_{s\,act}$ (actual maximum stillwater bending moment) picked out from loading manual is compared with M_s*.
As can be seen from this figure, most of single hull tankers and bulk carriers are designed within M_s* under both hogging and sagging conditions.
On the other hand, double hull tankers are subjected to large hogging moment under ballast conditions except two VLCCs, No.1 and No.6, which have ballast tanks inside double side hull.
In case of over-panamax container ships, $M_{s\,act}$ slightly exceeds M_s* under hogging condition, but sagging stillwater bending moments are very small independent on ship size.
Car carriers are subjected to a large hogging moment, but have sufficient section modulus because of deep depth configuration as mentioned later. They have no sagging stillwater bending moment.

2) $M_{s\,act}$ / $M_{s\,allow}$

$M_{s\,allow}$ (allowable stillwater bending moment) is also picked out from loading manual and compared with $M_{s\,act}$ as shown in Figure 7.2 (b).
Some margins are observed for double and single hull tankers under the sagging condition. Large sized bulk carriers also have some margins for both hogging and sagging conditions.
For container ships and car carriers, actual hogging moments are nearly equal to the allowable bending moments.

3) Surplus

Surplus of section modulus ((Z_{act} /Z -1) x 100 %) is plotted in Figure 7.3. These values correspond to longitudinal stress levels.
Generally speaking, in the design process of scantling determination, deck section modulus becomes decisive. On the other hand, bottom has sufficient section modulus because of double bottom structure except single hull tankers. In case of single hull tankers, bottom section modulus is slightly larger than deck section modulus because of the heavier scantlings to resist the sea pressure in addition to longitudinal bending.
In case of car carries, they have very large section moduli for both deck and bottom due to paticular configurations with deep depth and many internal car decks.
When discussing ultimate strength of a hull girder, design characteristics dependent on ship kinds have to be taken into consideration.

TABLE 7.2

SAFETY FACTOR AGAINST ULTIMATE HULL GIRDER STRENGTH

MOMENT (x 1,000 MN•m)

		D.H.TANKER			S.H.TANKER			CONTAINER SHIP			BULK CARRIER			REMARKS
		HOG.	SAG.	HOG/SAG	HOG.	SAG.	HOG/SAG	HOG.	SAG.	HOG/SAG	HOG.	SAG.	HOG/SAG	
Mdesign	Ms design	5.72	5.84	0.98	5.48	4.96	1.10	2.01	2.01	1.00	3.29	3.73	0.88	
	Mw rule	9.60	10.21	0.94	7.96	8.45	0.94	1.99	2.46	0.81	6.74	7.16	0.94	
	M total	15.32	16.05	0.95	13.44	13.41	1.00	4.00	4.47	0.89	10.04	10.89	0.92	
Mult	A	27.40	24.33	1.13	20.23	18.54	1.09	6.56	5.47	1.20	19.06	15.20	1.25	
	B	28.66	20.80	1.38	20.09	16.75	1.20	6.69	5.13	1.30	18.99	13.69	1.39	
	C	30.59	26.59	1.15	20.01	19.00	1.05	8.07	7.75	1.04	18.56	16.02	1.16	
	D	28.32	19.57	1.45	18.46	17.90	1.03	7.60	6.51	1.17	18.71	14.34	1.30	
	E	25.61	24.07	1.06	17.54	17.10	1.03	7.20	6.91	1.04	17.08	14.84	1.15	
	F	28.88	20.42	1.41	19.03	16.84	1.13	6.72	6.72	1.00	17.36	14.45	1.20	
	Mean	28.24	22.63	1.25	19.23	17.69	1.09	7.14	6.42	1.11	18.29	14.76	1.24	
	COV	5.4%	11.2%	12.3%	5.1%	4.9%	5.6%	7.7%	13.8%	9.6%	4.3%	5.0%	6.8%	
SAFETY	FACTOR	1.84	1.41		1.43	1.32		1.78	1.43		1.82	1.36		

NOTE ; 1) M total = Ms design + Mw rule (ref. Table 7.1)

2) Mult : refer to TABLE 4.7 ~ TABLE 4.10 ($M_{US}|_{(2)}$, $M_{UH}|_{(2)}$: with specified initial deflection and welding residual stress)

3) COV = Coefficient Of Variation

4) SAFETY FACTOR = Mult(Mean) / M total

7.1.2 Novel Ships and Topics

In case of novel ships such as Deep Sea Drilling Vessel, FPSO (= Floating Production and Storage Offshore Unit), longitudinal strength assessment is generally based on more direct method than conventional commercial ships, where extreme loads are estimated by direct calculations and the longitudinal strength is assessed based on the ultimate strength. Assessment is, in some cases, performed by reliability method.
Recent topics on conventional ships are as follows:

Bulk Carrier Safety
Reflecting many casualties happened in the early 1990's, many additional requirements have been established as "Bulk Carrier Safety". One of these requirements is the longitudinal strength requirement of a hull girder in flooded condition for single side skin bulk carriers (IACS UR S17). In this requirement, stillwater bending moment has to be calculated under one hold flooded condition and wave bending moment is assumed to be 80% of the ordinary Rule-based design bending moment. On the other hand, assessment is the same as an intact ship (section modulus requirement for conventional ships). Under such an extreme condition, it is considered to be reasonable to change strength criteria from conventional elastic strength to the ultimate strength.

Jack-knifying Casualties
Recent casualties concerning longitudinal strength such as MV *Derbyshire* and MV *Nakhodka* have caused discussions about design and maintenance methods for longitudinal strength including the considerations on strength deterioration due to corrosion.

7.2 Application of Ultimate Strength Criteria to Hull Girder Design

7.2.1 Comparison of Existing Elastic Criteria with Ultimate Strength Criteria

Safety factors obtained from design bending moment and ultimate strength analyses carried out in Chapter 4 are listed in Table 7.2. Followings can be observed from this table.
In general, design bending moments under hogging condition are smaller than those under sagging condition.
On the other hand, ultimate bending moments under hogging condition are larger than those under sagging condition.
As a consequence, safety factors under hogging condition becomes larger than those under sagging condition.
This result implies that more rational design could be realised when basing on ultimate strength criteria.

7.2.2 Requisite for Design Application

The present requirements for longitudinal strength are fundamentally based on elastic design criteria. When considering safety of the vessel, however, the actual capacity of longitudinal strength - ultimate hull girder strength - must be taken into consideration.
In order to obtain the accurate capacity, followings have to be clarified:

- Appropriate modelling of a hull girder and establishment of analysis procedure
- Estimation of the effects of initial imperfections (initial deformation, welding residual stress etc.) on the ultimate strength

On the other hand, the accuracy of design loads (demand) is required to enhance the level of assessment. Consistency of accuracy among load, strength and assessment is necessary.
In the actual ships, features of the ultimate strength and load are different according to kinds of ships. It depends on structural configuration and loading pattern. Therefore, these features are to be clarified through calculations.

There are many design factors which affects the ultimate strength and load, and they are not always the deterministic values. Therefore, stochastic nature of each factor has to be examined.
In addition to the above, strength is time-dependent. Effects of corrosion on the ultimate hull girder strength also have to be examined.
Many analyses have been performed under intact condition, but analysis under damaged condition are considered to be also necessary.
Considering above-mentioned aspects, practical method to assess the ultimate hull girder strength shall be proposed in the next chapter.

8 PROPOSAL FOR TECHNICAL GUIDE TO ASSESS ULTIMATE HULL GIRDER STRENGTH

8.1 Needs for the Assessment of Ultimate Hull Girder Strength

The estimation of the ultimate strength of the hull girder of vessels of conventional hull form under longitudinal bending can be applied:
(1) At the design stage, to achieving more rational design, that is, to reduce the weight of the structure whilst at the same time fulfilling strength requirements. This is possible by selecting configurations whose construction parameters (weight and fabrication cost) are minimised whilst at the same time satisfying local strength requirements.
(2) For existing structures, to the estimation of residual strength, a factor of paramount importance in aged structures that have suffered corrosion and other forms of wear and tear.
For certain ship types, the estimation of the ultimate strength forms an important part of the design process. Vessels such as dredgers and FPSOs are subjected to high bending loads under normal operating conditions and for this reason, the loads carried by the structure have to be carefully estimated. In vessels such as catamarans and other advanced crafts, the question of weight minimisation is important. At the same time, it is necessary to ensure that the structure performs satisfactorily when subjected to bending, torsional and impact loads. For vessels with such configurations care has to be taken when specifying ultimate strength requirements.

8.2 Levels of Analysis

The ultimate longitudinal strength can be represented either by the ultimate bending moment (M_u), which may exceed the initial yield moment, (M_Y), or by the curve of progressive collapse. This curve is obtained by plotting the actual bending moment in a selected, critical section (e.g. amidships), against the longitudinal curvature of the hull (ϕ). The use of the M-ϕ curve is based on the assumption that the girder behaves as a long beam with a hollow rectangular cross-section in bending, thus enabling the use of the beam analogy to be used. Clearly, this assumption has limitations, both because of the variety and configurations of actual hull forms and also because of the assumptions implicit in simple beam theory.

8.2.1 Finite Element Analysis

The complexity of hull forms, structural behaviour and imposed loads make it necessary to resort to the use of finite element analysis in several instances when assessing the strength of ship structural components. However, the modelling and analysis of a complete hull girder using a finite element program is a task of enormous magnitude. For this reason the analysis is more conveniently performed on a cross-section of the hull that extends in the longitudinal direction sufficiently enough to model the behaviour that is typical of the particular cross-section. Thus, an analysis may extend from one frame spacing to that of a whole compartment (cargo tank). These analyses have to be supplemented by information on the bending and

shear loads that act at the fore and aft loaded transverse sections.
In order to perform a full-range analysis it is necessary that the procedure has nonlinear capabilities (material and geometric non-linearities) and also that the post-collapse behaviour of individual structural elements such as panels and stiffeners can be simulated.
In most cases it is possible to take advantage of the symmetry of the structure, thus significantly reducing modelling and computing requirements. It therefore becomes important to specify the correct boundary conditions along the transverse edges and along the longitudinal vertical plane in way of the centre-line. Boundary conditions are determined in a rigorous manner by performing a full, coarse, analysis of the hull girder. It is also possible to specify the boundary conditions on the basis of previous analyses or by using simplified analytical considerations.
In FE analysis, loading is applied to the model by increasing the longitudinal curvature in finite increments. For each increment of curvature, the distributions of stresses and deformations are determined for each component. This approach enables a full-range analysis that includes post-collapse behaviour to be performed. The longitudinal stresses that are normal to one or more transverse sections are then used to determine the bending moment about the current neutral axis.
The use of finite element procedures in the estimation of ultimate strength in longitudinal bending of ships has shown that accuracy is limited because of the following factors:

a) The boundary conditions along the transverse sections to which the loading is applied cannot be modelled with satisfactory accuracy.
b) The position of the neutral axis of the cross-section along the length analysed varies and
c) The presence of residual stresses.

All these factors introduce uncertainties that limit the practical usefulness of the finite element method in assessing ultimate hull girder strength.
For these reasons it becomes necessary to consider other methods that are more easily applied and that can also be of assistance to the designer.

8.2.2 Simplified Methods for Progressive Collapse Analysis

As mentioned above, there exists a need for methods that can be easily applied and which can provide sufficiently accurate results. In these methods the result is, as in FE analysis, either a value of the ultimate bending moment or a curve of progressive collapse (M-ϕ).
A number of such approaches are based upon the Smith's method, according to which the analysis is performed in two stages. A transverse section of the vessel is first subdivided into elements, each consisting of a longitudinal stiffener and it's associated plating. A full-range analysis of each individual element is then performed, using either a numerical or an analytical procedure. The output of these analyses is a series of stress-strain curves that extend well beyond the collapse load.
During the second stage, these curves are used to estimate the bending moment carried by the complete transverse section (M). The contribution of each element (dM) depends on its location in the cross-section, and specifically on its distance from the current position of the neutral axis. The contribution will then also depend on the strain that is applied to it, since $\varepsilon = - z \phi$, where ϕ is the hull curvature and z is the distance from the neutral axis (simple beam assumption). The average stress-average strain curve (σ - ε) will then provide an estimate of the average longitudinal stress (and consequently load) acting on the particular section. Individual moments about the neutral axis are then summed to give the total bending moment for a particular curvature ϕ.
Simplified methods are thus based on Smith's approach that implies that simple beam theory holds for the whole cross-section. Deviations such as warping are thus ignored.
As mentioned above, it is possible to obtain individual element strength curves using either numerical or analytical methods. The sensitivity studies carried out and described in Chapter 4 indicate that the most important reason for which differences in estimates of the ultimate

bending moment occur in different methods is the form of the individual element stress-strain curves. The shape, as well as the peak value of the local strength curves, have an important influence on the ultimate strength of the complete hull girder. When the ultimate bending moment is reached, in several elements the stress will be at or near the peak stress, whereas in others it will be lower. The cross-section will therefore have residual strength, since not all members will be at peak load. At a later stage of loading, load-shedding at critical regions of the cross-ections occurs. On the other hand, components of the hull girder that are closer to the current neutral axis continue to carry load. This has the effect of "smoothing" of the moment-curvature curve in the vicinity of collapse.
It should also be borne in mind that the components that have not collapsed when the ultimate bending moment is reached will behave linearly. Since individual methods for the prediction of local stress-strain behaviour produce identical results for this range of loading, the differences in results are confined to those sections that are loaded in the nonlinear range. As a result, the observed discrepancies are smaller than would otherwise be the case. This is clear from the results included in the sensitivity studies in Chapter 4.
The differences that are attributable to the final stage in the development of a progressive collapse analysis should in comparison be negligible. That is, if the Smith's approach is used, there should be only minor discrepancies in the progressive collapse curves that are based on identical local stress-strain curves. The integration of the local strength curves should be performed in a standard manner, that allows for the calculation of the position of the neutral axis using longitudinal equilibrium considerations. These minor differences may arise because different ways of subdividing the cross-section into elements may be used (Stage 1, see *4.5*).

8.2.3 Direct Approximate Methods to Evaluate Ultimate Hull Girder Strength

Such methods aim at providing an estimate of the ultimate bending moment without attempting to providing an insight into the behaviour before, and more importantly, after, collapse of the cross-section. Such Methods can be used at early stages in design, when considering the layout of structural members. Similarly, the effect of corrosion and wear can be assessed by conducting studies for individual ship cross-sections.
The tracing out of a progressive collapse curve is replaced by the calculation of the ultimate bending moment for a particular distribution of stresses. The quality of the direct approximate method is directly dependent on the quality of the stress distribution at collapse. It is assumed that at collapse the tensile stresses are at yield throughout, whereas the compressive stresses are qual to the individual inelastic buckling stresses for each member. On this basis, the plastic neutral axis is estimated using considerations of longitudinal equilibrium. The ultimate bending moment is then the sum of individual moments of all elements about the plastic neutral axis.

8.2.4 Simple Methods using Elastic Parameters

Finally, it is possible in certain cases to obtain an estimate of the ultimate bending moment using simple considerations based on simple beam theory. It states that $M_0 = Z\ \sigma_0$ where σ_0 is the stress at the outer fibres of the cross-section and M_0 is the corresponding bending moment. The elastic section modulus, Z, is included in the above equation.
It has been found in Chapter 4 that the bending moment that corresponds to initial yielding of the deck, M_{ys}, can provide in general a little higher but reasonably accurate estimate of the ultimate hull girder strength under the sagging condition. On the other hand, in the hogging condition, the initial buckling strength, M_{bh}, of the bottom plate gives a slightly lower but reasonably accurate estimate of the ultimate hull girder strength. These in effect can provide a first estimate of the ultimate hull girder moment.
When yielding or buckling of the deck structure or the bottom structure brings about collapse of the

TABLE 8.1
ASSESSMENT OF AVAILABLE METHODS TO EVALUATE ULTIMATE HULL GIRDER STRENGTH
IN LONGITUDINAL BENDING

Capability	Sinmple Technique			Advanced Technique				Consequence of Omitting Capability
	Initial Yielding	Elastic Analysis	Assumed Stress Distribution	Progressive Collapse Analysis with Idealised σ-ε curves	Progressive Collapse Analysis with Calculated σ-ε curves	ISUM	Non-linear FEM	
Plate Buckling	-	2	3	4	5	5	5	H
Stiffened Plate Buckling	-	2	3	3	5	3	5	H
Plate Initial Deflection	-	1	2	2	5	5	5	M
Stiffener Initial Deflection	-	1	3	3	5	3	5	M
Plate Welding Residual Stress	-	2	3	3	4	4	4	H
Stiffener Welding Residual Stress	-	1	2	3	3	4	4	M
Post-Buckling Behaviour	-	-	-	3	5	5	5	H
Multi-Span Model	-	-	-	2	5	5	5	M
M-Φ Curve (Collapse Prediction)	-	-	-	3	5	5	5	H
Post Ultimate Strength	-	-	-	3	5	4	5	M
Damage	2	2	2	3	5	3	5	-
Material Modelling	1	1	1	3	5	5	5	-
Modelling/Data Preparation	5	4	4	3	3	3	1	-
Analysis/ Checking Results	5	3	3	3	3	3	1	-
Accuracy/Reliability of Results	2	1	2	3	4	3	4	-
Total (Full Score: 75)	15	19	30	43	67	56	63	-

Score:
1: Not Available
2: Poor Ability
3: Insufficient Accuracy
4: Acceptable
5: Excellent

Consequence of Omitting Capability
L: Low
M: Medium
H: High

whole cross-section, there is close agreement between the above estimate and the true ultimate bending moment. This arises when the cross-section of the longitudinal stiffeners

and their spacing are maintained constant. Such arrangements are encountered in tanker structures and in the bottom structure of bulk carriers.

8.3 Comparison of Available Methods to Evaluate Ultimate Hull Girder Strength

Table 8.1 provides an overview and comparative assessment of the methods considered previously. The grading of each method with respect to each "capability" is quantatively performed by scoring 1 through 5. It is also done qualitatively by indicating the consequence of omitting capabilities by High, Medium and Low.
Of these methods, *A* is an empirical method. Methods *B* and *C* are direct methods whereas the remaining methods have the capability to trace out the full sequence of progressive collapse behaviour of the hull girder.
It is seen that the most effective among all methods is Method *E*, the progressive collapse analysis with calculated stress-strain relationships, that involves the use of numerical methods to determine the stress-strain curves of individual plate and stiffened plate elements, which are then integrated following the assumptions of simple beam theory in order to trace out the progressive collapse curve. Method *F*, the ISUM, may also be an efficient method, but more rational elements have to be developed which can account the overall buckling as a stiffened panel and the tripping of stiffeners as well as the localisation of yielding and deformation in the post-ultimate strength range of individual structural members.

8.4 Selection of Suitable Method

A designer who wishes to select a method appropriate to his needs can introduce more than one method in the design procedure. Each of these should be appropriate to the level of accuracy and resources available to prepare the information and process it. Thus, at early stages of design, one of the simpler methods (e.g. *A*, *B* or *C*) can be used in order to obtain an estimate of the ultimate strength. At later stages, a more accurate method such as *E* or *G* can be used.
The accuracy of the selected method can be examined by performing calculations on the examples used for benchmark calculations in Chapters 3 and 4. It is also possible to examine the accuracy of a newly developed method of analysis in the same manner.

9 CONCLUSIONS

Through the research and investigation activities of the committee, it has been found that:

(1) The available methods for evaluation of the ultimate hull girder strength can be classified into two groups. One way is to perform progressive collapse analysis and the other is to calculate the ultimate hull girder strength directly applying empirical/theoretical formulae.
(2) The potentially most accurate method for progressive collapse analysis may be the elastoplastic large deflection analysis applying the FEM (Finite Element Method). Such an analysis is fundamentally possible but is presently not practical to perform due to large requirement to computer resources and modelling work, and very few results have been reported until now.
(3) An alternative method of progressive analysis is the Smith's method, which is a simplified method but is capable of simulating the progressive collapse behaviour of a ship hull girder subjected to longitudinal bending with relatively high accuracy. The ISUM (Idealized Structural Unit Method) can also be used for progressive collapse analysis. However, more accurate and sophisticated stiffened plate element has to be developed to achieve reliable results.
(4) In simplified methods of progressive collapse analysis, the accuracy of the calculated results largely depends on how accurately the collapse behaviour of individual structural

members can be determined. From this point of view, benchmark calculations were performed on ninty (90) stiffened plates with and without welding residual stresses applying existing simplified methods as well as the FEM.

(5) Some scatters were observed among calculated results applying different methods. On the other hand, it was shown that a simplified method predicts the ultimate strength very accurately if the assumed collapse mode is the same as the actual one. The most crucial point for a simplified method is that it is able to simulate the occurrence of overall buckling as a stiffened plate including tripping of longitudinal stiffeners.

(6) Benchmark calculations were performed also on four existing ship hull girders and one test girder to evaluate the ultimate hull girder strength under pure bending. It was shown that the buckling/plastic collapse of the deck and the bottom dominates the overall collapse of the cross-section under the sagging and the hogging condition, respectively. The influence of the collapse behaviour of structural members on collapse behaviour of the hull girder is clarified through sensitivity analysis.

(7) Initial yielding strength and initial buckling strength were calculated using the elastic section modulus, and are compared with the evaluated ultimate hull girder strength. It was shown that the initial yielding strength of the deck is a little higher than the ultimate hull girder strength under the sagging condition. Nevertheless, relatively good agreement was found. The initial buckling strength of the bottom is a little lower but in good agreement with the ultimate hull girder strength under the hogging condition.

(8) Research work on the effects of load combinations on ultimate strength were investigated. That is, the influences of transverse in-plane loading and also lateral pressure on structural members and hull girder were examined. It was found that transverse in-plane loading slightly reduces the ultimate strength of a stiffened plate. On the other hand, lateral pressure reduces the ultimate strength of a stiffened plate to a certain extent according to the magnitude of the pressure.

(9) For a certain type of ship or for a certain loading condition, the influences of bi-axial bending, bi-axial shear force and torsional moment have to be considered. As regards bi-axial bending, the ultimate strength interaction relationship is easily obtained applying Smith's method. To include the influences of shear force and torsional moment, approximate methods can be used. However, a more accurate evaluation of these influences remains as a future task.

(10) The thickness reduction due to corrosion reduces the ultimate hull girder strength. In the case of single hull tankers, it was reported that the strength reduction is almost proportional to the reduction of the section modulus. It was concluded that approximately 15% reduction in the section modulus is allowable from the viewpoint of ultimate hull girder strength.

(11) The sensitivity of the ultimate hull girder strength with variations of several design parameters was calculated for the four hull girders used in the benchmark calculations. It was shown that the thickness of the plating and the stiffeners as well as yield strength of the material have the largest impact on the ultimate hull girder strength. The influences of initial deflection and welding residual stress in plates and stiffeners were not so significant.

(12) The present design criteria related to longitudinal strength were investigated in relation to the ultimate hull girder strength. It was found that the safety factor for the sagging condition is in general lower than that for the hogging condition. It was concluded that design characteristics dependent on ship types should be taken into account for the design of individual ship types.

(13) Existing methods to calculate the ultimate hull girder strength were evaluated, and the results have been summarised in the Table 8.1. It was recommended to potential designers to examine this table carefully and to select the most appropriate method among the available methods according to the design stage and the designer's needs.

(14) The accuracy of the selected method can be examined by performing calculations on the examples used in the benchmark calculations in Chapters 3 and 4.

(15) The simplest measure of the ultimate hull girder strength is the initial yielding strength of the deck in the sagging condition. The local buckling strength of the bottom is a good simple measure in the hogging conditions. The former measure gives a slightly higher estimate and the latter a slightly lower one than the true value.

The committee is grateful to Dr. Yanagihara, Dr. Masaoka, Prof. Gordo and Prof. Guedes Soares for their contributions to the benchmark calculations and to Dr. Yanagihara and Messrs. Mukherjee and Murakami for their helps to provide electronic manuscript of the committee report.

REFERENCES

Bai, Y., Bendiksen, E. and Terndrup Pedersen, P. (1993). Collapse analysis of ship hulls. *Marine Structures* **6**, 485-507.

Beghin, D., Jastrzebski, T. and Taczala, M. (1995). Result - A computer code for evaluation of the ultimate longitudinal strength of hull girder. *Proc. of PRADS-5* Vol.2, Edt. Kim & Lee, Soc. Naval Arch. of Korea, 832-843.

Caldwell, J.B. (1965). Ultimate longitudinal strength. *Trans RINA* **107**, 411-430.

Carlsen C.A. (1980). A parametric study of collapse of stiffened plates in compression. *The Structural Engineers* **58B:2**, 33-40.

Chen, Y.K., Kutt, L.M., Piaszczyk, C.M. and Bieniek, M.P. (1983). Ultimate strength of ship structures. *SNAME Trans.* **91**, 149-168.

Cho, R.-S., Choi, B.-W. and Frieze, P.A. (1998a). Ultimate strength formulaton for ship's grillages under combined loadings. *Proc. PRADS'98*, The Hague, 125-132.

Cho, R.-S., Choi, B.-W. and Song, I.-C. (1998b), Post-ultimate behaviour of stiffened panels subjected to axial compression. *Proc. Int. 2nd Conf. Thin-Walled Structures*, Singapore, 433-440.

Dow, R.S. (1980). A computer program for elasto plastic, large deflection buckling and post-buckling of plane frames and stiffened panels. *Report AMTE(S)* **R80762**.

Dow, R.S., Hugill, R.C., Clarke, J.D. and Smith, C.S. (1981). Evaluation of ultimate ship hull strength. *Proc Symp on Extreme Loads Response*, Arlington, U.S.A., 133-148.

Dow, R.S. (1991). Testing and analysis of 1/3-scale welded steel frigate model. *Proc Int Conf on Advances in Marine Structures*, ARE, Dunfermline, Scotland, 749-773.

Dowling et al. (1991). Design of flat stiffened plating: Phase 1 report. *CESLIC Report* **SP 9**, Dept. of Civil Engineering, Imperial College, London.

DNV. (1995). Buckling strength analysis. Classification Notes **30.1**.

Endo, H., Tanaka, Y., Aoki, G., Inoue, H. and Yamamoto, Y. (1988). Longitudinal strength of the fore body of ships suffering from slamming. *J. Soc. Naval Arch. of Japan* **163**, 322-333 (in Japanese).

Faulkner, J.A., Clarke, J.D., Smith, C.S. and Faulkner, D. (1984). The loss of HMS COBRA - A reassessment. *Trans RINA* **127**, 125-151.

Frieze *et al.* (1991). Report of ISSC Committee V.1- Applied Design, *11th ISSC Conference*, Wuxi, China, Vol 2.

Fujikubo, M., Yao, T. and Varghese, B. (1997). Buckling and ultimate strength of plates subjected to combined loads. *Proc. 7-th Offshore and Polar Engineering Conf.* Vol.IV, 380-387.

Fujikubo, M., Yanagihara, D. and Yao, T. (1999a). Estimation of ultimate strength of continuous stiffened plates under thrust. *J. Soc. Naval Arch. of Japan* **185**, 203-212 (in Japanese).

Fujikubo, M., Yanagihara, D. and Yao, T. (1999b). Estimation of ultimate strength of continuous stiffened plates under thrust (2nd Report). *J. Soc. Naval Arch. of Japan* **186**, 631-638 (in Japanese).

Fujikubo, M., Kaeding, P. and Yao, T. (2000a). ISUM rectangular plate element with new

lateral shape function (1st Report) - Loagitudinal and transverse thrust -. *J. Soc. Naval Arch. of Japan* **187** (in printing).

Fujikubo, M. and Yao, T. (2000b). Elastic local buckling strength of stiffened plate considering plate/stiffener interaction and welding residual stress. *Marine Structures*, (in printing).

Gordo, J.M. and Guedes Soares, C. (1993). Approximate load shortening curves for stiffened plates under uniaxial compression. *Proc. Integrity of Offshore Structures – 5,* D. Faulkner *et al.* (Eds.), EMAS, 189-211.

Gordo, J.M. and Guedes Soares, C. (1996a). Approximate methods to evaluate the hull girder collapse strength. *Marine Structures* **9:3-4**, 449-470.

Gordo, J.M., Guedes Soares, C. and Faulkner, D. (1996b). Approximate assessment of the ultimate longitudinal strength of the hull girder. *J. Ship Research* **40:1**, 60-69.

Gordo, J.M. and Guedes Soares, C. (1997). Interaction equation for the collapse of tankers and containerships under combined vertical and horizontal bending moments. *J. Ship Research* **41:3**, 230-240.

Hughes, O.F. (1988). *Ship Structural Design : A Rationally-Based, Computer-Aided Optimization Approach.* Edited by the SNAME, New Jersey, 566p.

JMT (Japan Ministry of Transport) (1997). *Report on the Investigation of Causes of the Casualty of Nakhodka.* The Committee for the Investigation on Causes of the Casualty of Nakhodka.

JSRA (Japan Shipbuilding Research Association) (2000). Investigation into Structural Safety of Aged Ships. *Report of No. 74 Rule and Regulation Committee*, (in Japanese).

Jensen J.J. *et al.* (1994). Report of Committee III.1 Ductile Collapse. *Proc. 12th International Ship and Offshore Structures Congress*, Jeffery, N. E. and Kendrick, A. M. (Editors), Vol.1, 229-387.

John, W.G. (1874). On the strength of iron ship. *Trans. Inst. Naval Arch.* **15**, 74-93.

Kutt, L.M., Piaszczyk, C.M. and Chen, Y.K. (1985). Evaluation of longitudinal ultimate strength of various ship hull configurations. *SNAME Trans.* **93**, 33-55.

Maestro, M. and Marino, A. (1989). An assessment of the structural capacity of damaged ships: The plastic approach in longitudinal unsymmetrical bending and the influence of buckling. *Int. Shipbuilding Progress* **36:408**, 255-265.

Mansour, A.E., Yang, J.M. and Thayamballi, A. (1990). An experimental investigation of ship hull ultimate strength. *SNAME Trans.* **98**, 411-439.

Mansour, A.E., Lin, Y.H. and Paik, J.K. (1995). Ultimate strength of ships under combined vertical and horizontal moments. *Proc. 6th Int. Symp. PRADS*, Seoul, Korea, 2.844-851.

Masaoka, K., Okada, H. and Ueda, Y. (1998). A rectangular plate element for ultimate strength analysis. *Proc. 2nd Int. Conference on Thin-Walled Structures*, Singapore, 1-8.

Nishihara, S. (1983). Analysis of ultimate strength of stiffened rectangular plate (4th Report) - On the ultimate bending moment of ship hull girder -. *J. Soc. Naval Arch. of Japan* **154**, 367-375 (in Japanese).

Nitta, A., Arai, H. and Magaino, A. (1992). Basis of IACS unified longitudinal strength standard. *Marine Structures* **5**, 1-21.

Okamoto, T., Hori, T., Tateishi, M., Rashed, S.M.H. and Miwa, S. (1985). Strength evaluation of novel unidirectional-girder-system product oil carrier by reliability analysis. *SNAME Trans.* **93**, 55-77.

Ostapenko, A. (1981). Strength of ship hull girders under moment, shear and torque. *Proc. SSC-SNAME Symposium on Extreme Loads Response*, Arlington, U.S.A., 149-166.

Paik, J.-K. and Lee, D.-H. (1990a). Ultimate strength-based safety and reliability assessment of ship's hull girder. *J. Soc. Naval Arch. of Japan* **168**, 397-409.

Paik, J.-K. (1990b). Ultimate strength-based safety and reliability assessment of ship's hull girder (2nd Report) - Stiffened hull structure -. *J. Soc. Naval Arch. of Japan* **169**, 397-409.

Paik, J.-K., Kim, D.-H., Bong, H.-S., Kim, M.-S. and Han, S.-K. (1992a). Deterministic and probabilistic safety evaluation for a new double-hull tanker with transverseless system.

SNAME Trans. **100**, 173-198.
Paik J.-K. (1992b). Ultimate hull girder strength analysis using Idealized Structural Unit Method: A case study for double hull girder with transverseless system. *PRADS'92*, Elsevier, Vol 2, Newcastle upon Tyne, U.K., 745-763.
Paik J.-K. (1992c). *An efficient method for ultimate strength analysis of ship structures - The Idealized Structural Unit Method - (ALPS/ISUM theoretical manual).* Pusan National Univ., Korea
Paik, J.-K. (1994a). Hull collapse of aging bulk carrier under combined longitudinal and shearing force. *Trans. RINA* **136**, 217-228.
Paik, J.-K. (1994b). Tensile behaviour of local members on ship hull collapse. *J. Ship Research* **38**, 239-244.
Paik, J.-K. and Mansour A.E. (1995). A simple formulation for predicting the Ultimate strength of ships. *J. Marine Science and Technology* **1**, 52-62.
Paik, J.-K., Thayamballi A.K. and Jung S.C. (1996). Ultimate strength of ship hulls under combined vertical bending, horizontal bending and shearing forces. *SNAME Trans.* **104**, 31-59.
Paik, J.-K. and Thayamballi, A.K. (1997). An empirical formulation for predicting the ultimate compressive strength of stiffened panels. *Proc. 7th Int. Offshore and Polar Engineering. Conf.* Vol.IV, Homolulu, 328-338.
Paik, J.-K., Thayamballi, A.K., Sung, K.-K. and Soo, H.-Y. (1998). Ship hull ultimate strength reliability considering corrosion. *J. Ship Research* **42:2**, 154-165.
Paik, J.-K. (1999). *SPINE, A computer program for analysis of elastic-plastic large deflection behaviour of stiffened panels. User's manual,* Pusan National Univ., Korea.
Rahman R.K. and Chowdhury M. (1996). Estimation of ultimate longitudinal bending moment of ships and box girders. *J. of Ship Research,* **40:3**, 244-257.
Rigo, P. (1998). Constraints - Ultimate strength - Hull girder. Chap. IV of "LBR-5 an Optimization Model for Naval and Hydraulic Structures, These d'Agregation Ens. Sup.," Edt. ANAST, Liege Univ., Belgium, 1-128 (in French).
Rizzuto E. (1997). Discussion of Committee II.1 Report of ISCC'97. *Proc. of 13th ISSC*, T. Moan and S. Berge (eds), Pergamon Press - Elsevier Science, Vol 3, 69-71.
Rutherford, S.E. and Caldwell, J.B. (1990). Ultimate longitudinal strength of ships: A case study. *SNAME Trans.* **98**, 441-471.
Smith, C.S. (1977). Influence of local compressive failure on ultimate longitudinal strength of a ship's hull. *Proc. Int. Symp. on Practical Design in Shipbuilding*, Tokyo, Japan, 73-79.
Smith, C.S. (1983). Structural redundancy and damage tolerance in relation to ultimate ship hull strength. *Proc. Int. Symp. on The Role of Design, Inspection and Redundancy in Marine Structural Reliability*, Williamsburg, U.S.A.
Steen, E. (1995). Buckling of stiffened plates under combined loads - ABAQUS analysis. *DNV Report* **95-0445**.
Steen, E. and Balling Engelsen, A. (1997). "ABAQUA" analysis - Plate buckling/GL code. *DNV Report* **97-05606**.
Steen, E. (1999). Buckling of stiffened plates using a Shanley's model approach. *Research Report in Mechanics* **99-1**, Dept. Mechanics, Mechanics Division, University of Oslo.
Timoshenko, S.P. (1953). *History of Strength of Materials*. McGraw-Hill Book Co., New York
Ueda, Y. and Yao, T. (1982). The plastic node method: A new method of plastic analysis. *Comput. Methods for Appl. Mech. in Engng.* **34**, 1089-2004.
Ueda, Y., Rashed, S.M.H. and Paik, J.K. (1984). Plate and stiffened plate units of the idealized structural nuit method - Under in-plane loading -. *J. Soc. Naval Arch of Japan* **156**, 366-376 (in Japanese).
Ueda, Y. and Yao, T, (1985). The influence of complex initial deflection modes on the beghaviour and ultimate strength of rectangular plate in compression. *J. Constructional Steel Research* **5**, 265-302.
Ueda, Y. and Rashed, S.M.H. (1991). Advances in the application of ISUM to marine

structures. *Proc. Int. Conf. On Advances in Marine Structures-2*, ARE, Dunfirmline, U.K., 628-649.

Ueda, Y. and Masaoka, K. (1993). Ultimate strength analysis of thin plated structures using eigen-functions (1st Report); Rectangular plate element subjected to compression and shear. *J. Soc. Naval Arch. of Japan* **174**, 439-445 (in Japanese).

Ueda, Y. and Masaoka, K. (1995). Ultimate strength analysis of thin plated structures using eigen-functions (2nd Report); Rectangular plate element with initial imperfection. *J. Soc. Naval Arch. of Japan* **178**, 463-471 (in Japanese).

Valsgaard, S., Jorgensen L., Boe, A.A. and Thorkildsen, H. (1991). Ultimate hull girder strength margins and present class requirements. *Proc. SNAME Symp.'91 on Marine Structural Inspection, Maintenance and Monitoring*, Arlington, March, B.1-19.

Viner, A.C. (1986). Development of ship strength formulation. *Proc. Int. Conf. on Advances in Marine Structures*, ARE, Dunfirmline, U.K., 152-173.

Yao, T. and Nikolov, P.I. (1991). Progressive collapse analysis of a ship's hull under longitudinal bending. *J. Soc. Naval Arch. of Japan* **170**, 449-461.

Yao, T. and Nikolov, P.I. (1992). Progressive collapse analysis of a ship's hull under longitudinal bending (2nd Report). *J. Soc. Naval Arch. of Japan* **172**, 437-446.

Yao, T. (1993a). Analysis of ultimate longitudinal strength of a ship's hull. *Text Book of Mini-Symposium on "Buckling/Plastic Collapse and Fatigue Strength; State of The Art and Future Problems.* The West-Japan Soc. Naval Arch. 154-177 (in Japanese).

Yao, T. and Nikolov, P.I. (1993b). Ultimate longitudinal strength of a bulk carrier. *Proc. 3rd Int. Offshore and Polar Engineering Conf.,* Vol. IV, Singapore, 497-504.

Yao, T., Fujikubo M., Kondo K. and Nagahama S. (1994). Progressive collapse behaviour of double hull tanker under longitudinal bending. *Proc. 4th Int. Offshore and Polar Engineering Conf.*, Vol.VI, Osaka, Vol.IV, 570-577.

Yao, T., Niho, O., Fujikubo, M., Varghese, B. and Mizutani, K. (1997a). Buckling/ultimate strength of ship bottom plating. *Proc. Int. Conf. on Advances in Marine Structures III*, Paper **28**, Dunfermline, U.K.

Yao, T., Fujikubo, M., Varghese, B., Yamamura, K. and Niho, O. (1997b). Buckling/plastic collapse strength of rectangular plate under combined pressure and thrust. *J. Soc. Naval Arch. of Japan* **182**, 561-570.

Yao, T. (1999). Ultimate longitudinal strength of ship hull girder; Historical review and state of art. *Int. J. Offshore and Polar Engineering* **9:1**, 1-9.